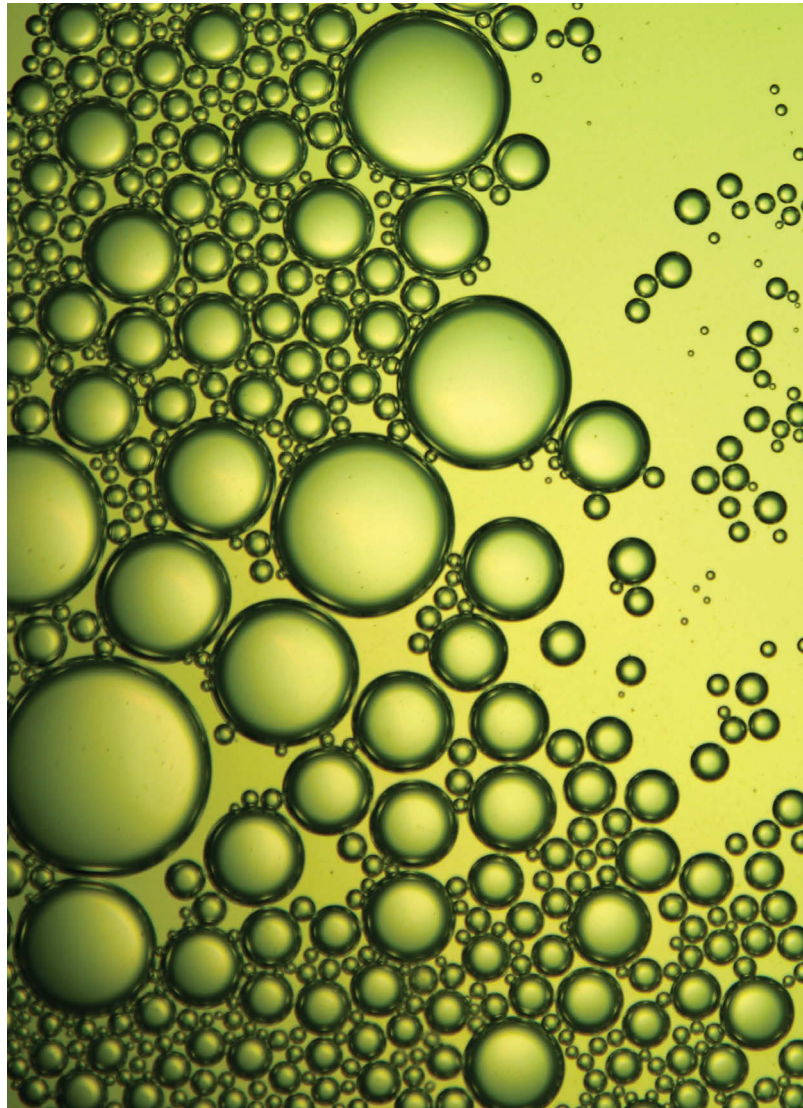


ENHANCING BIOFUEL PRODUCTION FROM A MARINE MICROALGAE- CONSTRAINTS OF CULTIVATION SCALE-UP



Dale T. Radford

B.Sc (Hons), MRes

Submitted in fulfillment of the requirements for the degree of Doctor of Philosophy in
Science,

Climate Change Cluster (C3),
School of Life Sciences,

University of Technology Sydney,

May 2016

Certificate of Original Authorship

I certify that the work in this thesis has not previously been submitted for a degree nor has it been submitted as part of requirements for a degree except as fully acknowledged within the text.

I also certify that the thesis has been written by me. Any quotations, ideas and help that I have received in my research work and during the preparation of the thesis itself have been acknowledged. In addition, I certify that all information sources and literature used are indicated in the thesis.

Signed: _____

Dale Radford (PhD candidate)

Acknowledgements

Thank you to my supervisors, Peter Ralph, John Raven, Milán Szabó and Martin Schliep for their support, guidance and critique throughout my candidature. Thank you to all members of the Algal Biosystems Group at UTS who have provided continued support both in technical and intellectual challenges that have allowed for the completion of this thesis. To my fellow PhD students, Kirralee Baker, Charlotte Robinson and Michaela Larsson, for their assistance overcoming laboratory challenges whilst also reminding me of the world outside of university and the beautiful country that is Australia. And, finally to the friendly faces at Knights Tea & Coffee Company for fulfilling my caffeine addiction over the past 3 years.

Preface

This thesis has been prepared in publication format, whereby each chapter represents a manuscript ready for submission to a peer-reviewed journal. As of yet, no individual chapter has been accepted for publication in a peer-reviewed journal.

In association with my PhD, I have been co-author on two publications that are relevant to the thesis, but does not contribute to it. The work presented in Tamburic et al .2014 lead up to the work presented in **Chapter 2**. The concepts and methods underlying Baker et al. 2016 provide the foundations for the work presented in **Chapter 3**.

Tamburic, B., Guruprasad, S., **Radford, D.T.**, Szabó, M., Lilley, R.M., Larkum, A.W.D., Franklin, J.B., Kramer, D.M., Blackburn, S.I., Raven, J. A, Schliep, M. & Ralph, P.J. 2014. The Effect of Diel Temperature and Light Cycles on the Growth of *Nannochloropsis oculata* in a Photobioreactor Matrix. *PloS one*, 9, 1, p. e86047.

Baker, K.G., Robinson, C.M., **Radford, D.T.**, McInnes, A.S., Evenhuis, C. and Doblin, M.A., 2016. Thermal performance curves of functional traits aid understanding of thermally induced changes in diatom-mediated biogeochemical fluxes. *Frontiers in Marine Science*, 3, p.44.

Table of Contents

Certificate of Original Authorship	ii
Acknowledgements	iii
Preface.....	iv
Table of Contents.....	v
List of Figures	ix
List of Tables	xiv
Supplementary Figures	xv
Supplementary Tables.....	xv
Abstract.....	xvi
Chapter 1 General Introduction	1
1.1. Global Energy Challenge	1
1.2. Biofuels	2
1.3. Algal biofuels	3
1.3.1. Overview	3
1.3.2. Energy balance	4
1.4. The microalgae biofuel production process	7
1.4.1. Microalgal cultivation.....	7
1.4.2. Downstream processing	8
1.5. Constraints in large-scale microalgae cultivations	10
1.5.1. Scale	10
1.5.2. Reactor design and mode of operation constraints	10
1.5.3. Algal strain selection	11
1.5.4. External abiotic environmental factors	12
1.5.5. Nutrient supply	15
1.5.6. Carbon supply	16
1.6. Summary	17
1.7. Thesis outline.....	17
1.8. General references	19

Chapter 2	Laboratory to large-scale: A multi-trait comparison of <i>Nannochloropsis oculata</i> cultivated under static and dynamic environmental conditions.	25
2.1	Introduction	26
2.2	Materials and Methods	29
2.2.1	Microalgal Cultures and medium	29
2.2.2	Photobioreactor set-up.....	29
2.2.3	Growth measurements.....	30
2.2.4	Fluorescence measurements.....	31
2.2.5	Nutrient analysis	31
2.2.6	Sampling regimes	32
2.2.7	Statistical analysis.....	32
2.3	Results.....	33
2.3.1	Growth of <i>N. oculata</i> at different light and temperature regimes	33
2.3.2	Nutrient limitation in simulated environmental growth.....	34
2.3.3	Relative photosynthetic electron transport rate.....	38
2.4	Discussion	40
2.5	Acknowledgments.....	45
2.6	References	45
2.7	Supplementary Figures.....	49
Chapter 3	Time-resolved thermal response of <i>Nannochloropsis oculata</i> improves large-scale cultivation reliability.	51
3.1	Introduction	52
3.2	Materials and methods	55
3.2.1	Stock microalgal culture and medium	55
3.2.2	In vivo chlorophyll fluorescence	55
3.2.3	Short-term (5 min) temperature stress analysis- MC-PAM	56
3.2.4	Long-term (4 day) temperature stress analysis	56
3.2.5	Statistical analysis.....	57
3.3	Results.....	58
3.3.1	Short-term thermal response on photophysiology of <i>N. oculata</i>	58
3.3.2	Thermal response following 24 hours exposure	59
3.3.3	Long-term thermal response	61

3.4	Discussion	64
3.5	Acknowledgements.....	68
3.6	References	68
3.7	Supplementary figures.....	72
Chapter 4 Satisfying the nutrient tank of <i>Nannochloropsis oculata</i> .74		
4.1	Introduction	75
4.2	Materials and methods	78
4.2.1	Microalgal culture and medium	78
4.2.2	Experimental nutrient matrix	78
4.2.3	Growth analysis	79
4.2.4	Nutrient analysis	80
4.2.5	Photophysiological analysis	80
4.2.6	Lipid content and fatty acid composition analysis	80
4.2.7	Statistical analysis.....	81
4.3	Results and discussion	82
4.3.1	Growth and nutrient uptake dynamics	82
4.3.2	Physiological dynamics:.....	85
4.3.3	Biochemical response	87
4.3.4	Implications to large-scale	91
4.3.5	Future directions	91
4.4	Acknowledgments.....	93
4.5	References	93
4.6	Supplementary Figures.....	97
Chapter 5 Assessing gas transfer rates as an essential link in scale-up studies for mass microalgal cultivation 98		
5.1	Introduction	99
5.2	Materials and methods	104
5.2.1	ePBR gas transfer characterisation set-up	104
5.2.2	Microalgal culture and medium	105
5.2.3	Static cultivation (tank reactor) setup	105
5.2.4	Simulated outdoor condition (ePBR) setup	105
5.2.5	Growth measurements.....	106
5.2.6	In situ photosynthesis, respiration rate and gas transfer calculations.....	106

5.2.7	Modeling gas-transfer rates, photosynthesis and respiration	108
5.3	Results	110
5.3.1	Gas transfer characterisation	110
5.3.2	Response to static growth conditions	112
5.3.3	Response to simulated outdoor growth conditions	112
5.4	Discussion	116
5.5	Acknowledgements	120
5.6	References	120
5.7	Supplementary Figures	125
Chapter 6	General Discussion	127
6.1	The ePBR platform - a suitable technique for improving large-scale biofuel production	127
6.2	New insights gained from an in-depth physiological characterisation of a biofuel candidate microalga. I. Understanding constraints on large-scale production. 129	
6.3	New insights gained from an in-depth physiological characterisation of a biofuel candidate microalga. II. Harnessing the natural capacity of microalgae..	131
6.4	Perspectives for future research	133
6.5	The future of microalgae biofuel production- concluding remarks	135
6.6	General References	137

List of Figures

Figure 1.1 Biofuel classification modified from Nigam & Singh (2011).....	2
Figure 1.2 A schematic representation of photosynthetic biofuel production (adapted from Schenk et al. 2008). Legend in top left explains arrows. Abbreviations; LHC, light harvesting complex; PSI/II, photosystem I/II; PQ, plastoquinone; PQH ₂ , reduced plastoquinone; Cyt b6f; Cytochrome b6/f complex; PC, plastocyanin; Fd, ferredoxin; FNR, ferredoxin/NADPH oxidoreductase; NADPH, reduced nicotinamide adenine dinucleotide phosphate; ADP, adenosine diphosphate; ATP, adenosine triphosphate; P _i , inorganic phosphate; TAG, triacylglycerol. Underlined products are used in biofuel production.....	6
Figure 1.3 Microalgal production process (modified from Pragya et al. 2013), where italics indicate possible downstream processes.....	7
Figure 1.4 Reactor design schematic- (a) an aerial view of and open raceway pond; (b) a tubular closed photobioreactor (PBR) with parallel horizontal tube (both taken from Chisti 2007).	8
Figure 1.5 A typical photosynthesis vs. irradiance (light intensity) curve: A typical photosynthesis response curve where; shaded area is dark respiration, P _{max} is maximum rate of photosynthesis, I _k is the half saturation irradiance.....	13
Figure 1.6 A typical growth rate vs. temperature response curve: A typical growth vs. temperature response curve; where T _{optimum} is the temperature at which growth is maximal; CT _{min} - minimum critical temperature and CT _{max} : maximum critical temperature- below and above this temperature no algal growth is observed.....	14
Figure 2.1: Experimental ePBR setup: (a) square wave light, constant temperature regime (b) square wave light, sinusoidal temperature regime, SqLSiT, (c); sinusoidal light, constant temperature regime, SiLCT, (d) sinusoidal light, sinusoidal temperature regime, SiLSiT. Lines represent light intensity (solid line) and temperature (broken line). All irradiance cycles were 12 h: 12 h light: dark cycles of square-wave light (1240 μmol photons m ⁻² s ⁻¹), sinusoidal light 0 to 1920 μmol photons m ⁻² s ⁻¹ , with peak irradiance occurring at midday. Temperature cycles were as follows, constant 25 °C ± 0.5°C and sinusoidal temperature fluctuating between 20 - 30 °C with peak temperature occurring at dusk.	30
Figure 2.2 Growth measurements: Cell abundance of <i>N. oculata</i> when cultivated in a ePBR under (a) square wave light, constant temperature, SqLCT (b) sinusoidal light, constant temperature regime, SiLCT, (c) square wave light, sinusoidal temperature regime, SqLSiT, and (d) sinusoidal light, sinusoidal temperature regime, SiLSiT. Symbols represent values for each replicate within each treatment; solid line represents the concatenated logistic fit (n=3) fitting using non-linear regression algorithm (OriginPRO 2015). The vertical coloured broken line represents the time at which, maximum oxygen concentration (blue), zero/minimal residue nitrate (magenta), zero/minimal residual orthophosphate (green) occurred. The dashed horizontal black line represents the predicted maximum cell number derived from the logistic fit.....	34

Figure 2.3 pO_2 profiles: *In situ* dissolved oxygen profiles of *N. oculata* when exposed to; (a) square wave light, constant temperature regime, SqLCT, (b) sinusoidal light, constant temperature regime, SiLCT (c) square wave light, constant temperature regime, SqLCT and (d) sinusoidal light, sinusoidal temperature regime, SiLSiT. Lines represent the average of 3 replicates (solid line) $n=3$, average \pm standard deviation (broken line) and a baseline (horizontal dotted line). The baseline value corresponds to the solubility of oxygen in seawater at 25 °C and 1 bar pressure. Dashed vertical lines correspond to the maximum oxygen concentration throughout growth..... 35

Figure 2.4 Dissolved nutrient concentrations: Concentration of dissolved nitrate (a, c, e) and orthophosphate (b, d, f) throughout time in experiments carried out with *N. oculata* under square wave light, sinusoidal temperature regime, SqLSiT (a, b) sinusoidal light, constant temperature regime, SiLCT (c, d) and sinusoidal light, sinusoidal temperature regime, SiLSiT (e, f). The concentrations are expressed in $\mu g L^{-1}$ each data point is represents and individual replicate, horizontal broken line represents 0 $\mu g L^{-1}$. Vertical broken lines correspond to time at which predicted zero residual nutrient or minimal nitrate (magenta) and orthophosphate (green) nutrient amount occurred..... 37

Figure 2.5 Dynamic oxygen and photophysiological response of *N. oculata*: Relative electron transport rate and *in situ* pO_2 profiles of *N. oculata* when cultivated under different light and temperature regimes; (a, b) square wave light, sinusoidal temperature, SqLSiT; (c, d) sinusoidal light, constant temperature, SiLCT and (e, f) sinusoidal light, sinusoidal temperature regime, SiLSiT. Measurements were recorded at early exponential (a, c, e) and stationary phase (b, d, f). Solid diamonds and lines represent the average of 3 replicates relative electron transport rate and *in situ* dissolved oxygen profiles (blue line); error bars represent standard deviation ($n=3$). The solid white area represents the light intensity at the surface of the culture. 39

Figure 3.1 (a, b) Rapid light curves performed in the MC-PAM of replete cultures of *N. oculata* after exposure to 98 $\mu mol photons m^{-2} s^{-1}$ (PAR; white light) for 5 min at (a) 10 °C and (b) 40 °C, where closed diamonds represent triplicate samples ($n=3$) and errors bars corresponding to ± 1 standard deviation. (c, d) Derived parameters of RLC curve fits at different temperature exposures where (c) maximum relative electron transport rate (circles) and (d) saturating irradiance (triangles)..... 58

Figure 3.2 Relative electron transport rate (rETR) of *N. oculata* at different temperatures: rETR was determined using the multi-colour PAM (MC-PAM, Walz, Germany), samples were exposed to temperature for 5 min under 98 $\mu mol photons m^{-2} s^{-1}$ (PAR; white light) prior to performing a rapid light curve (10 s step). rETR was derived from the 54 $\mu mol photons m^{-2} s^{-1}$ light step. 59

Figure 3.3 Relative electron transport rate (rETR) and maximum quantum yield of *N. oculata* after 24 hours at varying temperatures: (a) rETR corresponds to value at 2 seconds after induction of light performed on Imaging-PAM. (b) Maximum quantum yield was determined after dark adaption for 15 min. Symbols represent

the average of triplicates (n=3) with errors bars corresponding to ± 1 standard deviation. Square brackets cluster treatments where non-significant difference were found ($p > 0.05$), whilst letters correspond to statistical difference between groups ($p < 0.05$). 60

Figure 3.4 Physiological responses of *N. oculata* after 96 hours at varying temperatures: (a) specific growth rate (diamonds), (b) nitrate uptake rate (squares) and (c) orthophosphate uptake rate (circles) where symbols represent the average of triplicates (n=3) with errors corresponding to ± 1 standard deviation. Square brackets and letters represent groups of statistical different values ($p < 0.05$). 62

Figure 3.5 Relative electron transport rate (rETR) and maximum quantum yield of *N. oculata* after 96 hours at varying temperatures: (a) rETR corresponds to value at 2 seconds after induction of light performed on Imaging-PAM. (b) Maximum quantum yield was determined after dark adaption for 15 min. Symbols represent the average of triplicates (n=3) with errors corresponding to ± 1 standard deviation. 63

Figure 4.1 Schematic of nutrient supply experimental design. Solid diamonds represents treatments performed in this study with three replicates per treatment (n=3). Open diamonds represent treatments performed in Mayer et al. 2013 and open circles represent Rasdi and Qin 2015. Numbers represent treatment identification and asterisks indicate those samples chosen for total lipid quantification and fatty-acid methyl ester (FAME) analysis. Black diagonal line represents constant N:P ratios (24:1) with different magnitude of nutrient supply. Magenta and green broken lines represent samples cultivated under changing N:P, whilst maintaining consistent nitrogen and orthophosphate supply, respectively. The control treatment is traditional f/2 media (882 μM nitrate and 36.2 μM orthophosphate). 79

Figure 4.2: Specific growth rates of *N. oculata* cultivated under a matrix of varying nitrate and orthophosphate supply. Bubbles size corresponds to the magnitude of growth rate; bigger bubbles indicate higher growth rates. Each bubble represents the average of triplicate samples (n=3). Similarities between treatments are denoted by same letters (one way ANOVA with post hoc Tukeys $p > 0.05$), differences in treatments are denoted by different letters ($p < 0.05$). 83

Figure 4.3: Nutrient uptake dynamics of *N. oculata*; (a) Nitrate uptake (solid diamonds) and orthophosphate uptake (open circles) compared to the resulting cell specific growth rate. Solid and broken lines represent the linear regressions ($y = mx + c$) for nitrate ($m = 50.1$; $R^2 = 0.71$) and orthophosphate uptake ($m = 2.44$; $R^2 = 0.20$) respectively. (b) Moles of N uptake per mole of P taken up in *N. oculata* cultivated under different N:P supply ratio. Closed circles represent the average of triplicate samples (n=3) with error bars corresponding to ± 1 standard deviation, a Michaelis-Menten model was fitted to the data (solid line; $R^2 = 0.80$). 84

Figure 4.4 (a, b) Nutrient concentration of nitrate (solid diamonds), orthophosphate (solid circles) and maximum quantum yield, F_v/F_m (open squares) over a batch growth of *N. oculata* cultivated under (a) control (882 μM N and 36.2 μM P) and

(b) treatment 4 (176 μM N and 7.24 μM P) starting nutrient conditions. Vertical broken line represents the day in which nutrient depletion occurred, double headed arrow indicates time differential of nutrient depletion between the control and treatments 4. (c) Maximum quantum yield (F_V/F_M) of *N. oculata* cultivated under a nutrient matrix measured on the day of harvest. Bubbles size corresponds to the magnitude F_V/F_M ($n=3$) values are represented by scale-bar adjacent. Letters denote similarity to control (882 μM N and 36.2 μM P; one way ANOVA with post hoc Tukeys $p > 0.05$), numbers represent the different treatment identification..... 86

Figure 4.5 Biochemical analysis of *N. oculata* cultivated under a matrix of varying nitrate and orthophosphate supply. (a) Cellular lipid content (pg cell^{-1}), bubble size corresponds to the cellular lipid content according to scale adjacent, where values represents the average of duplicate samples. Letters denoted significant difference in lipid content when compared with control (one way ANOVA with post hoc Tukeys $p < 0.05$). (b) Eicosapentaenoic acid (EPA) percentage, bubble size corresponds to the magnitude of EPA % in scale adjacent. Each bubble represents the average of triplicate samples ($n=3$). Similarity in treatments are denoted by same letters (one way ANOVA with post hoc Tukeys $p > 0.05$), whilst different between treatments are denoted by different letters ($p < 0.05$)..... 90

Figure 5.1 Schematic of oxygen concentration trace (blue line) used to calculate the gas transfer coefficient. Gas transfer rates were derived from equation 5.1 where the red solid line represents a typical fit, $R^2 > 0.98$. The vertical broken line represents the switching of gas types from N_2 to ambient air and the horizontal broken line represents oxygen saturation..... 105

Figure 5.2 (a) A typical dissolved oxygen trace of microalgae (solid blue line) cultivated under square wave light, white and gray background represents light on and light off respectively. Where the spike in the dissolved oxygen trace (a) were used to calculate (b) net photosynthesis and (c) respiration rates, both indicated by blue lines and gas transfer coefficient ($k_L a$; b, c) indicated by red line..... 108

Figure 5.3 Characterisation of gas transfer coefficient at different gas flow rates provided through different needle diameters of 0.21 mm (open diamond) and 0.34 mm (solid diamond). 110

Figure 5.4 Characterisation of gas transfer coefficients at different (a) temperature, (b) pH and (c) salinity using the ePBR set-up, each symbol represents the individual replicates. Broken line represents the gas transfer coefficient at 450 mL min^{-1} at 26 $^{\circ}\text{C}$, 0 g L^{-1} and pH 5.93. 111

Figure 5.5 (a) Growth of *N. oculata* under laboratory conditions (light intensity, white blocks), where temperature (red line), cell number (closed diamonds) were monitored over the growth cycle. Modelled rates of gas transfer (green line), photosynthesis (blue line), and respiration (black line) are shown during lag (a, d) and exponential (b,c) growth phases..... 114

Figure 5.6 (a) Growth of *N. oculata* under simulated outdoor conditions obtained from raceway pond at UTS rooftop facility, where light intensity (white blocks),

temperature (red line) and cell number (closed diamonds) were monitored over the growth cycle. Modelled rates of gas transfer (green line), photosynthesis (blue line), and respiration (black line) are shown during lag (a, d) and exponential (b,c) growth phases. 115

Figure 6.1: Proposed method of bio-prospecting potential site for microalgae cultivation for biofuel production using the ePBR platform. 135

List of Tables

Table 1.1 Comparison of yield and land area requirement for common sources of biodiesel (modified from Chisti 2007). ^a Area required to produce 100% of Australia transport fuel (petrol and diesel), 30.6 billion litres (Australian Bureau of Statistics 2014). ^b 50% oil (by wt) in biomass.	4
Table 1.2 Biomass, lipid content and lipid productivity of different microalgae cultivated under continuous light at 25 °C, modified from Rodolfi et al. 2009.....	12
Table 2.1 Growth rate of <i>N. oculata</i> grown under square wave light, constant temperature (SqLCT) square wave light, sinusoidal temperature (SqLSiT); sinusoidal light, constant temperature (SiLCT) and sinusoidal light, sinusoidal temperature (SiLSiT). μ , growth rate expressed in d^{-1} and final cell abundance expressed as 10^7 cells per mL. Values are mean \pm 1 SD (n=3) calculated using derived parameters from a non-linear logistic fit of individuals in each treatment. Asterisks correspond to the differences between treatments (one way ANOVA with post hoc Tukeys $p < 0.05$)......	33
Table 2.2 Nutrient uptake kinetics of <i>N. oculata</i> grown under square wave light, constant temperature (SqLCT) square wave light, sinusoidal temperature (SqLSiT); sinusoidal light, constant temperature (SiLCT) and sinusoidal light, sinusoidal temperature (SiLSiT). Nutrient uptake rates are expressed as $\mu g L^{-1} d^{-1}$ where values are mean \pm 1 SD (n=3) calculated using derived parameters from a linear fit of individual replicates. Asterisk correspond to the differences between treatments (one way ANOVA with post hoc Tukeys $p < 0.05$).	36
Table 4.1 Fatty acid composition of <i>N. oculata</i> cultivated under different nutrient concentrations: Fatty acids are expressed as a % of total fatty acid. Values are means of triplicate samples (n=3), ± 1 standard deviation.	89

Supplementary Figures

Supplementary Figure 2.1 Dynamic oxygen and photophysiological response of *N. oculata*: Quantum yield of photosystem II and *in situ* pO_2 profiles of *N. oculata* when cultivated under different light and temperature regimes; (a, b) square wave light, sinusoidal temperature, SqLSiT; (c, d) sinusoidal light, constant temperature, SiLCT and (e, f) sinusoidal light, sinusoidal temperature regime, SiLSiT. Measurements were recorded at early exponential (a, c, e) and stationary phase (b, d, f). Open diamonds and lines represent the average of 3 replicates relative electron transport rate and *in situ* dissolved oxygen profiles (blue line); error bars represent standard deviation (n=3). The solid white area represents the light intensity at the surface of the culture..... 50

Supplementary Figure 3.1 Physiological responses of *N. oculata* after 24 hours at varying temperatures: (a) specific growth rate (diamonds), (b) nitrate uptake rate (squares) and (c) orthophosphate uptake rate (circles) where symbols represent the average of triplicates (n=3) with errors corresponding to ± 1 standard deviation. 72

Supplementary Figure 3.2 Steady state light curve of *N. oculata*: rETR was calculated using the Imaging-PAM (Walz, Germany), samples were exposed to 5 min actinic light prior determination of relative electron transport rate. Symbols represent the average of triplicates (n=3) with errors corresponding to ± 1 standard deviation. Data from this analysis was used to determine the actinic light required for the induction curves..... 73

Supplementary Figure 5.1 The environmental PBR set up used to determine gas transfer within the solution, the top two reservoirs allow for the water to be humidified, MFC are gas flow controllers and the solenoid switch allowed for the switching between nitrogen and air. 125

Supplementary Figure 5.2 Dissolved oxygen trace (pO_2) of *N. oculata* cultivated under (a) laboratory conditions (square- wave light) and (b) under simulated outdoor conditions. Spikes correspond to time points in which gas supply was switched off in order to calculate net photosynthesis/ dark respiration and gas transfer coefficients. 126

Supplementary Tables

Supplementary Table 2.1 Experimental photobioreactor set-up: All irradiance cycles were 12 h: 12 h light: dark cycles. **Error! Bookmark not defined.**

Supplementary Table 4.1 Starting macronutrient concentrations (NO_3^- and PO_4^{3-}): Asterisk (*) represent samples chosen for lipid/ fatty acid methyl ester (FAME) analysis..... 97

Abstract

The current global dependence on liquid fossil fuels is not sustainable and as a result, the development of alternative renewable liquid fuel sources is paramount for future economic, environmental and social security. The production of liquid biofuels from marine microalgae offers a solution, due to its carbon-neutral capacity (mitigating increasing anthropogenic carbon dioxide) and its minimal impact on existing food and freshwater resources. In order to satisfy global demand for liquid fuel, the cultivation of microalgae is required at commodity scales; however, major challenges exist in order to ensure production is economically and sustainably viable. The aim of this thesis was to assess some of the key environmental constraints of industrial scale cultivation of microalgae, including: exposure to complex abiotic conditions; effective delivery of nutrient inputs and harnessing algal physiology to improve the viability of microalgae cultivation for biofuel production. To accomplish these aims, the application of quantitative physiological techniques in conjunction with a novel photobioreactor platform (ePBR; Phenometrics®) enabled us to assess the biological response of a biofuel candidate algae strain, *Nannochloropsis oculata*, following exposure to different environmental conditions and nutrient input scenarios.

My thesis revealed complex responses of *N. oculata* to a variety of environmental conditions. The response to changing light and temperature environments was found to be influenced by the growth stage of the algal culture, whilst comparisons between productivity under laboratory versus simulated outdoor conditions showed sinusoidal light dominates the diel effect of temperature oscillations in determining final yields. Exposure of *N. oculata* to a range of temperature conditions emphasised the wide thermal envelope of growth and therefore, the suitability of this algae strain for use in biofuel production. Moreover, physiological algal traits were found to respond to the magnitude and duration of exposure to sub-optimal temperatures. Acclimation to nutrient conditions provide evidence of how natural cellular mechanisms can be harnessed to reduce the initial nutrient input, and how optimisation of nutrient delivery can be used to produce alternative products of interest. In my thesis, the suitability of the ePBR platform in conjunction with physiological methods such as *in vivo* chlorophyll fluorescence was used to examine the challenges of industrial cultivation. Several important avenues for future biofuel research are highlighted including: the better understanding of recovery of cultures from different magnitudes of environmental stress and harnessing the inherent acclimation process of microalgae to reduce system inputs will help to drive the future sustainability of the algal biofuels industry.

Chapter 1 General Introduction

1.1. Global Energy Challenge

The past half a century has seen a growing global population placing an ever increasing demand upon the major natural resources (freshwater and food) and fuel. In more recent years, the increased global industrialisation has resulted in a widespread dependence upon petroleum-based fuels (Tsita & Pilavachi 2013). It is estimated that 80% of the primary energy consumed worldwide is derived from fossil fuels, 58% being used in the transport sector (Escobar et al. 2009). With this dependence not likely to diminish in the foreseeable future, and our fossil fuels reserves ever-decreasing, there is increasing urgency for an alternative renewable resource of energy.

Technological advancements in recent decades have seen the development of effective and sustainable renewable energy industries: hydro-electric, wind and solar (photovoltaic) are now seen throughout the world, which are all capable of generating vast amounts of sustainable electricity suitable for human consumption (Diesendorf 2014). Currently, the inability to store these types of energy prevents these sources from meeting all of our entire energy requirements, especially the need for a mobile energy source. This highlights the need for the development of a transportable liquid fuel that can be retrofitted to current infrastructure. An alternative solution to fossil-derived fuels can be provided by the generation of a fuel from renewable biomass resources (i.e. biofuels; Nigam & Singh 2011), whereby improving the capacity of the renewable energy industry to provide social, economic and environmental benefits.

The development of a sustainable fuel market would provide a government/nation/economy with greater fuel security. Brazil's recent prominence as a major global economy can be used as a case study to demonstrate the advantages of becoming mostly energy-independent from fossil-derived fuel, an initiative stimulated by the global energy crisis in the 1970s (Robbins 2011). In addition to economic benefits, biofuels offer environmental benefits as they close the carbon loop, i.e. are carbon neutral, and provide an opportunity to aid the recent shift in global consensus in de-carbonising our society, culminating in the adoption of the Paris Agreement (United Nations 2015). The renewable energy objectives of the Paris Agreement were to reduce annual greenhouse gas emissions by 2020 with intentions of 'holding the increase in the global average temperature to well below 2 °C above pre-industrial levels' (United Nations 2015). In order to reach these targets, government mandates

are being implemented; for example, India intends to have 20% biofuel (ethanol) blending mandated by 2017 (currently 5%; Lane 2014). Increasing consistency of such initiatives will drive global demand/market for easily accessible biofuels, allowing biofuels to be traded as a commodity. However, increased demand requires greater production scale. At this scale, social and environmental impacts influence the feasibility of any biofuel production process (Rajagopal & Zilberman 2007; Fairley 2011; Robbins 2011).

1.2. Biofuels

Firstly, it is imperative to have a clear definition of what constitutes a biofuel. A common definition is a fuel generated from renewable biomass resources (Stöcker 2008) that can be sub-categorised as primary or secondary biofuels. Primary biofuels generate energy from the un-modified chemical energy present in natural unprocessed biomass (e.g., firewood). Secondary biofuels are considered as primary biofuels that have been processed prior to fuel generation and can be further classified based upon the feedstock and technology used in production. The three types are first-, second- and third-generation (advanced) biofuels (**Figure 1.1**; Nigam & Singh 2011).

Biofuel classification			
Primary	Secondary		
Direct combustion of firewood, wood chips, pellets, animal waste, forest and crop residues, landfill gas.	1st generation <i>Substrate:</i> seeds, grains or sugars. <i>Products:</i> Bioethanol or butanol by fermentation of starch (wheat, barely, corn, potato) or sugars (sugar-cane, sugar beet etc.) Biodiesel by transesterification of plant oils (rapeseed, soybeans, sunflower, palm, coconut, jatropha, used cooking oil animal fat etc.)	2nd generation <i>Substrate:</i> lignocellulosic biomass. <i>Products:</i> Bioethanol or butanol enzymatic hydrolysis. Methanol, Fischer-Tropsch gasoline and diesel, mixed alcohol, dimethyl ether and green diesel by thermochemical processes. Biomethane by anaerobic digestion.	3rd generation (advanced biofuel) <i>Substrate:</i> micro/macro-algae, bacteria or fungi. <i>Products:</i> Biodiesel by transesterification of microbial oils (microalgae, bacteria, fungi etc.) Biocrude from microalgae by thermochemical processes. Bioethanol from micro/macro algae. Biohydrogen from green algae.

Figure 1.1 Biofuel classification modified from Nigam & Singh (2011).

First-generation secondary biofuels derived from sugars, grains or seeds require simple processes to produce a refined fuel, many of which are currently in commercial production: ethanol produced from energy dense sugarcane is a prime example. This ethanol is then able to be blended with petroleum ranging from 10% ethanol (E10) to

85% ethanol (E85; Nigam & Singh 2011). Other first-generation biofuels include biodiesel produced from palm, soybean or rapeseed feedstocks.

Second generation fuels are derived from lignocellulosic biomass from agricultural crops, wood, grasses and non-edible residues of food crops. The polysaccharides (cellulose and hemicellulose) within the feedstock are converted to glucose, and then fermented (in the presence of yeast or bacteria) to produce alcoholic products such as ethanol and butanol which are capable of being directly blended with petroleum (Chisti 2008).

Despite many primary and secondary biofuels being commercially available, limitations have been identified when cultivated at large scales (Pickett et al. 2008; Schenk et al. 2008; Mata, Martins & Caetano 2010; Chisti 2013). Competition for land to produce food raises the question of the use of crops that are cultivated on most fertile soil; should they provide food or fuel?. Additionally, low yield per land area deem these fuels not economically favorable and as a result, while the global community is seeking an alternative biofuel production method that overcomes this limitation. The most recent shift in focus to biofuel production is the manipulation of micro-organisms' natural metabolic process to produce a renewable, alternative feedstock; microalgae are a good example (Berry 2010).

1.3. Algal biofuels

1.3.1. Overview

The idea of generating a renewable source of liquid fuel from microalgae has been around for over half a century. The first major documentation of large outdoor cultivation trials was in a publication of *"Algae Culture. From Laboratory to Pilot Plant"* (Burlew 1953) and triggered the industrial cultivation of microalgae for use as biofuels. One of the most extensive research programs to date took place almost two decades ago (between 1978 and 1996) which was performed by the United States National Renewable Energy Laboratory (NREL) to study the ability of microalgae to produce natural oils and resulted in advances in applied biology, algae production systems and resource availability (Sheenan et al. 1998). Furthermore, in 1990, the Japanese launched a major initiative that although not directly focused upon production of bioenergy, provided improved understanding of commercial-scale microalgae cultivation. The project aim was to develop 'effective and clean methods of biological fixation of CO₂ based on the effective integration of photosynthesis function of microorganisms' (Michiki 1995). The project provided important findings in the

cultivation of microalgae exposed to untreated flue-gas that allowed for future research into bioremediation and biofuel production from algae grown using flue-gas CO₂ as its sole carbon source. These programs are just two examples for a body of research which has driven our understanding of biofuel production ranging from biology and engineering to understanding economic constraints. Despite this, the current method of converting algae to fuel is not commercially competitive against current crude oil prices (Chisti 2013).

1.3.2. Energy balance

When compared with traditional methods of large-scale biofuel production such as ethanol from corn, microalgal biofuels is socially and environmentally more beneficial (Chisti 2007, 2013). This is because microalgae-derived biofuels have the capacity to produce a greater amount of biofuel per unit area and unit time (Georgianna & Mayfield 2012). Furthermore, the land required for cultivation does not compete with that use for cultivation of food, however, the use of marine (non-potable, brackish, saltwater) strains for production will not diminish our freshwater resources (Milly et al. 2005; Vasudevan et al. 2012; Gao et al. 2013).

Table 1.1 Comparison of yield and land area requirement for common sources of biodiesel (modified from Chisti 2007). ^aArea required to produce 100% of Australia transport fuel (petrol and diesel), 30.6 billion litres (Australian Bureau of Statistics 2014). ^b50% oil (by wt) in biomass.

Feedstock	Oil yield (L ha ⁻¹)	Land required to produce 100 % Australian annual transport fuel (M ha) ^a
Corn	172	178
Soybean	446	67
Canola	1 190	36
Jatropha	1 892	16
Coconut	2 689	11
Oil Palm	5 950	5
Microalgae ^b	58 700	0.5

Microalgae are capable of being converted into many different forms of biofuel products; commonly 'green crude' oil or biodiesel. In the former case, this is because they are capable of producing significant amounts of biomass via rapid cell division. In contrast, in the case of the latter, fuel precursor molecules can be extracted from high-neutral lipid containing cells; molecules that are synthesised through the conversion of light energy into chemical energy via the process of photosynthesis (**Figure 1.2**; Schenk et al. 2008).

The photosynthetic process involves the capture of light energy from the sun by light harvesting pigment molecules (carotenoids and chlorophylls) in the light harvesting complexes (LHC) within the thylakoid membrane. Here light energy is funneled to the chlorophyll *a* molecules of the reaction centres of the photosystems (PSII and PSI) where the primary charge separation occurs. The oxidised PSII reaction centre radical is then re-reduced by the electron that is obtained from the splitting of water. The stabilised charge separated state provides, on the reducing side, a linear electron flow along a series of redox components in the thylakoid membrane ending at the oxidising end of PSI. At some steps of the linear pathway, the electron flow is coupled to the pumping of hydrogen ions across the thylakoid membrane in the thylakoid lumen. Some of the protons deposited in the thylakoid lumen are products of the water splitting process, and some of the protons originate from the stroma (**Figure 1.2**). At the reducing end of PSI, the protons and electrons are recombined by ferredoxin-NADP⁺ oxidoreductase (FNR) to produce NADPH. The energy released in the return of the protons pumped into the thylakoid lumen back to the stroma converts adenosine diphosphate plus inorganic phosphate into adenosine triphosphate (ATP). These products, NADPH and ATP, provide the energy to drive the Calvin-Benson cycle that fixes carbon dioxide (CO₂) into sugars (initially glyceraldehyde-3-phosphate). These sugars are pre-cursors for other central metabolic pathways, for example, the fatty acid synthesis pathway that results in the production of triacylglycerides (lipids), a precursor molecule for biodiesel production (**Figure 1.2**; Falkowski & Raven 2007, Schenk et al. 2008). Due to the complexity of the photosynthetic process, numerous factors such as: incident light (**c.f. Chapter 1.5.4.1**), temperature (**c.f. Chapter 1.5.4.2**), carbon dioxide concentration (**c.f. Chapter 1.5.6**) and nutrient availability can influence photosynthetic efficiency of the cell and therefore affect downstream processes that use this energy, such as cellular growth.

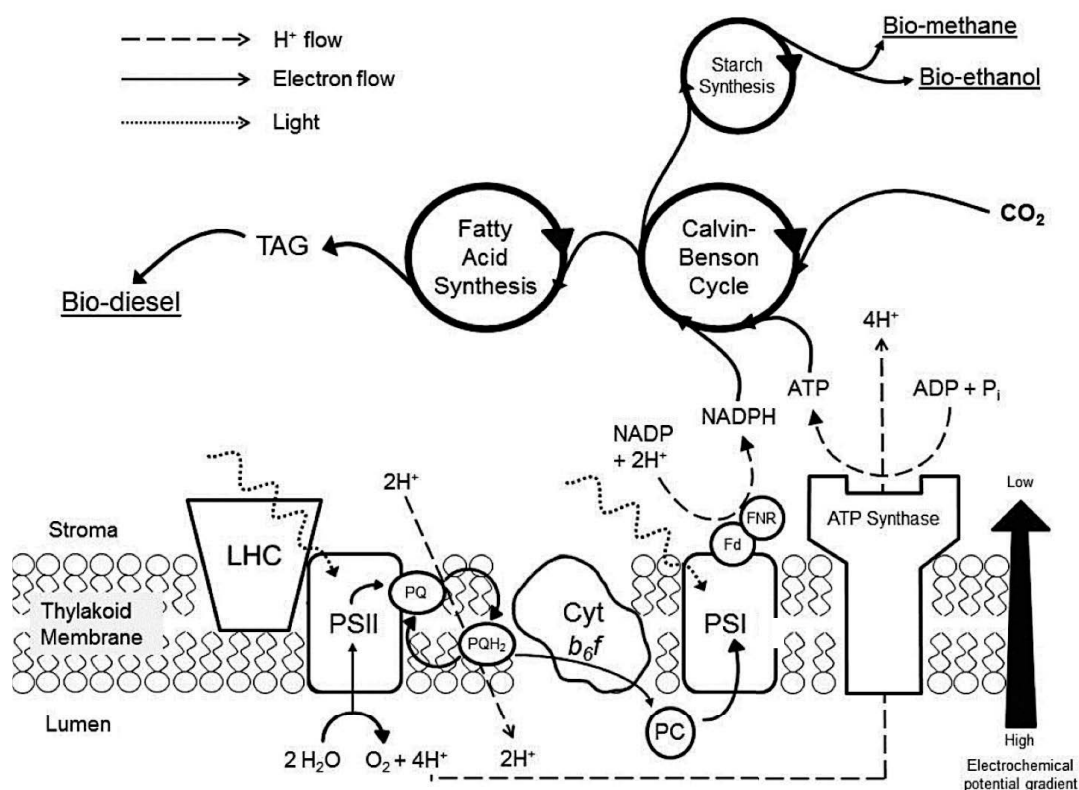


Figure 1.2 A schematic representation of photosynthetic biofuel production (adapted from Schenk et al. 2008). Legend in top left explains arrows. Abbreviations; LHC, light harvesting complex; PSI/II, photosystem I/II; PQ, plastoquinone; PQH₂, reduced plastoquinone; Cyt *b₆f*; Cytochrome *b₆/f* complex; PC, plastocyanin; Fd, ferredoxin; FNR, ferredoxin/NADPH oxidoreductase; NADPH, reduced nicotinamide adenine dinucleotide phosphate; ADP, adenosine diphosphate; ATP, adenosine triphosphate; P_i, inorganic phosphate; TAG, triacylglycerol. Underlined products are used in biofuel production.

1.4. The microalgae biofuel production process

The procedure to produce fuel from microalgae is complex and a multi-stage process that is summarised in **Figure 1.3**.

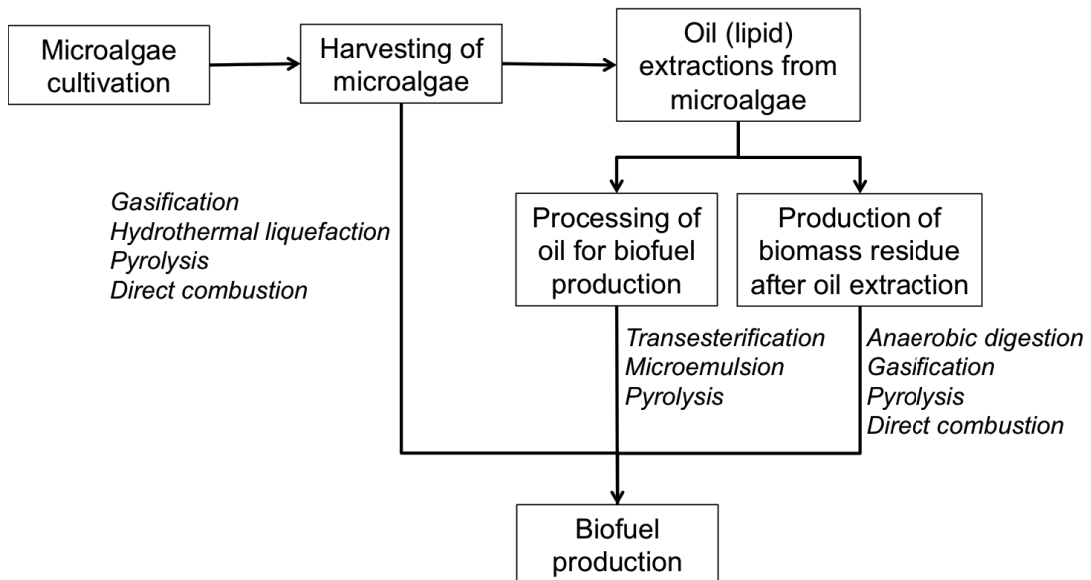


Figure 1.3 Microalgal production process (modified from Pragya et al. 2013), where italics indicate possible downstream processes.

1.4.1. Microalgal cultivation

The first stage in large-scale biofuel production is cultivation of the selected microalgae strain under specific abiotic conditions; addition of nutrients (macronutrients such as nitrogen and phosphorus, and micronutrients such as iron), carbon (commonly in the form of carbon dioxide; CO₂) and light. At large scales, this cultivation can occur in two major types of reactor design; raceway pond reactors and closed photobioreactors (PBRs; Chisti 2007). Basic raceway pond reactors are closed loop systems re-circulating systems that are mixed by a paddlewheel (**Figure 1.4a**). There is no specific design for closed PBRs; common types include tubular (horizontal, tubular or helical) or flat panel bioreactors (**Figure 1.4b**). Mixing is provided through the addition of air and a pump to circulate the culture around the system. Once the algae have been grown to the required biomass or specific cell content, the cells can be harvested (Grima et al. 1999; Borowitzka & Moheimani 2013a; Zittelli et al. 2013).

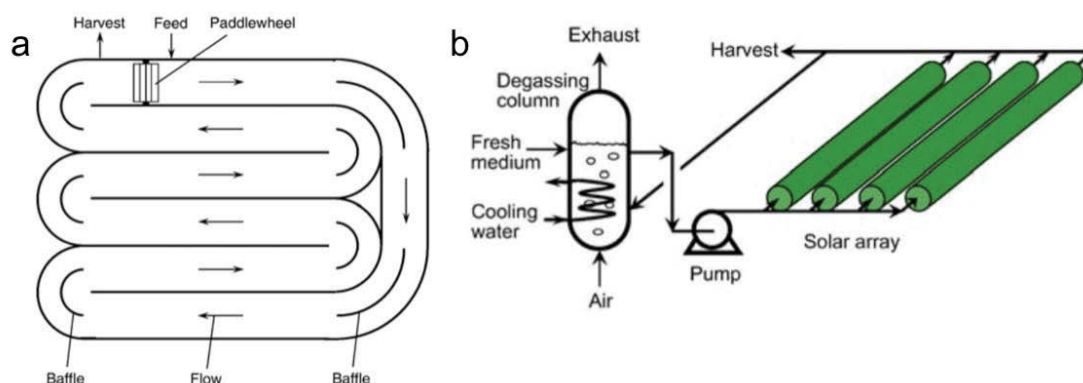


Figure 1.4 Reactor design schematic- (a) an aerial view of an open raceway pond; (b) a tubular closed photobioreactor (PBR) with parallel horizontal tube (both taken from Chisti 2007).

1.4.2. Downstream processing

To refine microalgae cellular components to the quality required to produce a marketable product, downstream processing is required, including harvesting and dewatering of the microalgae which amount to 20–30% of production cost (Mata et al. 2010). The major methods used include sedimentation, flocculation, floatation, centrifugation and filtrations. To date, no single method is optimal for maximising marketable product per unit cost of processing (Milledge & Heaven 2013). Once the majority of the water has been removed, the cells are ready to be refined further, where the specific downstream processing is dependent upon the specific end-product (Demirbas et al. 2009; Pragya et al. 2013).

The two major processes of refining the cells into marketable fuel products are: (i) lipid extraction; and (ii) hydrothermal liquefaction (HTL). Lipids are converted to 'biodiesel'; first intercellular cell constituents are extracted by rupturing of cells, then lipids are then extracted using solvents (commonly chloroform/methanol and hexane). The lipids are transesterified into biodiesel using an alcohol and catalyst which form fatty acid methyl esters (FAMES) (Scott et al. 2010) that have a similar molecular structure to diesel and are currently blended at ~80% with conventional diesel. Methods of thermochemical conversion have improved over recent years, particularly HTL as a result of commercial interest, as this process has the capacity to be integrated with existing petroleum-refining infrastructure (Liu et al. 2013). This method converts wet algae biomass (80 – 90 % water content) into different types of 'green crude' through exposure to high pressure (5 - 20 MPa) and high temperature (205 - 350 °C). The species of algae, reaction pressure and temperature dictate the yield of fuel from the HTL process. The resulting product, 'green' (bio) crude can be further refined to multiple fractions using conventional petroleum refining techniques (Suali & Sarbatly 2012). Other methods of thermochemical conversions include; gasification, pyrolysis,

anaerobic digestion and direct combustion (Liu et al. 2013; Pragya et al. 2013). Despite the level of research dedicated to improving these processes, current technology is still too inefficient, energy intensive, and the use of harsh chemicals in certain processes are prevalent, making them unsustainable options.

One cost-effective method for determining the overall economic viability of a biofuel production facility is to perform life cycle analysis (LCA). These analyses are used to describe and quantify inputs and emissions of the whole (or a specific) production process and consider both environmental and economic consequences (Scott et al. 2010). Often the outcomes of these LCAs have several layers of complexity that rely on a multidisciplinary solution. For example, engineers focus upon more cost and energy effective methods of harvesting microalgae, whilst chemists seek to improve the quality of bio-diesel products from intracellular lipids to align with the required regulation for sale and economists compare the suitability of production facilities at different locations to generate the most viable and profitable industries. The biologist's role in this multidisciplinary approach is to understand the photosynthetic and central metabolic processes of the microalgae that underpins the whole process. This role is becoming increasingly important as a general trend in LCA simulations show that only certain locations globally are favorable for the cultivation processes (Tredici 2010). LCA use dynamic models to predict microalgal productivity. These predictions are based upon the response of microalgae to different system inputs such as light intensity, temperature and nutrient availability (Geider, MacIntyre & Kana 1998). Data collected from short-term laboratory based experiments can be used to better understand the relationship between biotic (microalgae) and abiotic (physical-chemical; e.g. light) variables. These relationships can then be described by mathematical models that are parameterised to derive values of interest (e.g. growth rate coefficients) and are then able to directly predict actual production. Dynamic microalgae models pose additional challenges in comparison to other model biological organisms (e.g. bacteria) due to the photosynthetic nature of microalgae cells (Bernard 2011). These inherent characteristics make these systems more difficult to predict because of their ability to acclimate to the different surroundings (e.g. changes in pigments, photoacclimation, as a response to light). Initial models for large-scale cultivation systems focused upon the light and nutrient environment (Bernard 2011), advancing to consider the effect of dark respiration (Béchet, Shilton & Guieysse 2013) and more recently temperature (Béchet et al. 2015). Despite these recent advances, the data used to validate these models are often derived from studies maintained under static laboratory conditions and do not account for microalgae acclimation to

changes in diel fluctuations of light and temperature. In order to better inform these predictive models, detailed time resolved data collected over both hourly and daily time-scales exposed to fluctuating environmental conditions is required (Huesemann et al. 2016). These types of datasets will provide more relevant parameter values that will help to improve the accuracy of production predictions.

1.5. Constraints in large-scale microalgae cultivations

1.5.1. Scale

Our global dependence, along with the commodity usage of crude oil, means that for any significant replacement of petroleum with a microalgae derived liquid biofuel, cultivation is essential at minimal cost over extremely large scales. For example, the current annual demand of crude oil in Australia is approximately 53 billion litres (Department of Industry Innovation and Science 2015). Conservative estimates of algae cultivation (Georgianna & Mayfield 2012) suggest a land area of 1 million hectares is required to produce enough bio-crude to meet current Australian demands for crude oil (approximately the size of Sydney). At such scales every step of the cultivation process must be close to optimal. Reactor design will dictate the capital investment required for infrastructure construction and maintenance (Lardon et al. 2009). The location of the facility dictates; light and temperature conditions, proximity and type of water sources, each in turn influencing microalgae strain selection. Quantities of nutrient inputs at this scale, especially nitrogen (N), phosphorus (P) and carbon (C), will cause both environmental and economic concerns (Borowitzka & Moheimani 2013c).

1.5.2. Reactor design and mode of operation constraints

A major decision for large-scale cultivation is the type of reactor design to use. For low-cost products such as biofuels, raceway ponds are used because of their relatively inexpensive construction costs and low energy maintenance demands (Béchet et al. 2011; Borowitzka 1999). Trade-offs of their open design mean that cultures are exposed to variable natural conditions such as temperature fluctuations, contamination from unwanted algae and other microorganisms (e.g. grazers and zooplankton) and high evaporation rates. Finally, the inherent design of a raceway pond does not facilitate maximal utilisation of bubbled CO₂. This is due to non-optimal mixing between the gas-water interface. As a result of the poor CO₂ utilisation, raceway systems have low productivities as well as excessive CO₂ usage (Sheenan et al. 1998).

Unlike raceway ponds, higher productivity is found in closed photobioreactors (PBRs) that can have up to a 13-fold greater volumetric biomass productivity (Chisti 2007), however typically closed PBR's have shown to be 2-3 times as productive (Raes et al. 2014). Closed PBRs require a greater amount of energy to maintain optimal conditions (e.g. temperature control, removal of oxygen buildup through bubbling with carbon dioxide and a pump to provide highly turbulent flow preventing sedimentation; Weissman et al. 1988). As a result of the increased complexity of a PBR, initial construction costs are greater than raceway ponds and are deemed not feasible for large-scale production of a cheap commodity such as biofuel.

Another constraint in both type of reactor designs is the effect of biofouling. Biofouling is the accumulation of foreign material (i.e. organic matter, bacteria, cyanobacteria, other microalgae, zooplankton and invertebrates) on the surfaces and in the medium of the reactor (Harris et al. 2013). These have significant costs if left untreated, biologically on culture productivities and financially through equipment maintenance. To date there is no solution to biofouling except careful experimentation and regular, comprehensive cleaning procedure the latter is costly and labour intensive (Schultz et al. 2011).

In addition to reactor design, the mode of reactor operation is important. Both types of reactors can be operated in the following modes; batch, continuous (turbidostat or chemostat) or semi-continuous (Mata et al. 2010). Each mode of operation has advantages and disadvantages; for example, continuous cultures allow for consistent production of biomass (daily) but its complex operation require expensive equipment set up and maintenance costs. Because of this, the type of reactor and mode of operation is determined by the market value of the final product. Batch and semi-continuous operation is favored in most outdoor large-scale microalgae facilities (Sheenan et al. 1998). The research completed in this thesis used batch cultivation throughout.

1.5.3. Algal strain selection

The selection of the optimal strain is often seen as the 'million dollar question' for a successful biofuel production facility. Microalgae are a highly diverse group of organisms with the capacity to survive in a range of environments. The diverse nature of different strains yield varied cellular components (**Table 1.2**). For example, *Chlorella sorokiniana* is able to grow rapidly because it is capable of doubling biomass every 4 hours; a maximum specific growth rate of 5.64 d^{-1} under optimal growth conditions (Lee

& Pirt 1981). In contrast, *Nannochloropsis* sp. have the capacity to accumulate up to 30% of their dry cell mass as intracellular lipids (Larkum et al. 2012). Due to these differences in inherent cell properties, the final biofuel product ultimately determines the strain cultivated, i.e. either lipid-derived (FAME) or biomass-derived ('green crude'). An additional consideration for large-scale cultivation is the water requirement of the alga. Since there is an increasing human demand upon diminishing freshwater resources, cultivation of marine strains for large-scale production is preferable (Borowitzka & Moheimani 2013c), but shortcomings should also be considered, such as evaporation resulting in increased salinity. Despite their varied environments, all microalgal strains have optimal conditions for their light and temperature (Schenk et al. 2008). Characterisation of these conditions will enable the selection of the appropriate strain for the appropriate cultivation location and final product.

Table 1.2 Biomass, lipid content and lipid productivity of different microalgae cultivated under continuous light at 25 °C, modified from Rodolfi et al. 2009.

Microalgae	Biomass productivity (g L ⁻¹ day ⁻¹)	Lipid content (% biomass)	Lipid productivity (mg L ⁻¹ day ⁻¹)
Marine strains:			
<i>Porphyridium cruentum</i>	0.37	9.5	34.8
<i>Tetraselmis suecica</i> (F&M-M33)	0.32	8.5	27.0
<i>Phaeodactylum tricornutum</i> (F&M-M40)	0.24	18.7	44.8
<i>Nannochloropsis</i> sp. (F&M-M26)	0.21	29.6	61.0
<i>Nannochloropsis</i> sp. (CS 246)	0.17	29.2	49.7
<i>Isochrysis</i> sp (T-ISO) (CS 177)	0.17	22.4	37.7
<i>Skeletonema</i> sp. (CS 252)	0.09	31.8	27.3
<i>Thalassiosira pseudonana</i> (CS 173)	0.08	20.6	17.4
<i>Chaetoceros muelleri</i> (F&M-M43)	0.07	33.6	21.8
Freshwater strains:			
<i>Scenedesmus</i> sp. (DM)	0.26	21.1	53.9
<i>Chlorella sorokiniana</i> (IAM-212)	0.23	19.3	44.7
<i>Monodus subterraneus</i> (UTEX 151)	0.19	16.1	30.4
<i>Chlorella vulgaris</i> (CCAP 211/11b)	0.17	19.2	32.6

1.5.4. External abiotic environmental factors

1.5.4.1. Light intensity

Light energy drives the photosynthetic process within a microalgae cell; the products of which provide precursors for the cells to synthesise biofuel molecules (**Figure 1.2**). The intensity of the irradiance (light energy) controls the rate of photosynthesis following a typical relationship exhibited by all microalgae species (**Figure 1.5**; Falkowski & Raven 2007).

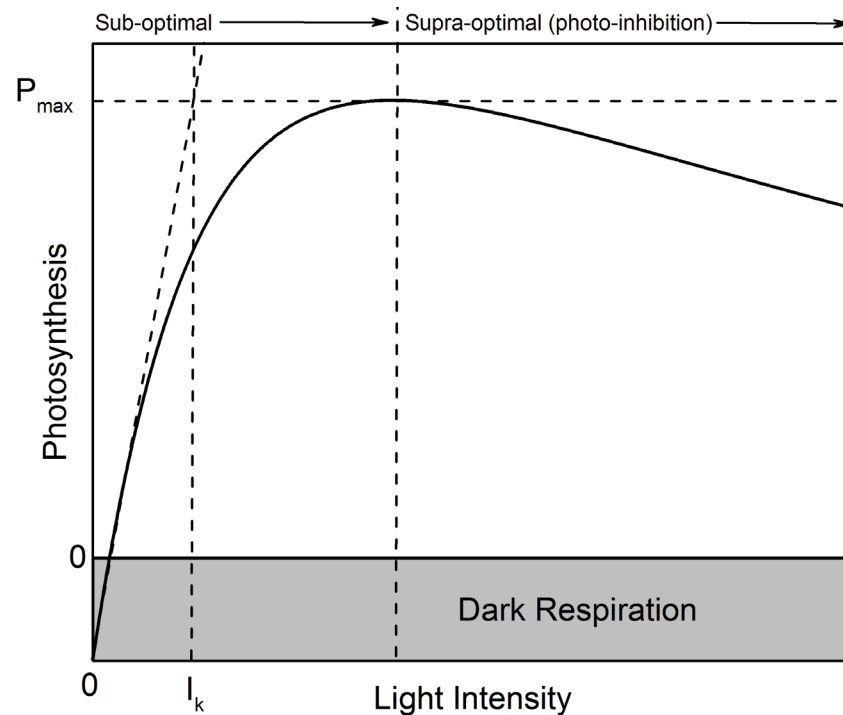


Figure 1.5 A typical photosynthesis vs. irradiance (light intensity) curve: A typical photosynthesis response curve where; shaded area is dark respiration, P_{\max} is maximum rate of photosynthesis, I_k is the half saturation irradiance.

Figure 1.5 shows regions of sub-/supra-optimal light intensities; here the irradiance is either too low or too high for maximal photosynthesis to occur. At sub-optimal intensities, photosynthesis is directly proportional to intensity and not sufficient for maximal photosynthesis. At supra-optimal intensities a reduction in photosynthesis occurs, linked to photoinhibition. If excessive and prolonged exposure to irradiance occurs this may result in irreversible cell damage (e.g. the damage (denaturing) of the D1 protein of PSII; Raven 2011). Other factors such as temperature, nutrient status, carbon-dioxide availability and cultivation history (photoacclimation) influence the nature of the photosynthesis-irradiance response (Eppeley 1972; Geider et al. 1998). The effect of light on photosynthetic rate is a strain-specific response; optimal light intensity can differ significantly between strains (Moore, Rocap & Chisholm 1998). For production at the scales required for biofuel production the cultivation will occur in outdoor environments (Weissman & Goebel 1987). Consequently, cultures will frequently experience sub-optimal light conditions throughout the cultivation process. Therefore, by understanding the underlying cellular mechanisms involved in adjusting to changing light conditions will assist with better management to minimise the associated detrimental effects on culture productivity.

1.5.4.2. Temperature

Outdoors, PBRs and shallow raceway ponds are susceptible to daily temperature fluctuations, in some cases experiencing diel changes between 10 °C and 45 °C (Belay 1997; Béchet et al. 2011). Temperature influences the physiology and biochemical properties of microalgae (Falkowski & Raven 2007). Enzyme-catalyzed reactions contribute to the majority of the reactions post-photosynthesis that culminate in the synthesis of biofuel 'precursors' molecules (e.g. intracellular lipids for lipid-derived biofuel or cell growth for biomass-derived biofuel). Supra-optimal temperatures are believed to primarily damage PSII (Berry & Bjorkman 1980) and in some cases have been demonstrated to inflict this damage via dissociation of manganese ions from the photocatalytic center (Allakhverdiev et al. 2008). These complex temperature interactions at subcellular scales impact overall microalgae growth rates, which can be described using an asymmetric bell-shape, see **Figure 1.6** (Eppley 1972; Schulte et al. 2011).

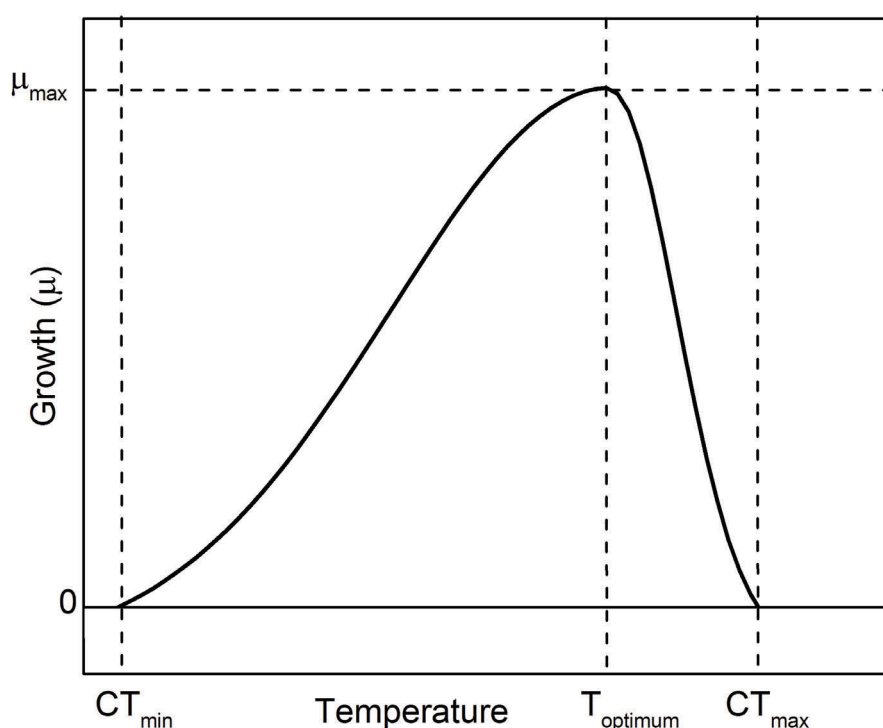


Figure 1.6 A typical growth rate vs. temperature response curve: A typical growth vs. temperature response curve; where $T_{optimum}$ is the temperature at which growth is maximal; CT_{min} - minimum critical temperature and CT_{max} - maximum critical temperature- below and above this temperature no algal growth is observed.

Growth rate increases with increasing temperatures from the minimum critical temperature (CT_{min}) until the thermal optimum ($T_{optimum}$), at this point, further increases in temperature result in a sharp decline in growth rate until the maximum critical temperature (CT_{max}).

The shape, magnitude and skew in the temperature-growth interaction is species-specific (Boyd et al. 2013). As a result, characterising the growth response of a biofuel candidate strain to different light and temperature conditions is the first step in understanding the capacity to be a successful biofuel strain. However, common laboratory experiments expose cultures to static, unnatural conditions, and only few have analysed the deviation in response when cultivated under diurnally fluctuating conditions (Renaud et al. 2002; Fabregas et al. 2004; Converti et al. 2009, Simionato et al. 2011). The combination of diel and seasonal changes of light and temperature conditions result in annual productivities constraining an economically viable biofuel industry (Borowitzka & Moheimani 2013b). However, the physiological responses of biofuel candidate algae have been scarcely examined under such conditions (Sukenic et al. 2009; Simionato et al. 2013; Tamburic et al. 2014). One of my thesis aims is to provide information on how microalgae respond to changing environments.

1.5.5. Nutrient supply

Microalgal elemental stoichiometry of C:N:P provides information about the macronutrient requirements of the strain. Whilst Redfield's ratio of 106:16:1 (C:N:P; Redfield 1958) provides a good starting point for understanding cellular elemental composition, it has been shown that this ratio is more dependent on the environmental conditions and species-specific requirements than previously thought (Geider & La Roche 2002). Inorganic N and P are acquired by a cell from the surrounding environments mostly through active transport via specific transporters in the plasmalemma (cell membrane), which is then assimilated into organic compounds within the cell (Raven 1984). Nitrogen plays a significant role in cellular biosynthesis and has an important structural function in the porphyrin ring of chlorophyll, an essential molecule in light harvesting and photosynthesis. Nitrogen-limitation has been shown to result in the accumulation of cellular lipids (Suen et al. 1987; Li et al. 2008; Gong et al. 2013), whereas, phosphorus is known to be the ultimate limiting element for microalgae growth in nature (Raven 2012). Phosphorus is a major building block in many cellular metabolites such as ATP which couples the light and dark reactions of photosynthesis and is involved in the cells capacity to assimilate carbon and nitrogen (Ticconi & Abel 2004).

It is estimated that up to 50 - 80 kg of nitrogen (N) and 5 kg of phosphate (P) are required to produce 1000 kg of algal biomass (Borowitzka & Moheimani 2013c), making the overall microalgae production process heavily reliant on the usage of fertilisers. The generation of nitrogen fertilisers is energy intensive and produces

significant amounts of CO₂, whilst phosphorus is mined from natural rock reserves that are estimated to be depleted within 100 - 400 years (Cordell, Drangert & White 2009; Fixen & Johnston 2012; Cordell & White 2014). Given that both sources are questionable in terms of their sustainability, it is clear that there is a need for alternative sources of fertilisers to secure a sustainable biofuel industry. As a result, we need to understand how we can supply these macronutrients in the quantities required to meet the physiological needs of the microalgae, the final product for the biofuel market, and at the same time, minimising the use of precious resources to ensure the sustainability of a microalgal biofuels industry.

1.5.6. Carbon supply

Carbon is an essential nutrient for microalgae to grow. In microalgae culture there are different chemical species of dissolved inorganic carbon (CO₂ (aq), HCO₃⁻ (aq), CO₃²⁻ (aq)) that are bioavailable for microalgae to use (Falkowski & Raven 2007). Inorganic carbon is taken into the cell via diffusion, where it is assimilated into biomass through the Calvin-Benson cycle (**Figure 1.2**). However, the concentration of carbon in atmospheric carbon dioxide (CO₂) of 0.039% (Kumar et al. 2010) which is too low to support dense cultures (Peng, Lan & Zhang 2013), despite many species containing cellular mechanisms to concentrate carbon (Giordano et al. 2005). The addition of CO₂ at higher than atmospheric concentrations is essential in order to achieve high productivities. It has been estimated that 1.8 kg CO₂ is fixed to produce 1 kg of algal biomass (Borowitzka & Moheimani 2013c). Because the production of a concentrated CO₂ source is expensive and energy-intensive, a large amount of research has focused upon using anthropogenic waste CO₂ sources (Michiki 1995; Ho, Chen & Chang 2012; Anjos et al. 2013), such as flue-gas from coal power stations and cement facilities providing an opportunity to mitigate industrial CO₂ emissions (Benemann 1997). A limiting factor with all reactor types is poor gas transfer rates (k_La). This is the rate at which gaseous CO₂ is dissolved into an aqueous state (Talbot et al. 1991), in an aqueous state the CO₂ is able to be utilised by the microalgae (Raeesossadati et al. 2014). An equally complex gas exchange problem is the super-saturation of oxygen in large-scale ponds which results in decreased biomass productivity (Moheimani & Borowitzka 2007; Peng, Lan & Zhang 2013). Overcoming practical constraints and the biological response of CO₂ supply is imperative in securing a future market for algal biofuels and is further explored within the scope of this thesis.

1.6. Summary

Continued commercial interest drives worldwide multi-disciplinary research to provide solutions to the current constraints that prevent the production of commodity biofuels. In the interim, the development of niche fuels (e.g. jet fuel) and production of high-value products (e.g. nutraceuticals) can stimulate development of effective algal production technologies and improve our understanding of the practicalities in large-scale management of algal production.

In order to develop an environmentally sustainable, economically viable, commercial scale cultivation system for the production of biofuel microalgae we need to provide a solution to the current issues that prevent viable production efficiencies. From a biological perspective, these issues mainly relate to the cultivation of microalgae at the large scales required to facilitate viable production efficiencies. These will require: (i) significant amounts of nutrients (N, P and CO₂); and (ii) cultivation outdoors in natural environments of fluctuating light and temperature conditions.

1.7. Thesis outline

My thesis investigates process constraints of large-scale cultivation of marine microalgae for biofuel production through the application of traditional physiological techniques along with use of an environmental photobioreactor (ePBR) platform. The ePBR platform allows for high resolution monitoring of simulated outdoor large-scale outdoor culture conditions. Physiological responses of the marine microalgae, biofuel candidate species, *Nannochloropsis oculata*, was assessed following exposure to a number of experimental conditions including: fluctuating light and temperature regimes; static thermal conditions; and various nutrient conditions to provide insights into how we can harness the physiological capacity of algae to improve its viability of cultivation for biofuel production.

The ePBR platform was used in **Chapter 2** to perform a multivariable design testing the effect of different light (square wave/sinusoidal) and temperature cycles (constant/sinusoidal) on growth rate, nutrient uptake and photosynthetic capacity of *N. oculata*. This experimental design allowed for comparison between laboratory-based studies and realistic outdoor (field) conditions to further understand the drivers behind growth rates and cellular yields obtained by large-scale cultivation.

Non-invasive fluorometric techniques are used in **Chapter 3** to advance our understanding of how the magnitude and duration of temperature change affects the

overall suitability of *N. oculata* cultivation at certain geographical locations. Time-resolved data acquired over a fine scale temperature range (15 - 40 °C) of growth and nutrient uptake capacity provide empirical data to better inform predictive production models and to assess whether algae traits can be used as 'early warning signs' to improve management practices in large-scale cultivation systems.

Further monitoring of functional traits in **Chapter 4** advances our understanding of how to effectively harness existing cellular mechanisms (e.g. acclimation) in order to reduce the nutrient input into large-scale cultivations. Here, the effect of different starting concentrations and ratios of macronutrients (nitrogen and phosphorus, compared with traditional f/2 concentrations and ratios) were explored and the affect upon growth rate, photosynthetic performance (photophysiology), nutrient uptake and quantity of lipid and quality of the final FAME product were analysed.

Chapter 5 aims to establish a scalable and transferable unit across various experimental designs and conditions for gas acquisition using the gas transfer of oxygen. Here the ePBR platform is used to describe the effect of different experimental set ups and physicochemical (such as salinity and pH) properties of the culture on the magnitude of gas transfer rates. Further experimental studies assessed the change in gas transfer rate through a growth cycle of *N. oculata* under laboratory and environmentally simulated conditions.

The general discussion (**Chapter 6**) summaries the key findings and highlights new insights on the process constraints involved in the large-scale microalgae cultivation for biofuel production. The implications for commercially viable microalgal biofuel production are evaluated and future research directions discussed.

1.8. General references

- Allakhverdiev, S., Kreslavski, V., Klimov, V., Los, D., Carpentier, R. & Mohanty, P. 2008, 'Heat stress: an overview of molecular responses in photosynthesis', *Photosynthesis Research*, vol. 98, no. 1, pp. 541–50.
- Anjos, M., Fernandes, B.D., Vicente, A.A., Teixeira, J.A. & Dragone, G. 2013, 'Optimization of CO₂ bio-mitigation by *Chlorella vulgaris*', *Bioresource Technology*, vol. 139, pp. 149–54.
- Australian Bureau of Statistics, . 2014, *9208.0 - Survey of Motor Vehicle Use*, Canberra, viewed 15 September 2015, <<http://www.abs.gov.au/ausstats/abs@.nsf/mf/9208.0/>>.
- Béchet, Q., Chambonnière, P., Shilton, A., Guizard, G. & Guieysse, B. 2015, 'Algal productivity modeling: A step toward accurate assessments of full-scale algal cultivation', *Biotechnology and Bioengineering*, vol. 112, no. 5, pp. 987–96.
- Béchet, Q., Shilton, A. & Guieysse, B. 2013, 'Modeling the effects of light and temperature on algae growth: state of the art and critical assessment for productivity prediction during outdoor cultivation.', *Biotechnology Advances*, vol. 31, no. 8, pp. 1648–63.
- Béchet, Q., Shilton, A., Park, J.B.K., Craggs, R.J. & Guieysse, B. 2011, 'Universal temperature model for shallow algal ponds provides improved accuracy.', *Environmental Science & Technology*, vol. 45, no. 8, pp. 3702–9.
- Belay, A. 1997, 'Mass culture of *Spirulina* outdoors- The Earthrise Farms experience', in A. Vonshak (ed.), *Spirulina platensis (Arthrospira): Physiology, Cell-biology and Biotechnology*, Taylor & Francis Ltd, London, pp. 131–58.
- Benemann, J.R. 1997, 'CO₂ mitigation with microalgae systems', *Energy Conversion and Management*, vol. 38, pp. S475-479.
- Bernard, O. 2011, 'Hurdles and challenges for modelling and control of microalgae for CO₂ mitigation and biofuel production', *Journal of Process Control*, vol. 21, no. 10, pp. 1378–89.
- Berry, D.A. 2010, 'Engineering organisms for industrial fuel production', *Bioengineered*, vol. 1, no. 5, pp. 303–8.
- Berry, J. & Bjorkman, O. 1980, 'Photosynthetic response and adaptation to temperature in higher plants', *Annual Review of Plant Physiology*, vol. 31, no. 1, article, pp. 491–543.
- Borowitzka, M.A. 1999, 'Commercial production of microalgae: ponds, tanks, tubes and fermenters', *Journal of Biotechnology*, vol. 70, no. 1, pp. 313–321.
- Borowitzka, M.A. & Moheimani, N.R. 2013a, 'Open Pond Culture Systems', in M.A. Borowitzka & N.R. Moheimani (eds), *Algae for Biofuels and Energy*, 1st edn., Springer Netherlands, Dordrecht, New York, pp. 133–52.
- Borowitzka, M.A. & Moheimani, N.R. 2013b, 'Sustainable biofuels from algae', *Mitigation and Adaptation Strategies for Global Change*, vol. 18, no. 1, pp. 13–25.
- Boyd, P.W., Ryneerson, T.A., Armstrong, E.A., Fu, F., Hayashi, K., Hu, Z., Hutchins, D.A., Kudela, R.M., Litchman, E., Mulholland, M.R., Passow, U., Strzepek, R.F., Whittaker, K.A., Yu, E. & Thomas, M.K. 2013, 'Marine phytoplankton temperature versus growth responses from polar to tropical waters--outcome of a scientific community-wide study.', *PloS One*, vol. 8, no. 5, p. e63091.
- Burlew, J.S. 1953, *Current status of the large-scale culture of algae*, J.S. Burlew (ed.), *Algal culture, From laboratory to pilot plant*, 1st edn, Carnegie Institution of Washington Publication 600, Washington DC.
- Chisti, Y. 2007, 'Biodiesel from microalgae', *Biotechnology Advances*, vol. 25, no. 3, pp.

294–306.

- Chisti, Y. 2008, 'Biodiesel from microalgae beats bioethanol.', *Trends in Biotechnology*, vol. 26, no. 3, pp. 126–31.
- Chisti, Y. 2013, 'Constraints to commercialization of algal fuels', *Journal of Biotechnology*, vol. 167, no. 3, pp. 201–14.
- Converti, A., Casazza, A.A., Ortiz, E.Y., Perego, P. & Del Borghi, M. 2009, 'Effect of temperature and nitrogen concentration on the growth and lipid content of *Nannochloropsis oculata* and *Chlorella vulgaris* for biodiesel production', *Chemical Engineering and Processing: Process Intensification*, vol. 48, no. 6, pp. 1146–51.
- Cordell, D., Drangert, J.-O. & White, S. 2009, 'The story of phosphorus: Global food security and food for thought', *Global Environmental Change*, vol. 19, no. 2, pp. 292–305.
- Cordell, D. & White, S. 2014, 'Life's bottleneck: sustaining the world's phosphorus for a food secure future', *Annual Review of Environment and Resources*, vol. 39, pp. 161–88.
- Demirbas, M.F., Balat, M. & Balat, H. 2009, 'Potential contribution of biomass to the sustainable energy development', *Energy Conversion and Management*, vol. 50, no. 7, pp. 1746–60.
- Department of Industry Innovation and Science 2015, *Resource and energy quarterly*, Canberra, pp. 1–71.
- Diesendorf, M. 2014, *Sustainable Energy Solutions for Climate Change*, 1st edn, NewSouth Publishing, Sydney.
- Eppeley, R.W. 1972, 'Temperature and phytoplankton growth in the sea', *Fishery Bulletin*, vol. 70, no. 4, pp. 1063–85.
- Escobar, J.C., Lora, E.S., Venturini, O.J., Yáñez, E.E., Castillo, E.F. & Almazan, O. 2009, 'Biofuels: Environment, technology and food security', *Renewable and Sustainable Energy Reviews*, vol. 13, no. 6–7, pp. 1275–87.
- Fábregas, J., Maseda, A., Domínguez, A., Ferreira, M. & Otero, A. 2002, 'Changes in the cell composition of the marine microalga, *Nannochloropsis gaditana*, during a light : dark cycle', *Biotechnology letters*, vol. 24, no. 20, pp. 1699–703.
- Fairley, P. 2011, 'Introduction: Next generation biofuels', *Nature*, vol. 474, no. 7352, pp. S2–5.
- Falkowski, P.G. & Raven, J.A. 2007, *Aquatic Photosynthesis*, 2nd edn., Princeton University Press, Princeton, NJ.
- Fixen, P.E. & Johnston, A.M. 2012, 'World fertilizer nutrient reserves: a view to the future', *Journal of the Science of Food and Agriculture*, vol. 92, no. 5, pp. 1001–5.
- Gao, X., Yu, Y. & Wu, H. 2013, 'Life cycle energy and carbon footprints of microalgal biodiesel production in Western Australia: A comparison of byproducts utilization strategies', *ACS Sustainable Chemistry and Engineering*, vol. 1, no. 11, pp. 1371–80.
- Geider, R. & La Roche, J. 2002, 'Redfield revisited : variability of C : N : P in marine microalgae and its biochemical basis', *European Journal of Phycology*, vol. 37, no. 1, pp. 1–17.
- Geider, R.J., MacIntyre, H.L. & Kana, T.M. 1998, 'A dynamic regulatory model of phytoplanktonic acclimation to light, nutrients, and temperature', *Limnology and Oceanography*, vol. 43, no. 4, pp. 679–94.
- Georgianna, D.R. & Mayfield, S.P. 2012, 'Exploiting diversity and synthetic biology for the production of algal biofuels', *Nature*, vol. 488, no. 7411, pp. 329–35.
- Giordano, M., Beardall, J. & Raven, J.A. 2005, 'CO₂ concentrating mechanisms in algae: Mechanisms, environmental modulation, and evolution', *Annual Review of*

- Plant Biology*, vol. 56, Annual Reviews, Palo Alto, pp. 99–131.
- Gong, Y., Guo, X., Wan, X., Liang, Z. & Jiang, M. 2013, 'Triacylglycerol accumulation and change in fatty acid content of four marine oleaginous microalgae under nutrient limitation and at different culture ages', *Journal of Basic Microbiology*, vol. 53, no. 1, pp. 29–36.
- Grima, E.M., Acien Fernández, F.G. & Chisti, Y. 1999, 'Photobioreactors : light regime, mass transfer and scaleup', *Journal of Biotechnology*, vol. 70, pp. 231–47.
- Harris, L., Tozzi, S., Wiley, P., Young, C., Richardson, T.-M.J., Clark, K. & Trent, J.D. 2013, 'Potential impact of biofouling on the photobioreactors of the Offshore Membrane Enclosures for Growing Algae (OMEGA) system', *Bioresource Technology*, vol. 144, article, pp. 420–8.
- Ho, S.-H., Chen, C.-Y. & Chang, J.-S. 2012, 'Effect of light intensity and nitrogen starvation on CO₂ fixation and lipid/carbohydrate production of an indigenous microalga *Scenedesmus obliquus* CNW-N.', *Bioresource technology*, vol. 113, pp. 244–52.
- Huesemann, M., Crowe, B., Waller, P., Chavis, A., Hobbs, S., Edmundson, S. & Wigmosta, M. 2016, 'A validated model to predict microalgae growth in outdoor pond cultures subjected to fluctuating light intensities and water temperatures', *Algal Research*, vol. 13, pp. 195–206.
- Kumar, A., Ergas, S., Yuan, X., Sahu, A., Zhang, Q., Dewulf, J., Malcata, F.X. & van Langenhove, H. 2010, 'Enhanced CO₂ fixation and biofuel production via microalgae: recent developments and future directions', *Trends in Biotechnology*, vol. 28, no. 7, pp. 371–80.
- Lane, J. 2014, 'Biofuel mandates around the world: 2015', *Biofuels Digest*, viewed 23 March 2015, <<http://www.biofuelsdigest.com/bdigest/2014/12/31/biofuels-mandates-around-the-world-2015/>>.
- Lardon, L., Hélias, A., Sialve, B., Steyer, J.-P. & Bernard, O. 2009, 'Life-cycle assessment of biodiesel production from microalgae', *Environmental Science & Technology*, vol. 43, no. 17, pp. 6475–81.
- Larkum, A.W.D., Ross, I.L., Kruse, O. & Hankamer, B. 2012, 'Selection, breeding and engineering of microalgae for bioenergy and biofuel production.', *Trends in biotechnology*, vol. 30, no. 4, pp. 198–205.
- Lee, Y.K. & Pirt, J. 1981, 'Energetic of photosynthetic alga growth: influences of intermittent illumination in short (40 s) cycles', *Journal of General Microbiology*, vol. 124, no. 1, pp. 43–52.
- Li, Y., Horsman, M., Wang, B., Wu, N. & Lan, C.Q. 2008, 'Effects of nitrogen sources on cell growth and lipid accumulation of green alga *Neochloris oleoabundans*', *Applied Microbiology and Biotechnology*, vol. 81, no. 4, pp. 629–36.
- Liu, X., Saydah, B., Eranki, P., Colosi, L.M., Greg Mitchell, B., Rhodes, J. & Clarens, A.F. 2013, 'Pilot-scale data provide enhanced estimates of the life cycle energy and emissions profile of algae biofuels produced via hydrothermal liquefaction', *Bioresource Technology*, vol. 148, pp. 163–71.
- Mata, T.M., Martins, A.A. & Caetano, N.S. 2010, 'Microalgae for biodiesel production and other applications: A review', *Renewable and Sustainable Energy Reviews*, vol. 14, no. 1, pp. 217–32.
- Michiki, H. 1995, 'Biological CO₂ fixation and utilization project', *Energy Conversion and Management*, vol. 36, no. 6–9, pp. 701–5.
- Milledge, J. & Heaven, S. 2013, 'A review of the harvesting of micro-algae for biofuel production', *Reviews in Environmental Science and Biotechnology*, vol. 12, no. 2, pp. 165–78.
- Milly, P.C.D., Dunne, K.A. & Vecchia, A. V 2005, 'Global pattern of trends in streamflow

- and water availability in a changing climate.', *Nature*, vol. 438, no. 7066, pp. 347–50.
- Moheimani, N.R. & Borowitzka, M.A. 2007, 'Limits to productivity of the alga *Pleurochrysis carterae* (Haptophyta) grown in outdoor raceway ponds', *Biotechnology and Bioengineering*, vol. 96, no. 1, pp. 27–36.
- Moore, L.R., Rocap, G. & Chisholm, S.W. 1998, 'Physiology and molecular phylogeny of coexisting *Prochlorococcus* ecotypes', *Nature*, vol. 393, no. 6684, pp. 464–7.
- Nigam, P.S. & Singh, A. 2011, 'Production of liquid biofuels from renewable resources', *Progress in Energy and Combustion Science*, vol. 37, no. 1, pp. 52–68.
- Peng, L., Lan, C.Q. & Zhang, Z. 2013, 'Evolution, detrimental effects, and removal of oxygen in microalga cultures: A review', *Environmental Progress & Sustainable Energy*, vol. 32, no. 4, pp. 982–8.
- Pickett, J., Anderson, D., Bowles, D., Bridgwater, T., Jarvis, P., Mortimer, N., Poliakov, M. & Woods, J. 2008, *Sustainable biofuels: prospects and challenges*, The Royal Society, London, UK.
- Pragya, N., Pandey, K.K. & Sahoo, P.K. 2013, 'A review on harvesting, oil extraction and biofuels production technologies from microalgae', *Renewable and Sustainable Energy Reviews*, vol. 24, pp. 159–71.
- Raesossadati, M.J., Ahmadzadeh, H., McHenry, M.P. & Moheimani, N.R. 2014, 'CO₂ bioremediation by microalgae in photobioreactors: Impacts of biomass and CO₂ concentrations, light, and temperature', *Algal Research*, vol. 6, pp. 78–85.
- Raes, E.J., Isdepsky, A., Muylaert, K., Borowitzka, M.A. & Moheimani, N.R. 2014, 'Comparison of growth of *Tetraselmis* in a tubular photobioreactor (Biocoil) and a raceway pond', *Journal of Applied Phycology*, vol. 26, no. 1, article, pp. 247–55.
- Rajagopal, D. & Zilberman, D. 2007, *Review of environmental, economic and policy aspects of biofuels*, World Bank Publication, The World Bank, Washington DC.
- Raven, J.A. 1984, 'A cost-benefit analysis of photon absorption by photosynthetic unicells', *New Phytologist*, vol. 98, no. 4, pp. 593–625.
- Raven, J.A. 2011, 'The cost of photoinhibition', *Physiologia Plantarum*, vol. 142, no. 1, pp. 87–104.
- Raven, J.A. 2012, 'Protein turnover and plant RNA and phosphorus requirements in relation to nitrogen fixation', *Plant Science*, vol. 188, pp. 25–35.
- Redfield, A.C. 1958, 'The biological control of chemical factors in the environment', *American Scientist*, vol. 46, no. 3, pp. 205–21.
- Renaud, S.M., Thinh, L.-V., Lambrinidis, G. & Parry, D.L. 2002, 'Effect of temperature on growth, chemical composition and fatty acid composition of tropical Australian microalgae grown in batch cultures', *Aquaculture*, vol. 211, no. 1–4, pp. 195–214.
- Robbins, M. 2011, 'Policy: Fuelling politics', *Nature*, vol. 474, no. 7352, pp. S22–4.
- Rodolfi, L., Chini Zittelli, G., Bassi, N., Padovani, G., Biondi, N., Bonini, G. & Tredici, M.R. 2009, 'Microalgae for oil: strain selection, induction of lipid synthesis and outdoor mass cultivation in a low-cost photobioreactor', *Biotechnology and Bioengineering*, vol. 102, no. 1, pp. 100–12.
- Schenk, P.M., Thomas-Hall, S.R., Stephens, E., Marx, U.C., Mussgnug, J.H., Posten, C., Kruse, O. & Hankamer, B. 2008, 'Second generation biofuels: high-efficiency microalgae for biodiesel production', *Bioenergy Research*, vol. 1, no. 1, pp. 20–43.
- Schulte, P., Healy, T. & Fanguy, N. 2011, 'Thermal performance curves, phenotypic plasticity, and the time scales of temperature exposure', *Integrative and Comparative Biology*, vol. 51, no. 1, pp. 691–702.
- Schultz, M.P., Bendick, J.A., Holm, E.R. & Hertel, W.M. 2011, 'Economic impact of biofouling on a naval surface ship', *Biofouling*, vol. 27, no. 1, article, pp. 87–98.

- Scott, S.A., Davey, M.P., Dennis, J.S., Horst, I., Howe, C.J., Lea-Smith, D.J. & Smith, A.G. 2010, 'Biodiesel from algae: challenges and prospects', *Current Opinion in Biotechnology*, vol. 21, no. 3, pp. 277–86.
- Sheenan, J., Dunahay, T., Benemann, J.R. & Roessler, P. 1998, *A look back at the U. S. Department of Energy's aquatic species program: biodiesel from algae*, National Renewable Energy Laboratory Report, Colorado.
- Simionato, D., Basso, S., Giacometti, G.M. & Morosinotto, T. 2013, 'Optimization of light use efficiency for biofuel production in algae', *Biophysical Chemistry*, vol. 182, pp. 71–8.
- Simionato, D., Sforza, E., Corteggiani Carpinelli, E., Bertucco, A., Giacometti, G.M. & Morosinotto, T. 2011, 'Acclimation of *Nannochloropsis gaditana* to different illumination regimes: effects on lipids accumulation.', *Bioresource technology*, vol. 102, no. 10, pp. 6026–32, viewed 21 January 2014, <<http://www.ncbi.nlm.nih.gov/pubmed/21429740>>.
- Stöcker, M. 2008, 'Biofuels and biomass-to-liquid fuels in the biorefinery: Catalytic conversion of lignocellulosic biomass using porous materials', *Angewandte Chemie International Edition*, vol. 47, no. 48, pp. 9200–11.
- Suali, E. & Sarbatly, R. 2012, 'Conversion of microalgae to biofuel', *Renewable and Sustainable Energy Reviews*, vol. 16, no. 6, pp. 4316–42.
- Suen, Y., Hubbard, J.S., Holzer, G. & Tornabene, T.G. 1987, 'Total lipid production of the green alga *Nannochloropsis* sp. QII under different nitrogen regimes', *Journal of Phycology*, vol. 296, no. s2, pp. 289–96.
- Sukenik, A., Beardall, J., Kromkamp, J.C., Kopecký, J., Masojídek, J., van Bergeijk, S., Gabai, S., Shaham, E. & Yamshon, A. 2009, 'Photosynthetic performance of outdoor *Nannochloropsis* mass cultures under a wide range of environmental conditions', *Aquatic Microbial Ecology*, vol. 56, no. 2–3, pp. 297–308.
- Talbot, P., Gortares, M.P., Lencki, R.W. & la Noüe, J. 1991, 'Absorption of CO₂ in algal mass culture systems: A different characterization approach', *Biotechnology and Bioengineering*, vol. 37, no. 9, pp. 834–42.
- Tamburic, B., Guruprasad, S., Radford, D.T., Szabó, M., Lilley, R.M., Larkum, A.W.D., Franklin, J.B., Kramer, D.M., Blackburn, S.I., Raven, J. a, Schliep, M. & Ralph, P.J. 2014, 'The effect of diel temperature and light cycles on the growth of *Nannochloropsis oculata* in a photobioreactor matrix.', *PloS One*, vol. 9, no. 1, p. e86047.
- Ticconi, C.A. & Abel, S. 2004, 'Short on phosphate: plant surveillance and countermeasures.', *Trends in Plant Science*, vol. 9, no. 11, pp. 548–55.
- Tredici, M.R. 2010, 'Photobiology of microalgae mass cultures: understanding the tools for the next green revolution', *Biofuels*, vol. 1, no. 1, pp. 143–62.
- Tsita, K.G. & Pilavachi, P.A. 2013, 'Evaluation of next generation biomass derived fuels for the transport sector', *Energy Policy*, vol. 62, pp. 443–55.
- United Nations 2015, 'Adoption of the Paris Agreement', *Framework Convention on Climate Change*, Paris, pp. 1–32.
- Vasudevan, V., Stratton, R.W., Pearlson, M.N., Jersey, G.R., Beyene, A.G., Weissman, J.C., Rubino, M. & Hileman, J.I. 2012, 'Environmental performance of algal biofuel technology options', *Environmental Science & Technology*, vol. 46, no. 4, pp. 2451–9.
- Weissman, J.C. & Goebel, R.P. 1987, *Desing and analysis of microalgal open pond systems for the purpose of producing fuels: a subcontract report*, Solar Energy Research Institute, US Department of Energy, Golden, CO.
- Weissman, J.C., Goebel, R.P. & Benemann, J.R. 1988, 'Photobioreactor design: Mixing, carbon utilization and oxygen accumulation', *Biotechnology and*

Bioengineering, vol. 31, no. 4, pp. 336–44.

Zittelli, G.C., Rodolfi, L., Bassi, N., Biondi, N. & Tredici, M. 2013, 'Photobioreactor for Microalgae Biofuel Production', in M.A. Borowitzka & N.R. Moheimani (eds), *Algae for Biofuels and Energy*, Springer Netherlands, Amsterdam, pp. 115–31.

Chapter 2 Laboratory to large-scale: A multi-trait comparison of *Nannochloropsis oculata* cultivated under static and dynamic environmental conditions.

Dale T. Radford¹, Chris Evenhuis¹, Kirralee G. Baker¹, Martin Schliep¹, John A. Raven^{1,2}, Milán Szabó^{1,3} and Peter J. Ralph¹

Affiliations

¹ Climate Change Cluster (C3), University of Technology Sydney, 2007 NSW, Australia

² Division of Plant Sciences, University of Dundee at the James Hutton Institute, Invergowrie, Dundee DD2 5DA, UK

³ Division of Plant Sciences, Research School of Biology, The Australian National University, Sullivans Creek Road, Acton, ACT 2601, Australia

Keywords

microalgae, light, temperature, diel fluctuations, sinusoidal, photobiology, biofuel, carbon limitation

Abbreviations

SqLSiT: square wave light- sinusoidal temperature

SiLCT: sinusoidal light- constant temperature

SiLSiT: sinusoidal light- sinusoidal temperature

rETR: relative electron transport rate

PSII: Photosystem II

ML: measuring light

SP: saturating pulse

pO_2 : dissolved oxygen concentration

2.1 Introduction

Diminishing reserves of fossil fuels coupled with increasing carbon dioxide emissions exemplifies the need for a sustainable and carbon-neutral fuel resource, and whilst solar, wind and tidal forms of renewable energy provide solutions for electricity, no suitable alternative for liquid fuel currently exists (Schenk et al. 2008). Biodiesel from microalgae provide a viable substitute compared with first/second generation biofuel feedstocks, showing potential to meet fuel demand, whilst minimising the impacts on food supply or other crop products (Chisti 2008).

At scales required to address consumer demands, industrial cultivation of microalgae under natural, outdoor conditions is required. These natural changes in abiotic conditions will ultimately dictate the amount of algal biomass that can be produced by a cultivation system which alters photosynthesis (Geider et al. 1998) and growth (Eppley 1972). Achieving optimal light is a 'balancing' act for microalgal cells; above optimal irradiance can result in inhibition of photosynthesis (photoinhibition) and potentially result in irreversible cell damage (Raven 2011), whilst insufficient light limits photosynthesis. Both conditions can reduce microalgal productivity. Temperature influences the ability of microalgae to photosynthesise (Davison 1991). For example, enzymatic reaction rates and electron transport are temperature-dependent (Raven & Geider 1988). Previous studies have analysed the effect of different constant temperatures on the ability of algae to grow (Converti et al. 2009). However, the examined ranges (20 to 30 °C) in these studies were constant and not realistic for large-scale microalgal cultivation where these are exposed to the weather and experience large seasonal fluctuations (Moheimani & Borowitzka 2007).

The majority of model predictions for efficiencies and yields of microalgae biofuel production have been based upon data obtained in the laboratory, using constant conditions that are not designed to simulate the real environment (Bernard 2011; Béchet et al. 2013). More recently, studies such as Tamburic et al. (2014) have simulated the effects of diel variation in temperature on the growth and photosynthetic capabilities of *Nannochloropsis oculata*. Algal growth was unaffected by the range of temperature fluctuations (15 to 25 °C) measured and are consistent with the use of this strain in outdoor cultivation systems. Despite these findings, it remains unclear how this biofuel candidate strain, *N. oculata*, will perform at temperature conditions outside this range. For example, at the cultivation locations deemed to be most suitable for biofuel microalgae production in Australia (north-west coast of Western Australia;

Borowitzka et al. 2012), where daily average temperatures are approximately 30 °C (BOM 2016). Furthermore, it is unknown how combinations of different environmental stress conditions affect the final product amount and quality (cell composition), especially diel changes in light and temperature; the magnitude and duration of which are unavoidable in outdoor cultivation and are not commercially viable to implement mitigation solutions (Borowitzka & Moheimani 2013b).

To improve the modeling of algal productivity of large-scale cultivation systems, empirical data derived from a factorial comparison of light and temperature environments where each factor is either constant or fluctuating is required (Béchet, Shilton & Guieysse 2013; Béchet et al. 2015; Huesemann et al. 2016). Due to the complexity of these types of experimental designs, inherent variation associated with optics, instrumental geometry and overall experimental systems makes it difficult to discriminate the biological response from the experimental setup and to ensure reproducibility between laboratories (Riebesell et al. 2010). To overcome these challenges, a standard platform is required, which consists of an array of unified high throughput control and analysis units. Such a standard platform is a matrix arrangement of environmental photobioreactors (ePBR) that can be used to imitate dynamic environmental conditions (e.g. diel fluctuations in temperature and light). By analysing the response of microalgae to these different conditions through parameters such as cell yield, growth and photosynthetic productivity provides high resolution data to allow for accurate comparisons under dynamic conditions (Lucker et al. 2014). Using this design, the effects of both irradiance (e.g. 0 - 2000 $\mu\text{mol photons m}^{-2} \text{s}^{-1}$) and temperature (e.g. 10 – 40 °C) upon algal photosynthesis and growth could be tested to provide further insight into the predictability and reliability as a biofuel microalgae when cultivated outdoors.

This study used environmental photobioreactors to replicate relevant outdoor environmental conditions, whilst allowing experiments to be performed in the laboratory without the large capital costs associated with constructing a pilot facility (Lucker et al. 2014; Tamburic et al. 2014). *N. oculata* was chosen as a model organism, as it has a naturally high content of lipids (Rodolfi et al. 2009), the ability to tolerate a wide range of environmental conditions (pH, salinity, etc.) and potential for genetic manipulations; making it the ideal candidate strain for large-scale biofuel production (Kilian et al. 2011). Conditions used here allow for comparison between laboratory-based studies and realistic outdoor (field) conditions to further understand the environmental drivers behind the growth rates and cellular yields obtained by large-scale cultivation

(Borowitzka & Moheimani 2013a). This study monitors the dynamics and plasticity of growth and photophysiological response of *N. oculata* throughout light: dark cycles over a single batch growth cycle.

2.2 Materials and Methods

2.2.1 Microalgal Cultures and medium

Nannochloropsis oculata (Droop) Green (CS-179) was obtained from the ANACC (Australian National Algae Culture Collection, CSIRO, Hobart, Australia) and grown in f/2 media (0.2 μm filtered artificial seawater enriched with; 8.82×10^{-4} M NaNO_3 ; 3.62×10^{-5} M, $\text{NaH}_2\text{PO}_4 \cdot \text{H}_2\text{O}$; trace metal solution and vitamin solution; Guillard & Ryther 1962).

2.2.2 Photobioreactor set-up

N. oculata was cultured in cylindrical photobioreactors (ePBR™ v1.1, Phenometrics, Lansing, MI, USA) with a 450 mL working volume (**Supplementary Figure 2.1**). *N. oculata* cultures were exposed to four different light and temperature treatments; square wave light- constant temperature (SqLCT), square wave light- sinusoidal temperature (SqLSiT), sinusoidal light- constant temperature (SiLCT) and sinusoidal light- sinusoidal temperature (SiLSiT). All PBRs were illuminated with LEDs, providing steady white light across the PAR region, 400 to 700 nm (Tamburic et al. 2014) under a 12 h: 12 h light: dark cycles. Irradiance regimes were either square wave, with constant irradiance of $1240 \mu\text{mol photons m}^{-2} \text{s}^{-1}$ or sinusoidal, where the irradiance ranged from 0 to $2000 \mu\text{mol photons m}^{-2} \text{s}^{-1}$, with maximum light intensity occurring at midday. This design allowed for all treatments to receive equal total quanta during each light phase. Two different temperature treatments were used; constant at $25^\circ\text{C} \pm 0.5^\circ\text{C}$ and sinusoidal ranging between a minimum of $20^\circ\text{C} \pm 0.5^\circ\text{C}$ and maximum of $30^\circ\text{C} \pm 0.5^\circ\text{C}$, with the peak temperature occurring around dusk (**Figure 2.1**). In order to mimic an outdoor cultivation system as closely as possible, no aeration was provided but a magnetic stirrer was used to ensure a well-mixed culture that allowed for homogeneity of invasive (e.g. cell counts) and non-invasive (e.g. fluorescence measurements) sample collection, that in turn assured accuracy of auxiliary data collection. Temperature and dissolved oxygen were measured continuously in all ePBRs using temperature probes (Phenometrics, Lansing, MI, USA) and dissolved oxygen bare fibre minisensors (OXB430-OI; Firesting O_2 , Pyroscience, Aachen, Germany), where $p\text{O}_2$ as a function of time was used as a proxy of photosynthesis.

Prior to experimental data collection, all *N. oculata* cultures were maintained in the ePBRs under semi-continuous growth to acclimate the cultures to the ePBR conditions. All experimental cultures were operated in triplicate ($n=3$) in batch mode.

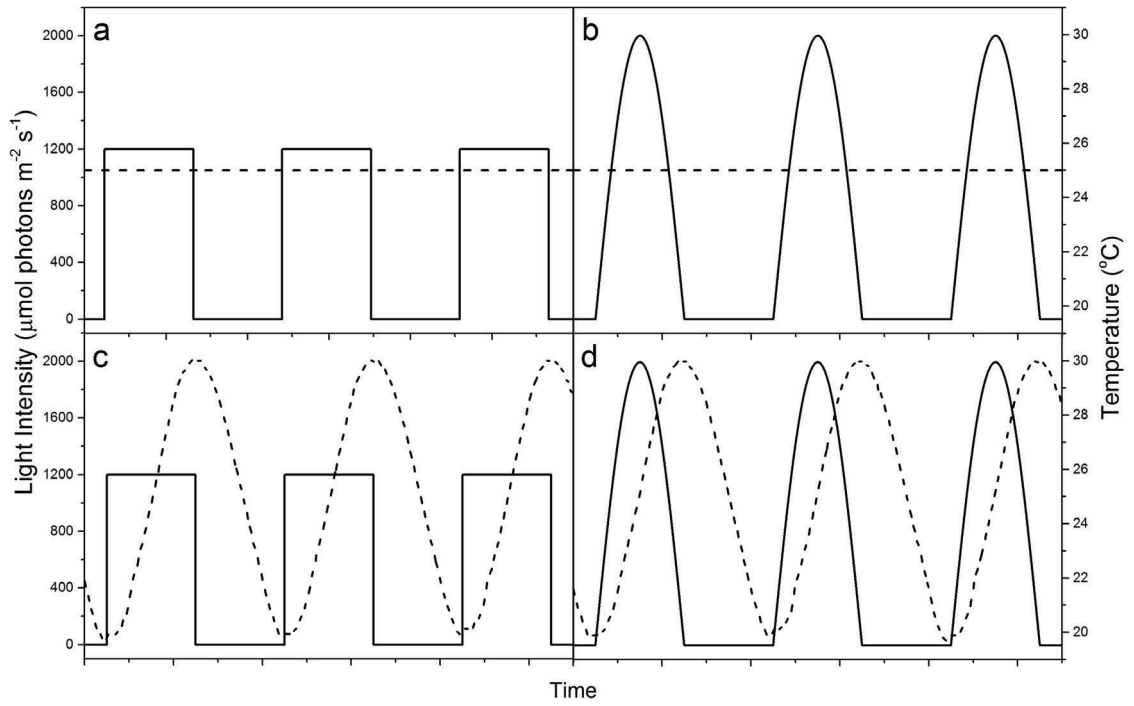


Figure 2.1: Experimental ePBR setup: (a) square wave light, constant temperature regime (b) square wave light, sinusoidal temperature regime, SqLSiT, (c); sinusoidal light, constant temperature regime, SiLCT, (d) sinusoidal light, sinusoidal temperature regime, SiLSiT. Lines represent light intensity (solid line) and temperature (broken line). All irradiance cycles were 12 h: 12 h light: dark cycles of square-wave light ($1240 \mu\text{mol photons m}^{-2} \text{s}^{-1}$), sinusoidal light 0 to $1920 \mu\text{mol photons m}^{-2} \text{s}^{-1}$, with peak irradiance occurring at midday. Temperature cycles were as follows, constant $25^\circ\text{C} \pm 0.5^\circ\text{C}$ and sinusoidal temperature fluctuating between $20 - 30^\circ\text{C}$ with peak temperature occurring at dusk.

2.2.3 Growth measurements

1 mL sub-samples per PBR were harvested and stored in Lugol's solution (Lovegrove 1960) 1% (v/v) final concentration. Cell counts were performed using a haemocytometer with a depth of $100 \mu\text{m}$ (Marienfeld- Superior, Neubauer improved, bright-line) and images were captured using an automated microscope set to capture at least 20 images per haemocytometer chamber (Ti-E, Nikon, x20 magnification). Images were processed and analysed using a user-defined script in the image analysis software, Fiji (Schindelin et al. 2012; Suggett et al. 2015). Over 400 cells were counted per sample to provide a 0.95 confidence interval of about 10% (Lund et al. 1958). To calculate growth rates the cell density data were fitted using the non-linear logistic model:

$$P(t) = \frac{a}{1 + e^{-k(t-t_c)}} \quad \text{(Equation 2.1)}$$

where, P is the cell density, a is maximum cell density, t is the time and k is the growth rate for the replicates of each different treatment.

2.2.4 Fluorescence measurements

In vivo chlorophyll fluorescence parameters were determined using a pulse amplitude-modulated chlorophyll fluorometer (Pocket-PAM, Walz, Effeltrich, Germany). This was performed by placing the Pocket-PAM head on the side of the vessel (10 cm from its base), providing a saturation pulse of light and analysing fluorescence parameters. Relative electron transport rate (rETR) was calculated using the following equation:

$$rETR = PAR \times \frac{F_M' - F'}{F_M'} \quad \text{(Equation 2.2)}$$

where, *PAR* is the incoming irradiance at the surface of the culture (PBR) and $(F_M' - F')/F_M'$ describes effective quantum yield of photosystem II in the light, in which, F' is minimal fluorescence, when all PSII reaction centers are open and F_M' is maximum fluorescence when all PSII reaction centers are closed (Schreiber et al. 1994). The Pocket-PAM settings were; measuring light (ML) intensity of $\sim 0.2 \mu\text{mol photons m}^{-2} \text{s}^{-1}$ PAR (ML setting 7), saturation pulse (SP) intensity $2600 \mu\text{mol photons m}^{-2} \text{s}^{-1}$ PAR (SP setting 12) and a block saturation pulse width of 0.8 s. Both ML and SP were provided by a blue LED source.

2.2.5 Nutrient analysis

Nitrate (NO_3^-), and orthophosphate (PO_4^{3-}) concentrations in the culture medium were determined in the supernatant following the centrifugation of 5 mL sample and subsequent filtration ($0.45 \mu\text{m}$, Minisardt, Supleco, Bellefonte, PA, USA,) to remove any residual cellular debris. Samples were then analysed using an automated ion analyser (Lachat QuickChem QC8500; Lachat Instruments, Milwaukee, WI, USA). The samples were analysed spectrophotometrically according to QuikChem Methods; 31-107-05-1-A and 31-115-01-1-G for NO_3^- and PO_4^{3-} , respectively.

Briefly, nitrite (NO_2^-) was diazotised (introduction of a diazo group [$\text{N}^+ \equiv \text{N}$]) under acidic conditions with sulfanilamide to form a diazonium ion. The resulting ion reacts with N-(1-naphthyl)ethylenediamine dihydrochloride to form a pink dye which absorbs at 520 nm, where the absorbance is proportional to the concentration of nitrite in the sample.

To determine NO_3^- , samples were reduced to NO_2^- by the passage of the sample through a cadmium column. The resulting NO_2^- was then determined according to the method described above. NO_3^- concentrations were then obtained by subtracting the NO_2^- values (previously determined) from the $\text{NO}_2^- + \text{NO}_3^-$ values (reduced using cadmium column). The limit of detection in both NO_2^- and NO_3^- analysis is $10 \mu\text{g N/L}$.

PO_4^{3-} was determined by reacting the sample under acidic conditions with ammonium molybdate and antimony potassium tartrate. As a result a blue complex is formed which absorbs light at 880 nm. The absorbance value at 880 nm is proportional to the concentration of PO_4^{3-} in the sample, the limit of detection of the analysis is 0.3 $\mu\text{g P/L}$.

Nutrient uptake rates were calculated from the linear region of nutrient removal and the time at which the regression crossed the x-axis was determined to be when culture became nutrient deplete.

2.2.6 *Sampling regimes*

Daily cell counts were performed at 09:00 h. A pilot study was completed to pre-determine days that best represented lag, exponential and stationary growth. Based on these findings, sampling was performed on lag phase (day 1), exponential phase (day 4) and stationary phase (day 13). *In vivo* chlorophyll fluorescence measurements were performed at 05:45, 06:15, 09:00, 12:00, 15:00, and 17:45. Samples for nutrient analysis were taken at 06:00, 12:00 and 18:00.

2.2.7 *Statistical analysis*

Comparisons of growth rate, final cell abundance and nutrient uptake rates were performed by one-way analysis of variance (ANOVA). The growth rate data were non-normal when analysed using a Shapiro-Wilks test, and were subsequently log-transformed. If the ANOVA result was significant ($p < 0.05$), a Tukey's Post Hoc Analysis was performed on the comparisons between means. All statistical analyses were computed using OriginPRO 2015 software (version b9.2.272).

2.3 Results

2.3.1 Growth of *N. oculata* at different light and temperature regimes

Cell density was used as a proxy for biomass. The greatest growth rate ($0.727 \pm 0.250 \text{ d}^{-1}$) of *N. oculata* was achieved when cultivated under square wave light and sinusoidal temperature (SqLSiT; **Table 2.1**). Other treatments had reduced growth rates that were not statistically different (one way ANOVA; $\text{df} = 3$, $p = 0.489$) of $0.521 \pm 0.097 \text{ d}^{-1}$, $0.531 \pm 0.123 \text{ d}^{-1}$ and $0.534 \pm 0.111 \text{ d}^{-1}$ for SqLCiT, SiLCT and SiLSiT, respectively. As a result of the high variability within treatments, statistically significant differences in final cell abundance were only found between SqLCT and SiLCT ($p = 0.048$). In general the SqL treatments attained ~30% higher yield compared with SiL with a final cell abundance of $2.22 \times 10^7 \text{ cells mL}^{-1}$ and $2.07 \times 10^7 \text{ cells mL}^{-1}$ in comparison to 1.47×10^7 and $1.56 \times 10^7 \text{ cells mL}^{-1}$, respectively. **Figure 2.2** provides daily cell numbers used to calculate the growth rates and yield data provided in **Table 2.1**.

Table 2.1 Growth rate of *N. oculata* grown under square wave light, constant temperature (SqLCT) square wave light, sinusoidal temperature (SqLSiT); sinusoidal light, constant temperature (SiLCT) and sinusoidal light, sinusoidal temperature (SiLSiT). μ , growth rate expressed in d^{-1} and final cell abundance expressed as 10^7 cells per mL. Values are mean ± 1 SD ($n=3$) calculated using derived parameters from a non-linear logistic fit of individuals in each treatment. Asterisks correspond to the differences between treatments (one way ANOVA with post hoc Tukeys $p < 0.05$).

Treatment	μ (cell d^{-1})	Final Cell abundance ($\times 10^7$ cells mL^{-1})
SqLCT	0.531 ± 0.041	$2.22 \pm 0.150^*$
SqLSiT	0.727 ± 0.250	2.06 ± 0.288
SiLCT	0.567 ± 0.076	$1.48 \pm 0.062^*$
SiLSiT	0.539 ± 0.176	1.56 ± 0.452

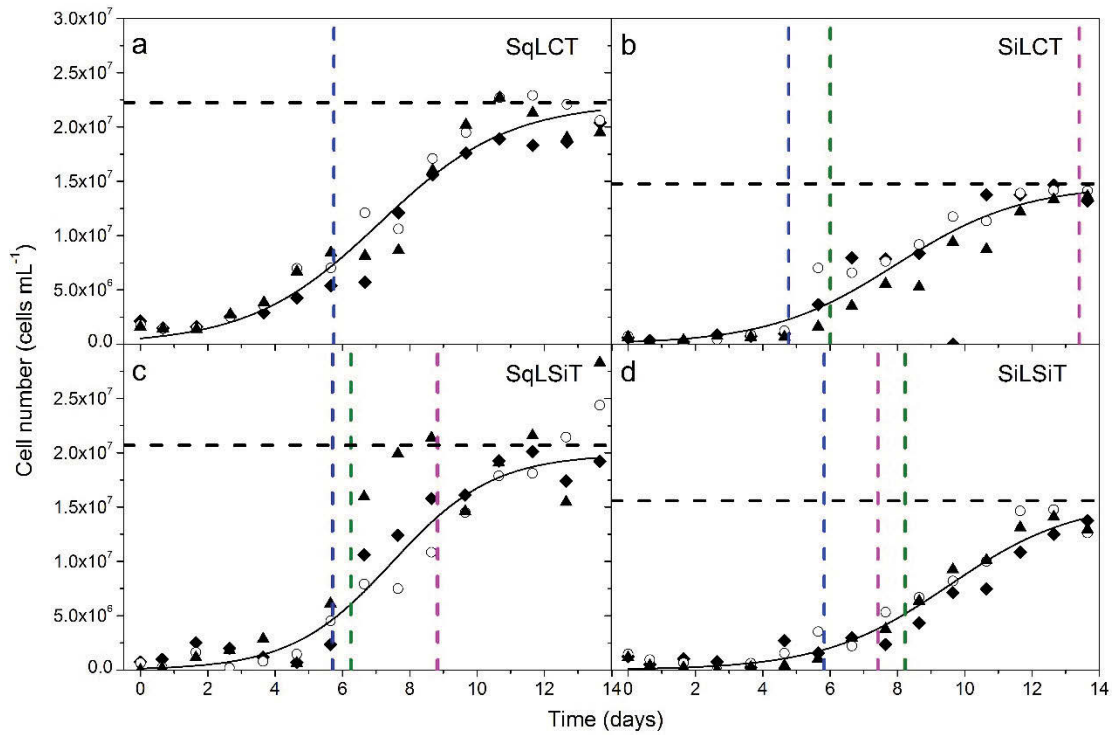


Figure 2.2 Growth measurements: Cell abundance of *N. oculata* when cultivated in a ePBR under (a) square wave light, constant temperature, SqLCT (b) sinusoidal light, constant temperature regime, SiLCT, (c) square wave light, sinusoidal temperature regime, SqLSiT, and (d) sinusoidal light, sinusoidal temperature regime, SiLSiT. Symbols represent values for each replicate within each treatment; solid line represents the concatenated logistic fit ($n=3$) fitting using non-linear regression algorithm (OriginPRO 2015). The vertical coloured broken line represents the time at which, maximum oxygen concentration (blue), minimal residual nitrate (magenta), minimal residual orthophosphate (green) occurred. The dashed horizontal black line represents the predicted maximum cell number derived from the logistic fit.

2.3.2 Nutrient limitation in simulated environmental growth

In order to understand differences between potential limitations due to inorganic carbon availability and nutrient requirements between environmental regimes, pO_2 concentrations and residual nitrate and orthophosphate amounts were measured throughout the growth period. *In situ* pO_2 concentrations plotted as a function of time during the diel cycles can provide a proxy for photosynthesis activity. *In situ* pO_2 concentrations were found to fluctuate throughout the diel cycle (**Figure 2.3**) and over the culture period. Maximum pO_2 values occurred between day 5 and 6 for all treatments (denoted blue line in both **Figure 2.2** and **Figure 2.3**) and declined towards stationary growth (day 14). Concurrent with this decrease in daily maximum pO_2 , a daily hysteresis was observed in all treatments.

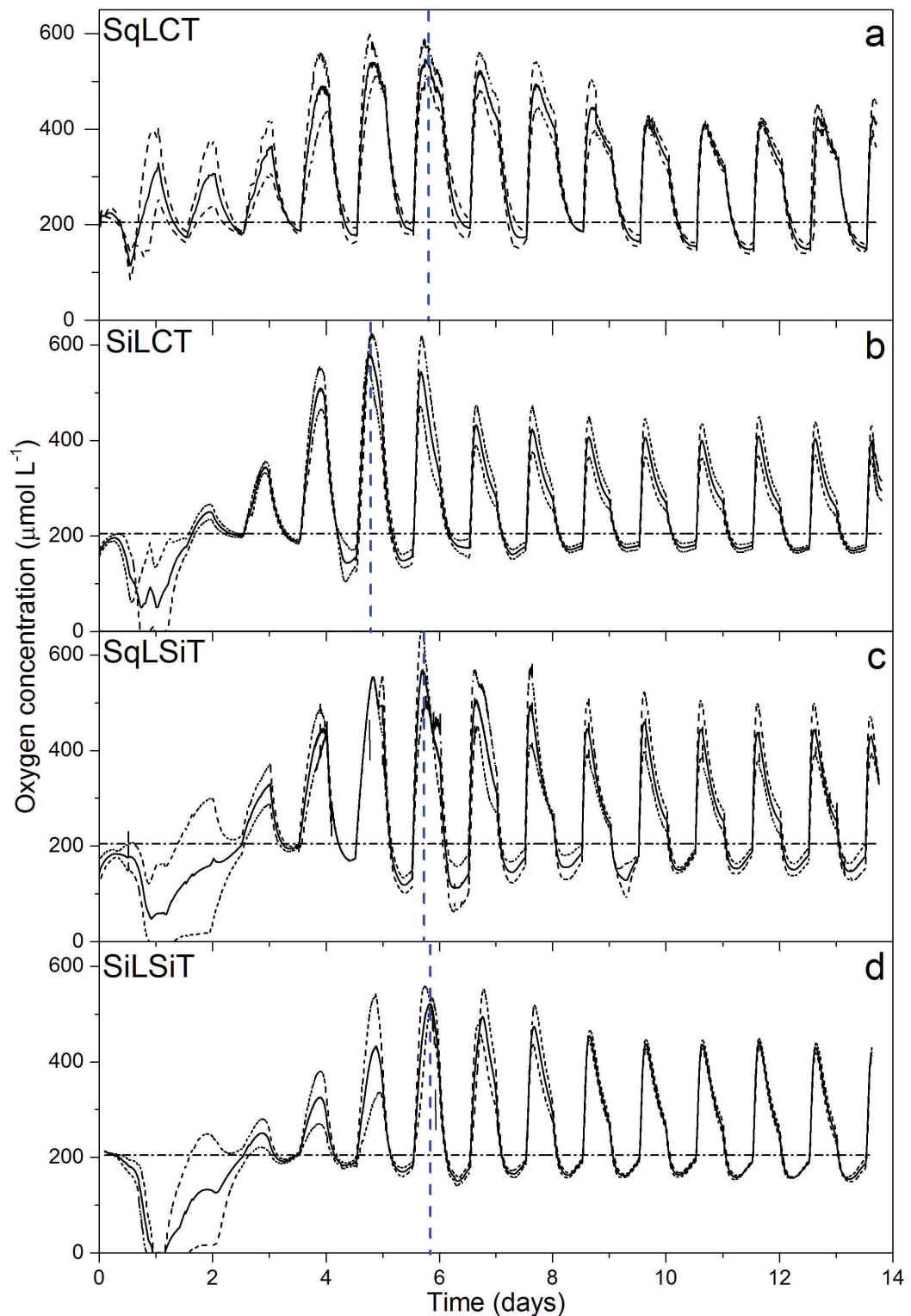


Figure 2.3 $p\text{O}_2$ profiles: *In situ* dissolved oxygen profiles of *N. oculata* when exposed to; (a) square wave light, constant temperature regime, SqLCT, (b) sinusoidal light, constant temperature regime, SiLCT (c) square wave light, constant temperature regime, SqLCT and (d) sinusoidal light, sinusoidal temperature regime, SiLSiT. Lines represent the average of 3 replicates (solid line) $n=3$, average \pm standard deviation (broken line) and a baseline (horizontal dotted line). The baseline value corresponds to the solubility of oxygen in seawater at 25 °C and 1 bar pressure. Dashed vertical lines correspond to the maximum oxygen concentration throughout growth.

Nutrient depletion among treatments occurred at different times during growth. This study defines nutrient depletion when minimal residual nutrients remain within the media (**Figure 2.2**, magenta or green dotted line; **Figure 2.4**). In all treatments, orthophosphate became depleted before nitrate and in one treatment (SiLCT) nitrate was not completely depleted (**Figure 2.4c**). There were no observed significant differences in nitrate uptake rate between treatments tested (**Table 2.2**), whilst SiLSiT exhibited significantly decreased orthophosphate uptake of $151 \pm 16.4 \mu\text{g L}^{-1} \text{d}^{-1}$ ($p < 0.05$).

Table 2.2 Nutrient uptake kinetics of *N. oculata* grown under square wave light, constant temperature (SqLCT) square wave light, sinusoidal temperature (SqLSiT); sinusoidal light, constant temperature (SiLCT) and sinusoidal light, sinusoidal temperature (SiLSiT). Nutrient uptake rates are expressed as $\mu\text{g L}^{-1} \text{d}^{-1}$ where values are mean \pm 1 SD (n=3) calculated using derived parameters from a linear fit of individual replicates. Asterisk correspond to the differences between treatments (one way ANOVA with post hoc Tukeys $p < 0.05$).

Treatment	Nitrate uptake ($\mu\text{g L}^{-1} \text{d}^{-1}$)	Orthophosphate uptake ($\mu\text{g L}^{-1} \text{d}^{-1}$)
SqLSiT	410 ± 125	223 ± 34.0
SiLCT	431 ± 78.0	245 ± 19.1
SiLSiT	618 ± 225	$154 \pm 16.4^*$

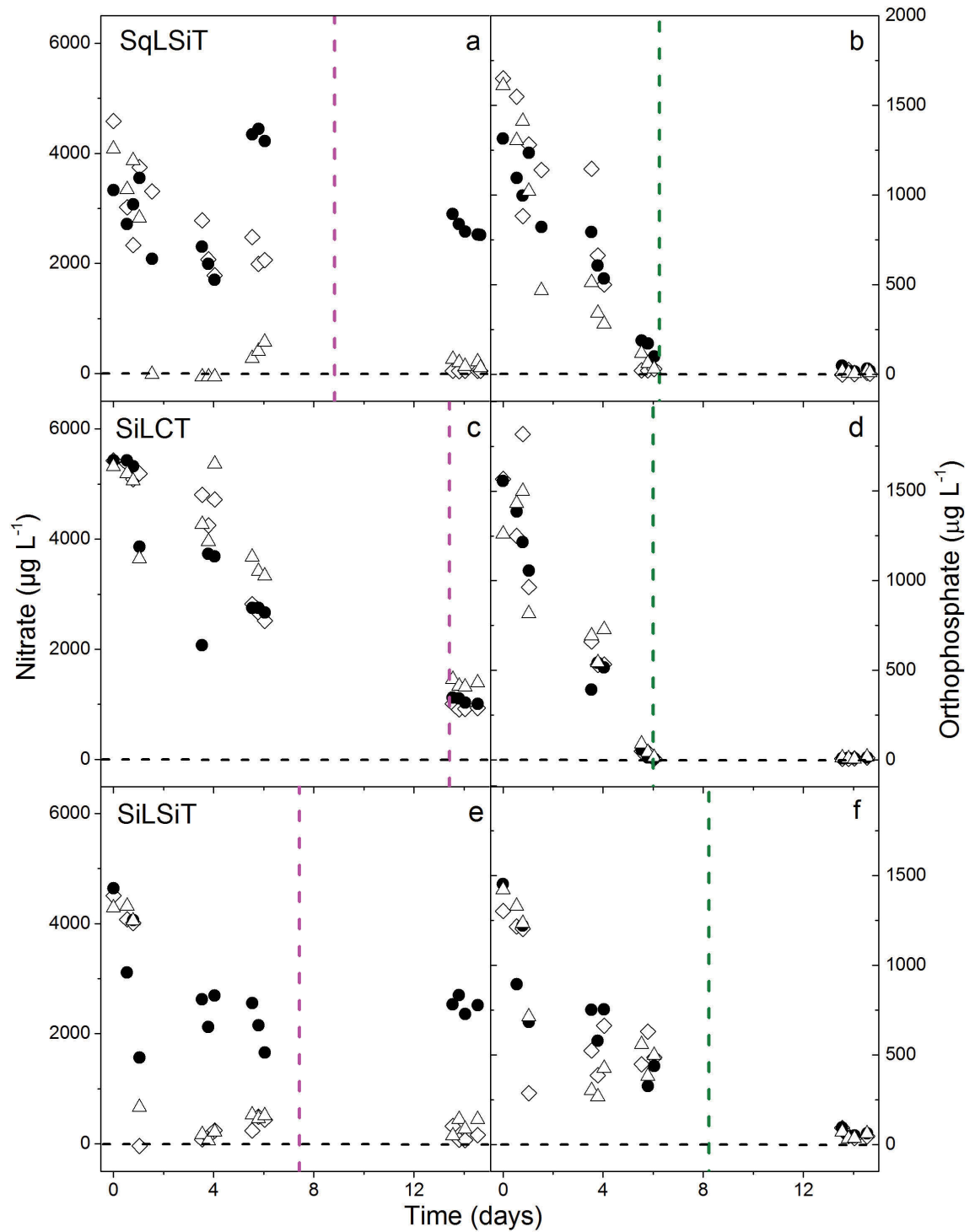


Figure 2.4 Dissolved nutrient concentrations: Concentration of dissolved nitrate (a, c, e) and orthophosphate (b, d, f) throughout time in experiments carried out with *N. oculata* under square wave light, sinusoidal temperature regime, SqLSiT (a, b) sinusoidal light, constant temperature regime, SiLCT (c, d) and sinusoidal light, sinusoidal temperature regime, SiLSiT (e, f). The concentrations are expressed in $\mu\text{g L}^{-1}$ each data point is represents and individual replicate, horizontal broken line represents 0 $\mu\text{g L}^{-1}$. Vertical broken lines correspond to time at which predicted minimal residual nutrient or minimal nitrate (magenta) and orthophosphate (green) nutrient amount occurred.

2.3.3 *Relative photosynthetic electron transport rate*

In order to analyse photosynthesis in greater detail for cells at different growth stages, relative electron transport rate (rETR) was plotted along *in situ* pO_2 concentrations (**Figure 2.5**). During the exponential growth phase an increase in rETR occurs when cells were cultivated under square wave light (**Figure 2.5a**), whereas under sinusoidal irradiance the rETR follows the trend of incident irradiance (**Figure 2.5c, e**). For all samples in this growth phase, the pO_2 concentration increased linearly up until approximately midday where a decreased rate of pO_2 accumulation occurred. In late afternoon a decrease in pO_2 was observed, being more pronounced in the sinusoidal light treatments.

The observed response of rETR and pO_2 in the stationary phase showed different trends. Under square wave light conditions, the rETR decreased over the light phase (**Figure 2.5b**), whereas both sinusoidal light treatments showed increased rETR at mid-morning (09:00) and subsequently decreased over the remainder of the light phase (**Figure 2.5f, g**). The pO_2 responses between treatments were somewhat similar, at the onset of light; there is an increase in pO_2 until approximately 08:30 - 09:00 where the daily maximum oxygen concentration occurred after which a decrease and apparent hysteresis occurred.

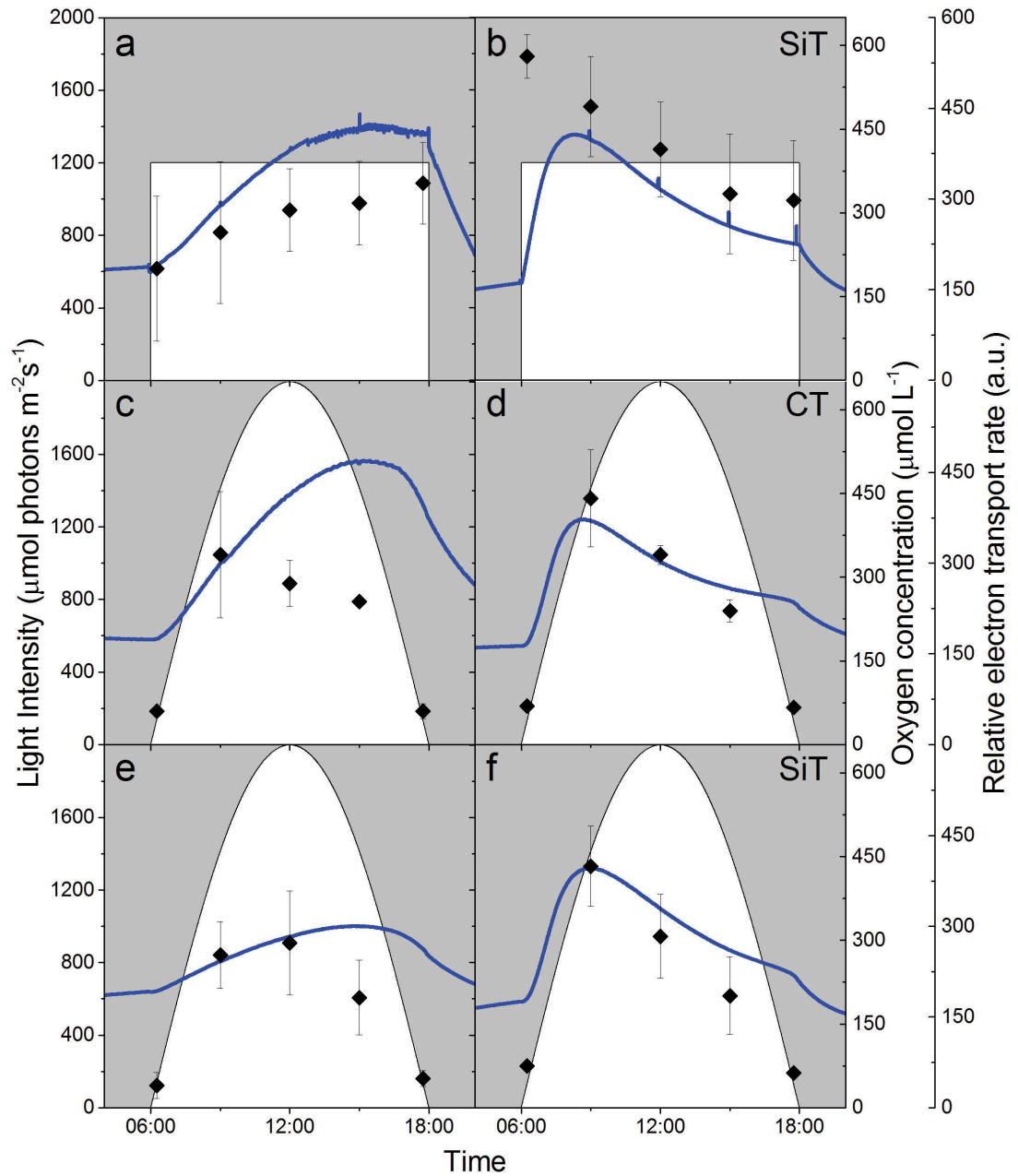


Figure 2.5 Dynamic oxygen and photophysiological response of *N. oculata*: Relative electron transport rate and *in situ* pO_2 profiles of *N. oculata* when cultivated under different light and temperature regimes; (a, b) square wave light, sinusoidal temperature, SqLSiT; (c, d) sinusoidal light, constant temperature, SiLCT and (e, f) sinusoidal light, sinusoidal temperature regime, SiLSiT. Measurements were recorded at early exponential (a, c, e) and stationary phase (b, d, f). Solid diamonds and lines represent the average of 3 replicates relative electron transport rate and *in situ* dissolved oxygen profiles (blue line); error bars represent standard deviation (n=3). The solid white area represents the light intensity at the surface of the culture.

2.4 Discussion

In this study, we provided evidence supporting the hypothesis that diel light variation contributes to reduced microalgae yields in outdoor cultivation systems, and may explain the differential yields observed in comparison to cultures grown in the laboratory. In general, the response of growth rates to fluctuating light have been shown to be species- and light intensity-dependent (Litchman 2000) and until now, the dynamic photophysiological response of *N. oculata* over a diel cycle has not been studied as extensively as presented in this study.

In comparison to cultures grown under static light regimes, we observed no significant difference in growth rate, but found a 30% reduction in cell yield under sinusoidal light regimes (**Figure 2.2** and **Table 2.1**). These findings suggest that the cumulative effect of small and statistically undetectable differences in growth rate on a daily basis culminates in significant differences in cell yield at final harvest. This is likely because under sinusoidal light conditions, cellular adjustment to non-optimal light of sub- and supra-saturating conditions over a diel timescale are likely to involve significant metabolic energy costs and consequently decreases growth rates and final cell yield (Raven 2011). These cellular adjustments (acclimation) may include those within the photosynthetic machinery: maximising light harvesting efficiency and triggering photoprotective and repair mechanisms over a short timescale. When light is sub-saturating in the morning and afternoon, cells may synthesise chlorophyll and increase antenna size to capture more light energy (Raven 2011). The rate biomass loss at night through respiration may also impact growth rate and yield, unfortunately the data collected is unable to determine its importance but should be considered in future experiments.

In contrast, at midday when the irradiance is equal to or above photosynthetic saturation rates levels of PSII photoinactivation are increased (Tamburic et al. 2012). This photoinactivation can have a multitude of affect upon the cellular metabolism, whereby energy that could otherwise be directed towards growth is required to repair any damage. Furthermore, the magnitude of supra-saturating irradiance could be an additional contributing affect upon the decreased growth rates of the sinusoidal light treatments. Whilst the daily quanta between light treatments is equal at midday the sinusoidal light treatment receives $800 \mu\text{mol photons m}^{-2} \text{ s}^{-1}$ quanta more than the square wave light treatment, levels of is higher. Previous studies suggest that at these supra-saturating conditions reaction centres become 'silent', resulting the inability to

reduce Q_A or returning the excitation energy to the antennae (Grobelaar 2007). Thus, when the magnitude of light saturation is greater, as in the sinusoidal light treatment the level of silencing is enhanced contributing to lower growth rates. These photosynthetic adjustments to sinusoidal light regimes were likely facilitated by the acclimation state of the culture and previous light history as these factors are known to influence a species growth capacity (Litchman & Klausmeier 2001). The acclimation period used in this study (at least 70 generations; approx. 2 weeks), was likely long enough for cells to alter their photosynthetic machinery to maximise light harvesting efficiency (Eberhard et al. 2008) and our findings suggest that harnessing these inherent acclimatory processes of microalgae may improve growth rates and productivity under outdoor cultivation conditions.

Similarly, thermal acclimation may have proved beneficial for cells, because periods of pre-exposure to a selected temperature regime (transgenerational acclimation) can have positive effects on offspring, specifically with regards to their ability to tolerate previously unexperienced conditions such as high temperature (Munday et al. 2013). As a result, sinusoidal temperature regimes that exposed cells to 30 °C (ambient + 5 °C) did not affect growth rate or final cell yield of *N. oculata*. Additionally, it is possible that the length of exposure to high temperatures (30 °C) was not long enough to negatively affect growth, as previous work has demonstrated 30 °C to be sub-optimal for this species (optimal growth between 20 and 25 °C; Cho et al. 2007; Converti et al. 2009; Day et al. 2013). It remains unclear whether the thermal characteristics of *N. oculata* are similar to those previously reported for this genus (critical maximum temperature of 32 °C in *N. oceanica*; Sandnes et al. 2005; Sukenik et al. 2009). In order to understand what locations will be suitable for large-scale growth, understanding the upper thermal tolerance for growth and photosynthesis in *N. oculata* warrants further investigation, as these thermal characteristics are known to be species-specific (Boyd et al. 2013).

Cellular requirements for nitrogen and phosphate remained unaffected by sinusoidal light and temperature, and whilst carbon-limitation was evident, increased environmental complexity did not increase demand for CO₂ (**Figure 2.3**). Carbon limitation during the afternoon was consistent between all treatments (pO_2 hysteresis; Tamburic et al. 2015) providing evidence that sinusoidal temperature, sinusoidal light or a combination of both treatments neither alleviates nor further exacerbates carbon limitation (**Figure 2.3**) at least under the conditions tested in this study. Injection of CO₂ into these systems may help to maintain high levels of photosynthesis during the

afternoon period (Tamburic et al. 2015) and may help to enhance overall culture productivity. In order for stakeholders to better understand when injections of CO₂ into these systems are necessary, a non-invasive tool is preferred that can provide high-resolution monitoring such as using fluorometry to track photophysiology (Hancke et al. 2008; Kromkamp et al. 2009).

Using a standard platform and non-invasive fluorometry techniques, we have traced the dynamic photophysiological response of *N. oculata* to observe diel trends in rETR that respond as a function of the incident irradiance, either square wave or sinusoidal. So far only a few studies have had the ability to strictly test the photophysiology response to different light and temperature using an experimental setup with consistent light geometries (Simionato et al. 2013; Tamburic et al. 2014). In doing so, we have shown photophysiological changes in response to light conditions, specifically, that square wave light exhibits a linear response to constant light with a positive or negative relationship over the light phase (**Figure 2.5a, b**). These findings are in agreement with previous studies for this genus when exposed to variable light and temperature in both laboratory-based studies (Sforza, Simionato, et al. 2012; Tamburic et al. 2014), as well as in complex outdoor conditions (Kromkamp et al. 2009). Monitoring the photophysiology in such high resolution also facilitated diel tracking of the photosynthetic response to dynamic light and temperature conditions (**Figure 2.5 and Supplementary Figure 2.2**) The daily recovery of photosynthesis suggests that damage to photosynthetic processes are not permanent under the conditions tested in this study, and may be a result of efficient photoprotective mechanisms and protein repair in *Nannochloropsis* (Sforza, Simionato, et al. 2012; Tamburic et al. 2014). It is likely that these protective mechanisms would be overpowered by more stressful conditions, such as exposures to temperatures of greater duration or magnitude (e.g. 40 °C) and permanent damage would occur (Sukenik et al. 2009). Further high resolution monitoring under these conditions would improve our understanding of this strain under more harsh outdoor conditions.

We present evidence that these photophysiological responses are further affected by the stage of growth that is likely a result of reduced cellular capacity to synthesise compounds to allow for maximal light utilisation (Havelkova-Dousova et al. 2004). Whilst under sinusoidal light, both treatments had similar rETR responses at exponential and stationary growth phases of the culture, suggesting a minimal effect of increasing the temperature from 20 °C to 30 °C compared to a constant 25 °C (**Figure 2.5c, d, e, f**). On day 4, the rETR response mimics the sinusoidal light levels,

suggesting photosynthesis is not limited and the cells are actively growing, evidenced by the increase in cell number in the following days (**Figure 2.2**). In all treatments, on day 13, the rETR was shown to be different than that of actively growing cells. The reduction of rETR occurring after mid-morning, concurrent with the pO_2 hysteresis suggests that carbon becomes the proximate limiting factor for photosynthesis.

As a result, the use of photophysiology techniques such as fluorometry for monitoring large-scale cultivation systems offers new capacity as it provides a non-invasive probe to provide detailed high-resolution information regarding the photosynthesis performance of a culture, as well as potential information to limitations within the culture (other than that of light) such as inorganic carbon. Furthermore, many studies have shown the relationship between photosynthetic measurements and the production of organic matter (Litchman 2000; Hancke et al. 2008; Brindley, Acién & Fernández-Sevilla 2010) and used oxygen evolution (as a proxy for assimilation of organic matter) to apply these techniques in outdoor cultivation (Sukeník et al. 2009). Despite these advances, the suitability of this tool for predicting expected growth rates and yields remains inconclusive in some cases because an uncoupling may occur due to alternative oxygen consuming cellular mechanisms (such as chlororespiration, Mehler reaction; Wagner et al. 2006). To better improve models on algal dynamics it is imperative to complete species-specific studies under the conditions expected in outdoor cultivation to understand what series of conditions trigger the cellular mechanisms that lead to sub optimal growth rates, as well as, modifying the reliability of oxygen and fluorescence-based photosynthetic performance.

In this study, we highlighted complex biological responses to realistic environmental conditions of sinusoidal light and temperature. We showed that changes in diel light mainly drive changes in productivity through small, undetectable daily effects that can culminate in significant differences in final cell yield. Despite these effects on final cell yield, we show that *Nannochloropsis oculata* is a highly plastic algal strain with the capacity to photosynthetically recover following exposure to light intensities equivalent to direct sunlight ($2000 \mu\text{mol photons m}^{-2} \text{s}^{-1}$). Whilst these environmentally complex conditions do not appear to change cellular nitrogen, phosphorus or carbon requirements, the occurrence of carbon limitation in the afternoon should be alleviated in order to enhance culture production. Furthermore, we demonstrated that by applying a standard platform in conjunction with non-invasive tools such as chlorophyll fluorometry we can accurately discriminate the biological response as a function of environmental conditions from the potential artifacts that may originate from the

experimental set-up. This technology allowed for accurate testing of challenges posed by large-scale algae cultivation such as daily changes in algal dynamics as a response to changes in light, nutrient and carbon conditions. Further research in this area could assess the implications of these fluctuations through the use of non-invasive tools to better inform the decision-making process with respect to whether periods of exposure to unfavorable conditions may have downstream implications on final harvest.

2.5 Acknowledgments

The authors would like to thank the Climate Change Cluster (C3), University of Technology Sydney for financial support.

The University of Dundee is a registered Scottish charity. No.SC015096.

2.6 References

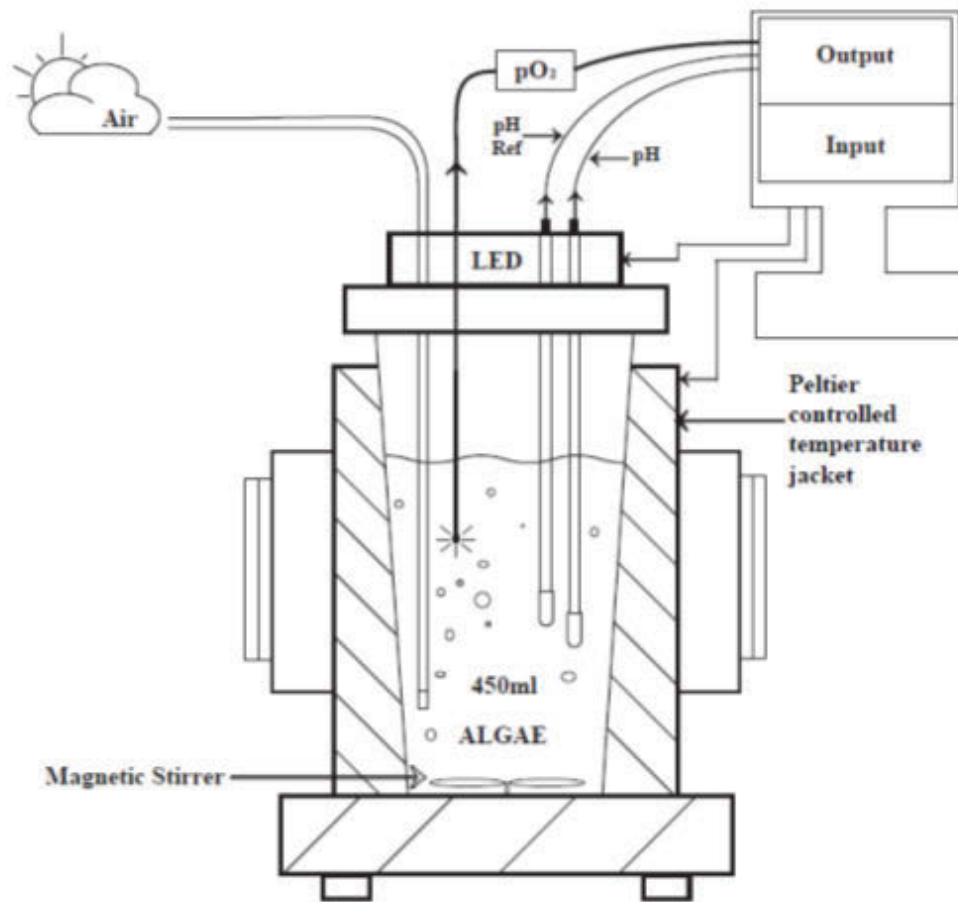
- Béchet, Q., Chambonnière, P., Shilton, A., Guizard, G. & Guieysse, B. 2015, 'Algal productivity modeling: A step toward accurate assessments of full-scale algal cultivation', *Biotechnology and Bioengineering*, vol. 112, no. 5, pp. 987–96.
- Béchet, Q., Shilton, A. & Guieysse, B. 2013, 'Modeling the effects of light and temperature on algae growth: state of the art and critical assessment for productivity prediction during outdoor cultivation.', *Biotechnology Advances*, vol. 31, no. 8, pp. 1648–63.
- Bernard, O. 2011, 'Hurdles and challenges for modelling and control of microalgae for CO₂ mitigation and biofuel production', *Journal of Process Control*, vol. 21, no. 10, pp. 1378–89.
- BOM 2016, 'Climate Data Online', *Bureau of Meteorology Climate Data online*, viewed 3 February 2016, <<http://www.bom.gov.au/climate/data/>>.
- Borowitzka, M.A., Boruff, B.J., Moheimani, N.R., Pauli, N., Cao, T., Smith, H., Michael A., B., Bryan J, B., Navid R., M., Natasha, P., Yinghui, C. & Helen, S. 2012, 'Identification of the optimum sites for industrial- scale microalgae biofuel production in WA using a GIS Model', *The Centre for Research into Energy for Sustainable Transport (CREST)*, pp. 1–35.
- Borowitzka, M.A. & Moheimani, N.R. 2013a, *Algae for Biofuels and Energy*, M.A. Borowitzka & N.R. Moheimani (eds), *Algae for Biofuels and Energy*, 1st edn., Springer Netherlands, Dordrecht, New York.
- Borowitzka, M.A. & Moheimani, N.R. 2013b, 'Open Pond Culture Systems', in M.A. Borowitzka & N.R. Moheimani (eds), *Algae for Biofuels and Energy*, 1st edn., Springer Netherlands, Dordrecht, New York, pp. 133–52.
- Boyd, P.W., Rynearson, T.A., Armstrong, E.A., Fu, F., Hayashi, K., Hu, Z., Hutchins, D.A., Kudela, R.M., Litchman, E., Mulholland, M.R., Passow, U., Strzepek, R.F., Whittaker, K.A., Yu, E. & Thomas, M.K. 2013, 'Marine phytoplankton temperature versus growth responses from polar to tropical waters--outcome of a scientific community-wide study.', *PloS One*, vol. 8, no. 5, e63091.
- Brindley, C., Acién, F.G. & Fernández-Sevilla, J.M. 2010, 'The oxygen evolution methodology affects photosynthetic rate measurements of microalgae in well-defined light regimes', *Biotechnology and Bioengineering*, vol. 106, no. 2, pp. 228–37.
- Chisti, Y. 2008, 'Biodiesel from microalgae beats bioethanol.', *Trends in Biotechnology*, vol. 26, no. 3, pp. 126–31.
- Cho, S.H., Ji, S.-C., Hur, S.B., Bae, J., Park, I.-S. & Song, Y.-C. 2007, 'Optimum temperature and salinity conditions for growth of green algae *Chlorella ellipsoidea* and *Nannochloris oculata*', *Fisheries Science*, vol. 73, no. 5, pp. 1050–6.
- Converti, A., Casazza, A.A., Ortiz, E.Y., Perego, P. & Del Borghi, M. 2009, 'Effect of

- temperature and nitrogen concentration on the growth and lipid content of *Nannochloropsis oculata* and *Chlorella vulgaris* for biodiesel production', *Chemical Engineering and Processing: Process Intensification*, vol. 48, no. 6, pp. 1146–51.
- Davison, I.R. 1991, 'Environmental effects on algal photosynthesis: Temperature', *Journal of Phycology*, no. 27, pp. 2–8.
- Day, J.G., Burt, D.J., Achilles-Day, U.E.M. & Stanley, M.S. 2013, 'Future algal biofuels: implications of environmental temperature on production strain selection', *International Journal of Ambient Energy*, vol. 36, no. 5, pp. 248–52.
- Eberhard, S., Finazzi, G. & Wollman, F.-A. 2008, 'The dynamics of photosynthesis', *Annual Review of Genetics*, vol. 42, pp. 463–515.
- Eppley, R.W. 1972, 'Temperature and phytoplankton growth in the sea', *Fishery Bulletin*, vol. 70, no. 4, pp. 1063–85.
- Geider, R.J., MacIntyre, H.L. & Kana, T.M. 1998, 'A dynamic regulatory model of phytoplanktonic acclimation to light, nutrients, and temperature', *Limnology and Oceanography*, vol. 43, no. 4, pp. 679–94.
- Grobbelaar, J.U. 2007, 'Photosynthetic characteristics of *Spirulina platensis* grown in commercial-scale open outdoor raceway ponds: What do the organisms tell us?', *Journal of Applied Phycology*, vol. 19, pp. 591–8.
- Guillard, R. & Ryther, J. 1962, 'Studies of marine planktonic diatoms: I. *Cyclotella nana* Hustedt, and *Dentonula confervacea* (Cleve) Gran', *Canadian Journal of Microbiology*, vol. 8, pp. 229–39.
- Hancke, K., Hancke, T.B., Olsen, L.M., Johnsen, G. & Glud, R.N. 2008, 'Temperature effects on microalgal photosynthesis-light responses measured by O₂ production, pulse-amplitude-modulated fluorescence, and ¹⁴C assimilation', *Journal of Phycology*, vol. 44, no. 2, pp. 501–14.
- Havelková-Doušová, H., Prášil, O. & Behrenfeld, M.J. 2004, 'Photoacclimation of *Dunaliella tertiolecta* (Chlorophyceae) under fluctuating irradiance', *Photosynthetica*, vol. 42, no. 2, pp. 273–81.
- Huesemann, M., Crowe, B., Waller, P., Chavis, A., Hobbs, S., Edmundson, S. & Wigmosta, M. 2016, 'A validated model to predict microalgae growth in outdoor pond cultures subjected to fluctuating light intensities and water temperatures', *Algal Research*, vol. 13, pp. 195–206.
- Kilian, O., Benemann, C.S.E., Niyogi, K.K. & Vick, B. 2011, 'From the Cover: High-efficiency homologous recombination in the oil-producing alga *Nannochloropsis* sp.', *Proceedings of the National Academy of Sciences*, vol. 108, no. 52, pp. 21265–9.
- Kromkamp, J.C., Beardall, J., Sukenik, A., Kopecky, J., Masojidek, J., Bergeijk, van S., Gabai, S., Shaham, E. & Yamson, A. 2009, 'Short-term variations in photosynthetic parameters of *Nannochloropsis* cultures grown in two types of outdoor mass cultivation systems', *Aquatic Microbial Ecology*, vol. 56, no. 2–3, pp. 309–22.
- Litchman, E. 2000, 'Growth rates of phytoplankton under fluctuating light', *Freshwater Biology*, vol. 44, no. 2, article, pp. 223–35.
- Litchman, E. & Klausmeier, C.A. 2001, 'Competition of phytoplankton under fluctuating light', *The American Naturalist*, vol. 157, no. 2, pp. 170–87.
- Lovegrove, T. 1960, 'An improved form of sedimentation apparatus for use with an inverted microscope', *Journal du Conseil*, vol. 25, no. 3, pp. 279–84.
- Lucker, B.F., Hall, C.C., Zegarac, R. & Kramer, D.M. 2014, 'The environmental photobioreactor (ePBR): An algal culturing platform for simulating dynamic natural

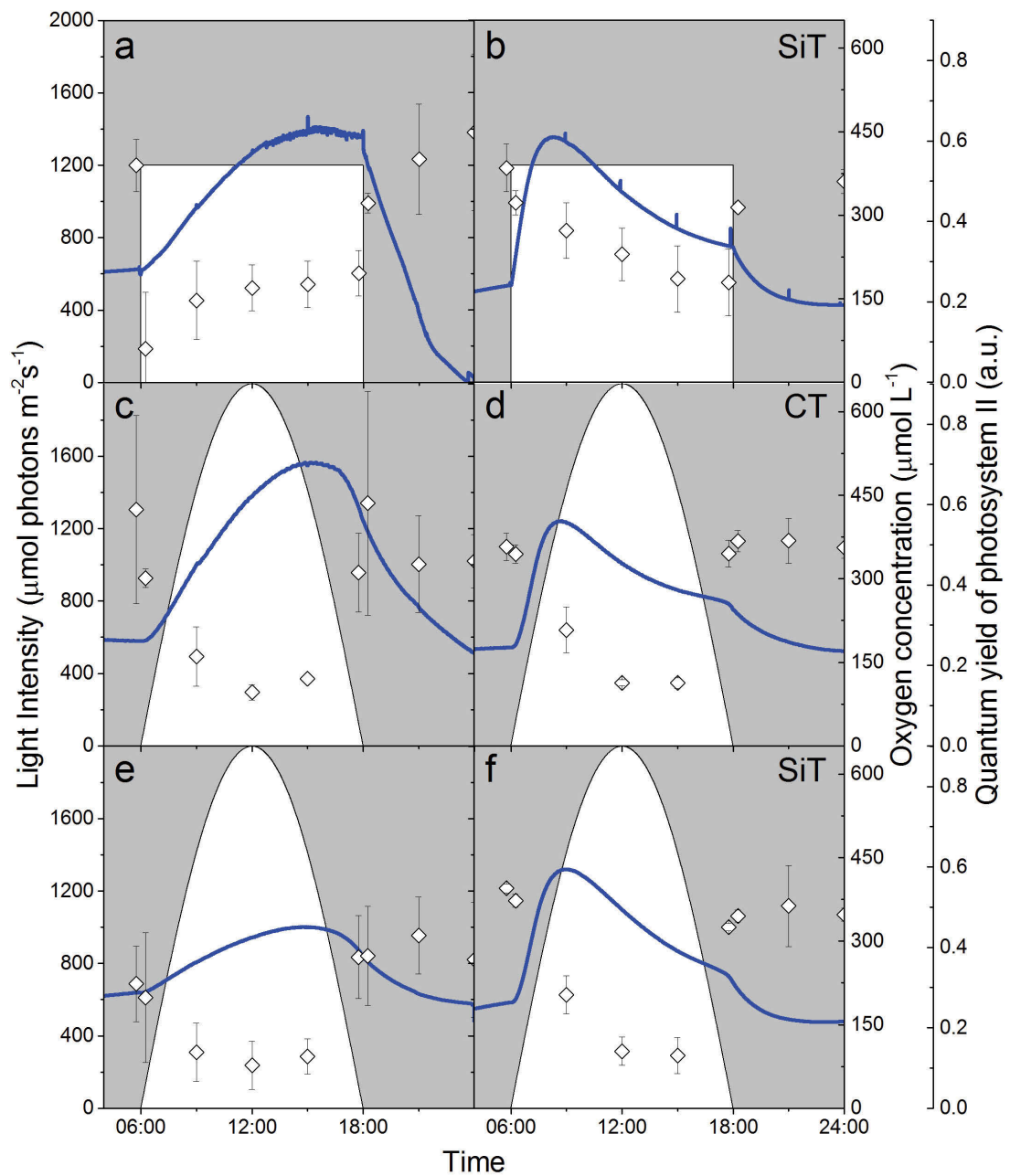
- environments', *Algal Research*, vol. 6 Part B, pp. 242–9.
- Lund, J.W.G., Kipling, C., Le Cren, E.D. & House, T.F. 1958, 'The inverted microscope method of estimating algal numbers and the statistical basis of estimations by counting', *Hydrobiologia*, vol. 11, no. 2, pp. 143–70.
- Moheimani, N.R. & Borowitzka, M.A. 2007, 'Limits to productivity of the alga *Pleurochrysis carterae* (Haptophyta) grown in outdoor raceway ponds', *Biotechnology and Bioengineering*, vol. 96, no. 1, pp. 27–36.
- Munday, P.L., Warner, R.R., Monro, K., Pandolfi, J.M. & Marshall, D.J. 2013, 'Predicting evolutionary responses to climate change in the sea.', *Ecology Letters*, vol. 16, no. 12, pp. 1488–500.
- Raven, J.A. 2011, 'The cost of photoinhibition', *Physiologia Plantarum*, vol. 142, no. 1, pp. 87–104.
- Raven, J.A. & Geider, R.J. 1988, 'Temperature and algal growth', *New Phytologist*, vol. 110, no. 4, pp. 441–61.
- Renaud, S.M., Thinh, L.-V., Lambrinidis, G. & Parry, D.L. 2002, 'Effect of temperature on growth, chemical composition and fatty acid composition of tropical Australian microalgae grown in batch cultures', *Aquaculture*, vol. 211, no. 1–4, pp. 195–214.
- Riebesell, U., Fabry, V.J., Hansson, L. & Gattuso, J.-P. 2010, *Guide to best practices for ocean acidification research and data reporting*, U. Riebesell, V.J. Fabry, L. Hansson & J.-P. Gattuso (eds), 1st edn., vol. 260, Publications Office of the European Union Luxembourg, Luxembourg.
- Rodolfi, L., Chini Zittelli, G., Bassi, N., Padovani, G., Biondi, N., Bonini, G. & Tredici, M.R. 2009, 'Microalgae for oil: strain selection, induction of lipid synthesis and outdoor mass cultivation in a low-cost photobioreactor', *Biotechnology and Bioengineering*, vol. 102, no. 1, pp. 100–12.
- Sandnes, J.M., Wenner, D., Källqvist, T., Wenner, D. & Gislerød, H.R. 2005, 'Combined influence of light and temperature on growth rates of *Nannochloropsis oceanica*: linking cellular responses to large-scale biomass production', *Journal of Applied Phycology*, vol. 17, no. 6, pp. 515–25.
- Schenk, P.M., Thomas-Hall, S.R., Stephens, E., Marx, U.C., Mussgnug, J.H., Posten, C., Kruse, O. & Hankamer, B. 2008, 'Second generation biofuels: high-efficiency microalgae for biodiesel production', *Bioenergy Research*, vol. 1, no. 1, pp. 20–43.
- Schindelin, J., Arganda-Carreras, I., Frise, E., Kaynig, V., Longair, M., Pietzsch, T., Preibisch, S., Rueden, C., Saalfeld, S., Schmid, B., Tinevez, J., White, D.J., Hartenstein, V., Eliceiri, K., Tomancak, P. & Cardona, A. 2012, 'Fiji: an open-source platform for biological-image analysis.', *Nature Methods*, vol. 9, no. 7, pp. 676–82.
- Schreiber, U., Bilger, W. & Neubauer, C. 1994, 'Chlorophyll fluorescence as a nonintrusive indicator for rapid assessment of *in vivo* photosynthesis', *Ecophysiology of Photosynthesis*, vol. 100, pp. 49–70.
- Sforza, E., Simionato, D., Giacometti, G.M., Bertuccio, A. & Morosinotto, T. 2012, 'Adjusted light and dark cycles can optimize photosynthetic efficiency in algae growing in photobioreactors.', *PLoS One*, vol. 7, no. 6, e38975.
- Simionato, D., Basso, S., Giacometti, G.M. & Morosinotto, T. 2013, 'Optimization of light use efficiency for biofuel production in algae', *Biophysical Chemistry*, vol. 182, pp. 71–8.
- Suggett, D.J., Goyen, S., Evenhuis, C., Szabó, M., Pettay, D.T., Warner, M.E. & Ralph, P.J. 2015, 'Functional diversity of photobiological traits within the genus *Symbiodinium* appears to be governed by the interaction of cell size with cladal

- designation.', *The New Phytologist*, vol. 208, no. 2, pp. 370–81.
- Sukenik, A., Beardall, J., Kromkamp, J.C., Kopecký, J., Masojídek, J., van Bergeijk, S., Gabai, S., Shaham, E. & Yamshon, A. 2009, 'Photosynthetic performance of outdoor *Nannochloropsis* mass cultures under a wide range of environmental conditions', *Aquatic Microbial Ecology*, vol. 56, no. 2–3, pp. 297–308.
- Tamburic, B., Evenhuis, C.R., Suggett, D.J., Larkum, A.W.D., Raven, J.A. & Ralph, P.J. 2015, 'Gas transfer controls carbon limitation during biomass production by marine microalgae', *ChemSusChem*, vol. 8, no. 16, pp. 2727–36.
- Tamburic, B., Guruprasad, S., Radford, D.T., Szabó, M., Lilley, R.M., Larkum, A.W.D., Franklin, J.B., Kramer, D.M., Blackburn, S.I., Raven, J.A., Schliep, M. & Ralph, P.J. 2014, 'The effect of diel temperature and light cycles on the growth of *Nannochloropsis oculata* in a photobioreactor matrix.', *PloS One*, vol. 9, no. 1, e86047.
- Tamburic, B., Zemichael, F.W., Maitland, G.C. & Hellgardt, K. 2012, 'Effect of the light regime and phototrophic conditions on growth of the H₂-producing green alga *Chlamydomonas reinhardtii*', *Energy Procedia*, vol. 29, pp. 710–9.
- Wagner, H., Jakob, T. & Wilhelm, C. 2006, 'Balancing the energy flow from captured light to biomass under fluctuating light conditions', *New Phytologist*, vol. 169, no. 1, pp. 95–108.

2.7 Supplementary Figures



Supplementary Figure 2.1 Phenometrics ePBR schematic diagram (taken from Tamburic et al. 2014: Light intensity is controlled using a white light LED array and culture temperature is controlled with a Peltier controlled temperature jacket. The PBR is comprised of a magnetically-stirred and dissolved oxygen (pO₂) is measured optically (PyroScience).



Supplementary Figure 2.2 Dynamic oxygen and photophysiological response of *N. oculata*: Quantum yield of photosystem II and *in situ* pO_2 profiles of *N. oculata* when cultivated under different light and temperature regimes; (a, b) square wave light, sinusoidal temperature, SqLSiT; (c, d) sinusoidal light, constant temperature, SiLCT and (e, f) sinusoidal light, sinusoidal temperature regime, SiLSiT. Measurements were recorded at early exponential (a, c, e) and stationary phase (b, d, f). Open diamonds and lines represent the average of 3 replicates relative electron transport rate and *in situ* dissolved oxygen profiles (blue line); error bars represent standard deviation ($n=3$). The solid white area represents the light intensity at the surface of the culture.

Chapter 3 Time-resolved thermal response of *Nannochloropsis oculata* improves large-scale cultivation reliability.

Dale T. Radford¹, Kirralee G. Baker¹, Milán Szabó^{1,2}, John A. Raven^{1,3} and Peter J. Ralph¹

Affiliations

¹ Climate Change Cluster (C3), University of Technology Sydney, 2007 NSW, Australia

² Division of Plant Sciences, Research School of Biology, The Australian National University, Sullivans Creek Road, Acton, ACT 2601, Australia

³ Division of Plant Sciences, University of Dundee at the James Hutton Institute, Invergowrie, Dundee DD2 5DA, UK

Keywords

Nannochloropsis oculata, thermal performance curve, large-scale cultivation, photophysiology, nutrient uptake, growth

Abbreviations

TPC: thermal performance curve

T_{opt} : optimum temperature (thermal optimum).

CT_{min} : minimum critical temperature.

CT_{max} : maximum critical temperature.

SP: saturation pulse

MC-PAM: Multiple Excitation Wavelength Chlorophyll Fluorescence analyser

RLC: Rapid light curve

rETR_{max}: Relative maximum electron transport rate

PAR: photosynthetically active radiation

NO₃⁻: nitrate

NO₂⁻: nitrite

PO₄³⁻: orthophosphate

3.1 Introduction

Microalgae are attractive sources for many commercial biotechnological applications, such as their potential to clean wastewater (Mallick 2002), generating high-value products (Borowitzka 1999, 2013) or as a sustainable feedstock for biofuel production (Chisti 2007). In order to meet market demands, mass cultivation of microalgae is required and often large-scale outdoor systems such as open ponds are used in order to produce the commercial scales required (Fon Sing et al. 2013). In these systems, microalgae experience natural abiotic fluctuations in both light and temperature over diurnal, seasonal and annual timescales- presenting numerous challenges in order to provide consistent production for the market.

Microalgae exhibit numerous biochemical mechanisms that enable them to photoacclimate to their light surroundings allowing for maximal utilisation, such as adjustments of intracellular pigment composition (Raven & Geider 2003; Sforza, Simionato, et al. 2012). Processes involved in photo-acclimation have been well studied in the field of photophysiology (see review, Falkowski & LaRoche 1991) and specifically on biofuel candidate genera such as *Nannochloropsis* (Fisher et al. 1996). This knowledge has been applied in the context of biofuels to optimise light provision through strategies such as alteration of culture depth or adjustment of cell density (Moheimani & Borowitzka 2007). In contrast, approaches to mitigate large fluctuations in temperature in commercial-scale ponds are non-existent or not economically viable (Borowitzka 1999). The most favorable solution to this challenge is the strategic selection of microalgae that has optimal growth/productivity for the temperature regimes prevalent at the cultivation system's location (Lundquist et al. 2010).

In order to inform this selection process, a better understanding of thermal responses in biofuel candidate species is required. This can be conducted through thermal screening using thermal performance curves (TPCs). TPCs are used to describe the relationship between temperature and the response of an organism's trait (e.g. growth) and have a characteristic bell-curve shape where maximal performance occurs at an 'optimal' temperature (T_{opt}) (Huey & Stevenson 1979). Typically, this curve is asymmetric, where the rise in temperature from the minimum critical temperature (CT_{min}) is a gentle slope towards the T_{opt} , but further increases result in a steep decline towards the maximum critical temperature (CT_{max}) (**Figure 1.6**; Huey & Stevenson 1979). This thermal function provides insight into common problems associated with outdoor cultivation. For example, when sub-optimal periods are experienced by

microalgae during the early morning and as a result, decreased photosynthetic rates and daily biomass production are often observed (Richmond et al. 1980; Moheimani & Borowitzka 2007). In summer, supra-optimal temperatures are often experienced by microalgae, where high temperatures often result in the closure of algae farms during periods of excessive heat, restricting the annual operational period, thus reducing the annual productivity (Belay 1997).

In order to improve predictive growth models that inform life-cycle analyses (LCAs), there is a need for more comprehensive data on algal TPCs, as these environmental processes play a key role in determining the location and feasibility of future cultivation systems (Borowitzka et al. 2012). To date, TPC characterisation in biofuel candidate species has revealed considerable variation between and within species, in terms of thermal optimum and overall shape. For example, some model species such as *Chlamydomonas reinhardtii* have shown to be thermal ‘specialists’ as they exhibit relatively high T_{opt} (30 °C) over a relatively narrow thermal range (Lukeš et al. 2014), whereas other more ‘generalist’ species such as *Nannochloropsis oculata* have a wider thermal range demonstrating comparable growth between 20 and 30 °C (Chen et al. 2012). These TPCs can, however, shift depending on the ‘trait of interest’ (e.g. growth rate or lipid accumulation), acclimation period and time of temperature exposure (Huey et al. 2012). To date, the majority of TPCs have been collected following a week or more of exposure (Sandnes et al. 2005), and as a result, it remains unclear whether the acclimation rate of these TPCs are more rapid and can occur over shorter exposure times (minutes-hours-days). Furthermore, it remains unknown how TPCs for other algal traits that are relevant to the biofuel industry, such as nutrient uptake (initial seed inputs) and photophysiology (reflective of culture productivity) mirror that of growth or if these traits can acclimate more rapidly to changes in temperature. Understanding how the magnitude and time scale of temperature exposures affect cell physiology in terms of short- (e.g. photophysiology) and long-term (e.g. growth) responses would better inform stakeholders about the quality of the algal product. Additionally, this information could improve management practices to reduce costs (e.g. the early harvest of cultures prior to a period of unfavorable growth conditions).

In order to refine appropriate locations for the cultivation of the biofuel candidate microalgae, *Nannochloropsis oculata*, we applied a screening process specifically designed to assess the thermal tolerance of this strain to different magnitudes and durations of temperature exposure. Through quantitative physiology, we obtained thermal performance curves (TPCs) at different timescales of exposure in order to

examine the response of overall growth, photophysiology and nutrient uptake dynamics of *N. oculata* over a wide range of continuous temperature conditions, in order to (i) provide empirical data to better inform predictive growth models used to determine the location and feasibility of future cultivation systems, and (ii) understand whether some algae traits (such as photophysiology) can be used as ‘early warning signs’ to improve management practices in large-scale cultivation systems.

3.2 Materials and methods

3.2.1 Stock microalgal culture and medium

Nannochloropsis oculata (Droop) Green (CS-179) was obtained from the ANACC (Australian National Algae Culture Collection, CSIRO, Hobart, Australia) and grown in f/2 media (0.2 µm filtered artificial seawater enriched with; 8.82×10^{-4} M NaNO₃; 3.62×10^{-5} M, NaH₂PO₄·H₂O; trace metal solution and vitamin solution; (Guillard & Ryther 1962). Stock cultures of *N. oculata* were maintained at 25 °C under cool-white fluorescent irradiance at 120 ± 10 µmol photons m⁻² s⁻¹ (12 h: 12 h light: dark cycle).

3.2.2 In vivo chlorophyll fluorescence

This study used *in vivo* chlorophyll fluorescence techniques to probe the photochemical reactions of photosynthesis (i.e. the transfer of light energy into chemically fixed energy; Schreiber 2004) such as maximum quantum yield of photosystem II (F_V/F_M) and relative electron transport rate (rETR) to examine the response of *N. oculata* over a range of temperatures.

To measure F_V/F_M , samples were dark-adapted for 15 min and subjected to a saturation pulse (SP; 3000 µmol photons m⁻² s⁻¹, 800 milliseconds). Maximum quantum efficiency (F_V/F_M) was calculated using the following equation (Genty, Briantais & Baker 1989):

$$\text{Maximum quantum yield } \left(\frac{F_V}{F_M}\right) = \frac{F_M - F_0}{F_M} \quad (\text{Equation 3.1})$$

Where, F_0 and F_m are the minimum and maximum fluorescence yield of PSII in the dark-adapted state, respectively. In order to measure rETR, samples were exposed to light of known intensity and then subjected to a SP (3000 µmol photons m⁻² s⁻¹, 800 milliseconds). From the values obtained the rETR was derived using the following equation (Genty, Briantais & Baker 1989):

$$rETR = PAR \times \frac{F_M' - F_0'}{F_M'} \quad (\text{Equation 3.2})$$

Where, F_0' is the minimal fluorescence yield and F_m' the maximum fluorescence yield both in the light-adapted state and PAR is the photosynthetically active radiation. All of the fluorometric photosynthetic measurements used in this study were derived using pulse-amplitude modulation (PAM) instruments. The different PAM instruments used in this study were to serve different purposes. The Multiple Excitation Wavelength Chlorophyll Fluorescence analyser (MC-PAM; Heinz Walz GmbH, Germany) was used to provide precision measurements at multiple wavelengths, whereas the Imaging-PAM

(Heinz Walz GmbH, Germany) allowed for screening of multiple samples simultaneously at fixed wavelength.

3.2.3 Short-term (5 min) temperature stress analysis- MC-PAM

To examine the short-term effects of temperature (5 min), nutrient and carbon-replete cultures of *N. oculata* were exposed to short-term temperature exposures ranging from 10 - 50 °C. An MC-PAM fitted with a temperature control unit (US-T, Heinz Walz GmbH, Germany) provided 98 $\mu\text{mol photons m}^{-2} \text{s}^{-1}$ PAR (white light) for 5 min at the different temperatures. Following the 5 min temperature exposure, a rapid light curve (RLC; 10 s white actinic light steps) was performed. For each light step the rETR was calculated according to **Equation 3.2**. Maximum relative electron transport (rETR_{max}), and the irradiance at which photosynthesis is saturated (E_k) **Supplementary Figure 3.2** was derived from the RLC curve fit according to methods used in Ralph & Gademann (2005).

3.2.4 Long-term (4 day) temperature stress analysis

To examine the longer-term effects (hours to days) of the response of *N. oculata* to different temperatures a growth experiment was performed as described below.

3.2.4.1 Experimental conditions

35 mL cultures were grown for 4 days over a gradient of temperatures between 17.2 °C and 39.9 °C. A temperature gradient was generated using an aluminum block (dimensions, l x w x h: 1200 cm x 30 cm x 15 cm) heated and cooled at each end with circulation thermo-regulated cold (15 °C) and hot (40 °C) water, respectively. 50 $\mu\text{mol photons m}^{-2} \text{s}^{-1}$ of cool-white light was provided by an array of LEDs (Schenzen Cidly Group, China) programmed to a 12 h: 12 h light: dark cycle.

3.2.4.2 Growth measurements

Sub-samples were harvested daily and optical density measurements were performed at 750 nm using a microplate spectrophotometer (Infinite 200 PRO series, TECAN) and then fixed in 1% (v/v) glutaraldehyde solution. A correlation analysis of optical density and cell counts ($R^2=0.950$) was performed, where cell counts were determined using the image analysis method described earlier (**Chapter 2.2.3**; Suggett et al. 2015).

3.2.4.3 Imaging PAM

Daily *in vivo* chlorophyll fluorescence of *N. oculata* was performed with an Imaging-PAM (Heinz Walz GmbH, Germany), allowing for the simultaneous analysis of multiple

treatments (12 samples total). Dark-adapted samples were subjected to an SP then illuminated with an actinic light intensity of $21 \mu\text{mol photons m}^{-2} \text{s}^{-1}$ (blue light; 450 nm), with saturation pulses occurring every 30 s to allow for calculation of F_V/F_M and rETR according to Equation 3.1 and 3.2, respectively. In order to ensure saturating actinic light intensity was used for the calculation of rETR, a steady state light curve was performed on samples of inoculum (**Supplementary Figure 3.2**), whereby $21 \mu\text{mol photons m}^{-2} \text{s}^{-1}$ was found to be appropriate. Whilst the absolute values of rETR cannot be directly compared to those measured at 5 min exposure (due to geometrical differences between the two instruments, different types of actinic sources, and different absorbance in the experimental setup), the trends and relative values in photosynthetic electron transport rate under the applied temperatures can be analysed.

3.2.4.4 Nutrient uptake analysis

Cell suspensions of *N. oculata* were centrifuged at 5000 g for 5 min (Eppendorf 5424R), the supernatant was removed and stored at -20°C until analysis. Nutrient uptake rates were calculated as a difference between the initial nutrient concentration at the beginning and residual concentration at the end of the experiment. Analysis of nitrate (NO_3^-), nitrite (NO_2^-) and orthophosphate (PO_4^{3-}) were performed according to the methods described in Baker et al. (2016). Briefly, NO_3^- were determined indirectly as described in Schnetger & Lehnert (2014), where NO_2^- analysed by the Griess-Ilsovoy method were subtracted from values of total nitrogen (NO_x) obtained through reduction with vanadium (III) chloride analysed spectrophotometrically at 540 nm. The nitrate values were linear between 1 and 100 μM and the detection limit was 0.15 μM . Orthophosphate concentrations were determined spectrophotometrically at 620 nm using the method described in Hoenig et al. (1989) where values were linear between 1 and 15 μM and the detection limit was 0.95 μM .

3.2.5 Statistical analysis

Data were analysed with either a one-way or two-way repeated measures analysis of variance (RM-ANOVA) with subsequent Bonferroni comparison tests to identify significant differences between groups; a p value of <0.05 was regarded as significant. Data were checked for the assumption of sphericity using the Mauchly's test. When these assumptions were violated the Greenhouse-Geisser or Huynh-Feldt correction were used when the epsilon was >0.75 or <0.75 , respectively, according to Girden (1992). All statistical analysis was computed using OriginPRO 2015 (version b9.2.272).

3.3 Results

3.3.1 Short-term thermal response on photophysiology of *N. oculata*

In order to study the short-term thermal response of *N. oculata*, the photosynthetic response was measured at different temperatures up to 40 °C. Relative electron transport rate (rETR) provides an estimate of photosynthetic response to PAR (Kroon et al. 1992) and was determined from a rapid light curve (RLC) following a short exposure (5 min) over a range of temperatures (10 - 40 °C). Temperature was shown to affect both the $rETR_{max}$ and I_K . For example, the $rETR_{max}$ increased with temperature i.e. 11.1 ± 0.1 (a.u.) and 27.0 ± 2.4 (a.u.) at 10 °C and 40 °C, respectively (**Figure 3.1**). For comparison with the growth experiment, the rETR at $54 \mu\text{mol photons m}^{-2} \text{s}^{-1}$ after 5 min exposure to the different magnitude of temperature treatment were derived (**Figure 3.2**). At this light intensity, rETR was shown to have a wide thermal optimum (T_{opt}) of 32.5 ± 7.5 °C (**Figure 3.2**). Slight reductions in rETR were seen as the temperature decreased from the optimum, whereas a steep decline is evident at elevated temperatures (> 40 °C).

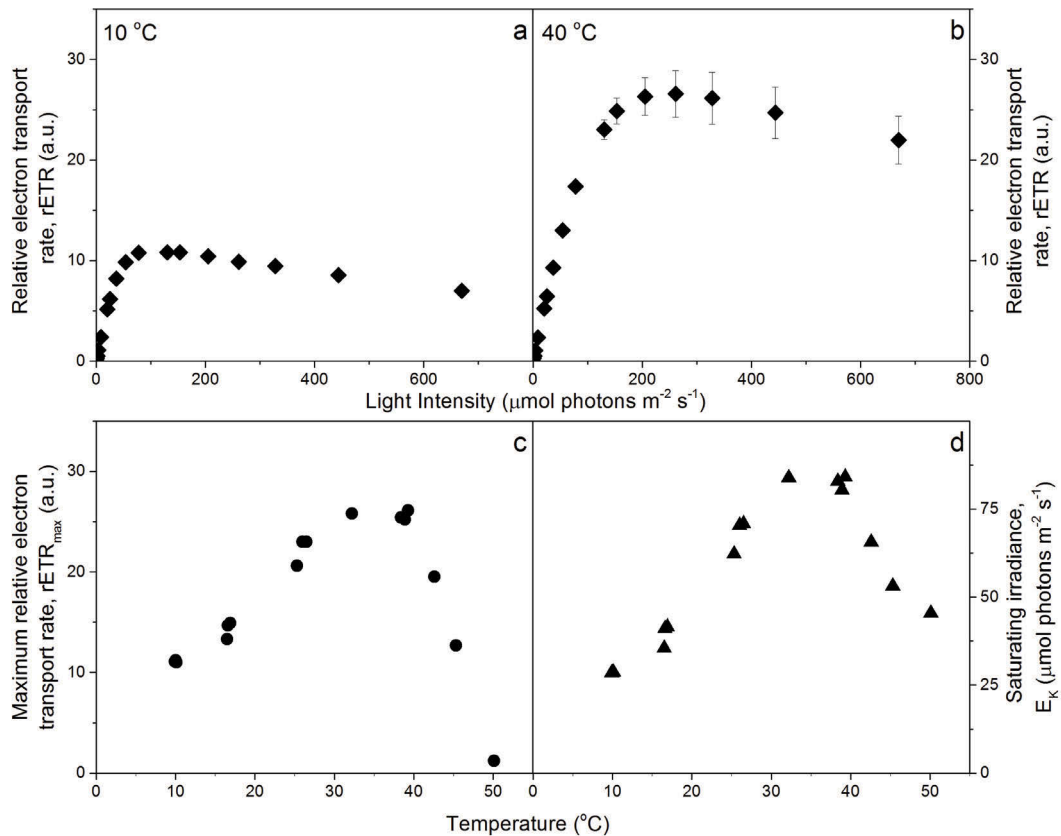


Figure 3.1 (a, b) Rapid light curves performed in the MC-PAM of nutrient replete cultures of *N. oculata* after exposure to $98 \mu\text{mol photons m}^{-2} \text{s}^{-1}$ (PAR; white light) for 5 min at (a) 10 °C and (b) 40 °C, where closed diamonds represent triplicate samples ($n=3$) and errors bars corresponding to ± 1 standard deviation. (c, d) Derived parameters of RLC curve fits at different temperature exposures where (c) maximum relative electron transport rate (circles) and (d) saturating irradiance (triangles).

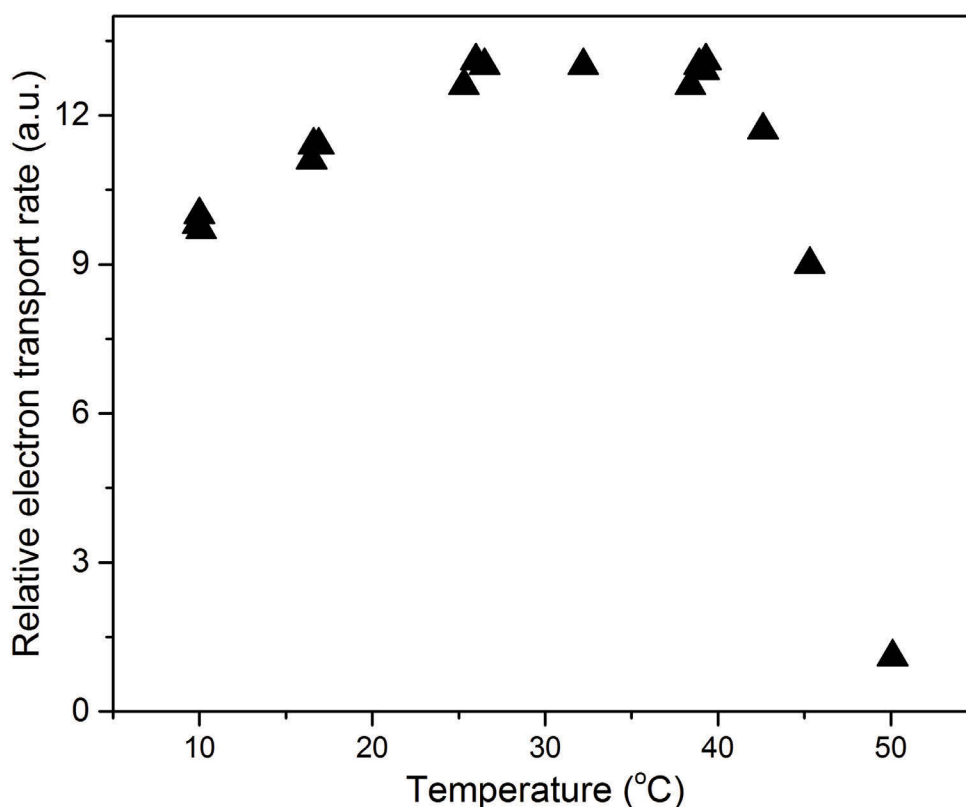


Figure 3.2 Relative electron transport rate (rETR) of *N. oculata* at different temperatures: rETR was determined using the multi-colour PAM (MC-PAM, Walz, Germany), samples were exposed to temperature for 5 min under $98 \mu\text{mol photons m}^{-2}\text{s}^{-1}$ (PAR; white light) prior to performing a rapid light curve (10 s step). rETR was derived from the $54 \mu\text{mol photons m}^{-2}\text{s}^{-1}$ light step.

3.3.2 Thermal response following 24 hours exposure

To understand how the photosynthetic response changes through time (hours – days), cultures of *N. oculata* were grown over a range of temperatures (17.2 - 39.9 °C). After 24 h exposure, increasing temperature resulted in decreased rETR (**Figure 3.3a**). This decrease is most significant in temperatures above 32.9 °C ($p < 0.001$), with values found to be zero above 36.2 °C. A flatter response is seen in F_V/F_M between 17.2 - 32.9 °C, with significantly reduced values present under 36.2 °C (**Figure 3.3b**). Despite the flat response (17.2 - 32.9 °C), statistical analysis shows a clustering (denoted a and b; $p < 0.05$), with colder temperatures (17.2 - 20.8 °C) having increased F_V/F_M values. Growth and nutrient uptake rates (nitrate and orthophosphate) tested after 24 h were found to be highly variable (**Supplementary Figure 3.1**).

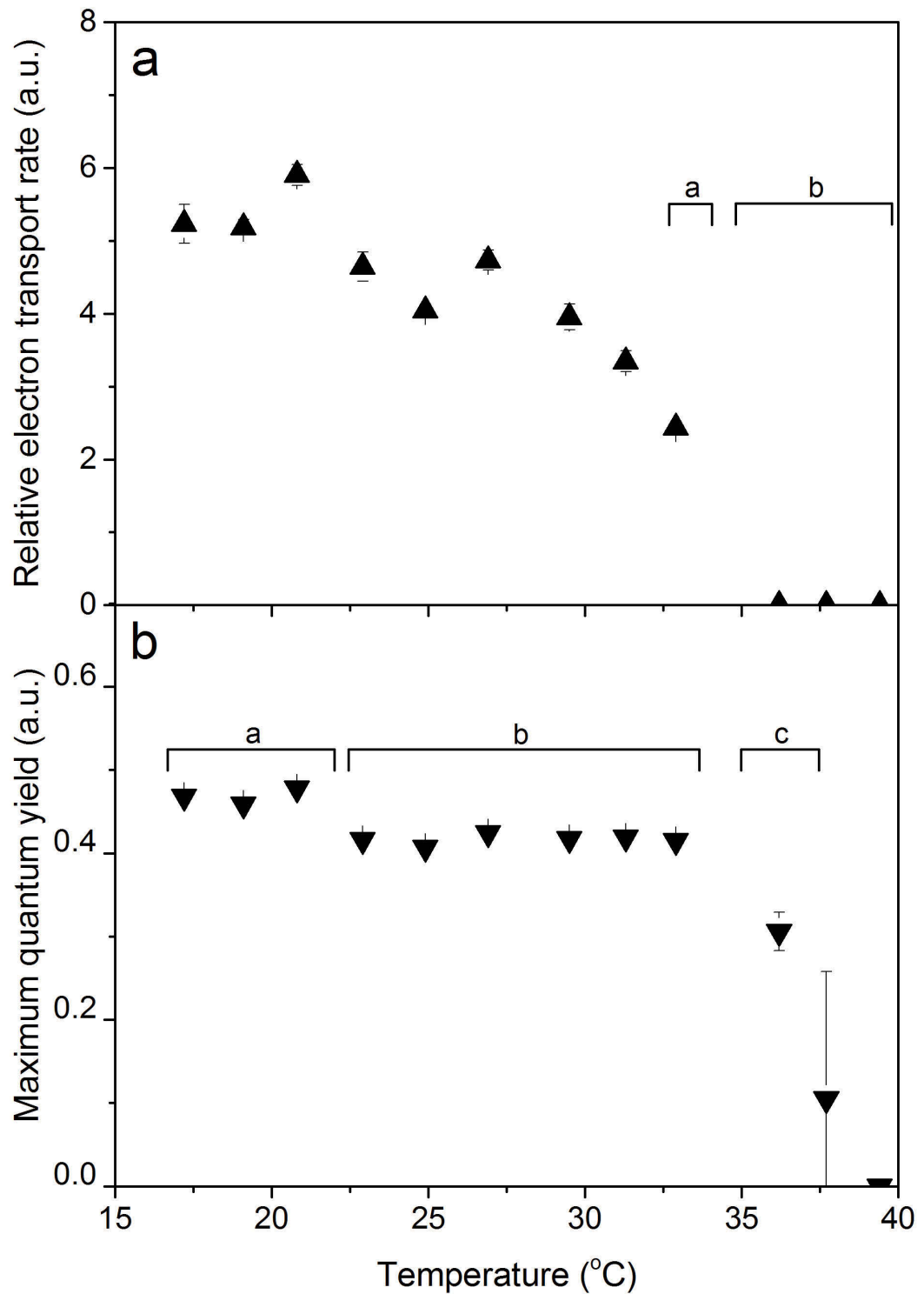


Figure 3.3 Relative electron transport rate (rETR) and maximum quantum yield of *N. oculata* after 24 hours at varying temperatures: (a) rETR corresponds to value at 2 seconds after induction of light performed on Imaging-PAM. (b) Maximum quantum yield was determined after dark adaption for 15 min. Symbols represent the average of triplicates ($n=3$) with errors bars corresponding to ± 1 standard deviation. Square brackets cluster treatments where non-significant difference were found ($p > 0.05$), whilst letters correspond to statistical difference between groups ($p < 0.05$).

3.3.3 Long-term thermal response

Although variability is seen in the physiological response after 24 h, a typical thermal growth response is evident after 96 h (**Figure 3.4a**). Here growth rate increases slowly as temperature increases towards T_{opt} (26.9 °C), at which point any further increase in temperature resulted in a sharp decline until no growth was observed (36.2 °C). Due to high variability between replicates, there is no statistical difference in the growth rates except at extremely high temperatures where no growth was observed (one way repeated measures ANOVA; $p < 0.05$). Nutrient uptake was determined from the residual nitrate and orthophosphate in the medium relative to the initial concentration. Uptake of either nutrient was shown to have a similar relationship; nutrient uptake decreased with increasing temperature (**Figure 3.4b, c**). Due to reduced variability, a larger response to increased temperature was observed in orthophosphate uptake than nitrate uptake. Despite this, *N. oculata* exhibited the capacity to uptake both nutrients in the treatments. No growth was observed after 96 h (above 36.2 °C).

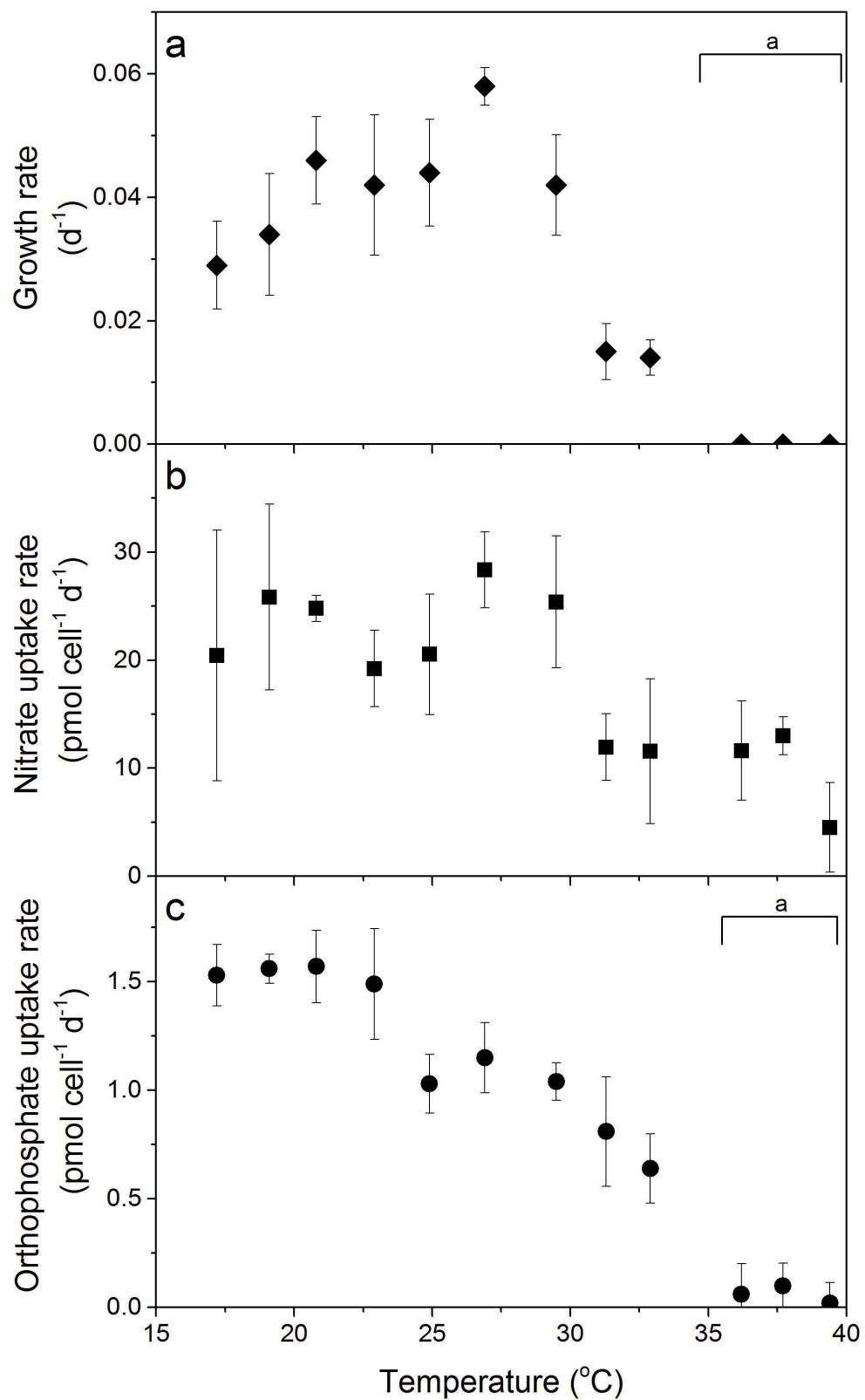


Figure 3.4 Physiological responses of *N. oculata* after 96 hours at varying temperatures: (a) specific growth rate (diamonds), (b) nitrate uptake rate (squares) and (c) orthophosphate uptake rate (circles) where symbols represent the average of triplicates ($n=3$) with errors corresponding to ± 1 standard deviation. Square brackets and letters represent groups of statistical different values ($p < 0.05$).

In terms of photophysiological response of *N. oculata* following 96 h (**Figure 3.5**), rETR was significantly greater between 20.8 and 29.5 °C (denoted a; **Figure 3.5a**) with no observed photosynthesis at 36.2 °C where rETR was zero ($p < 0.05$). Comparatively, F_v/F_m shows a near flat response between 17.2 and 32.9 °C and zero values above 36.2 °C (**Figure 3.5b**). Unlike at 24 h, rETR and F_v/F_m increased significantly after 96 h exposure in treatments where growth was observed (17.2 - 32.9 °C; **Figure 3.3**, **Figure 3.5**, respectively). However, unlike F_v/F_m that showed a similar thermal response through time (flat), the decreased rETR at elevated temperatures (> 29 °C) after 24 h was not evident after 96 h (**Figure 3.3** and **Figure 3.5a**, respectively).

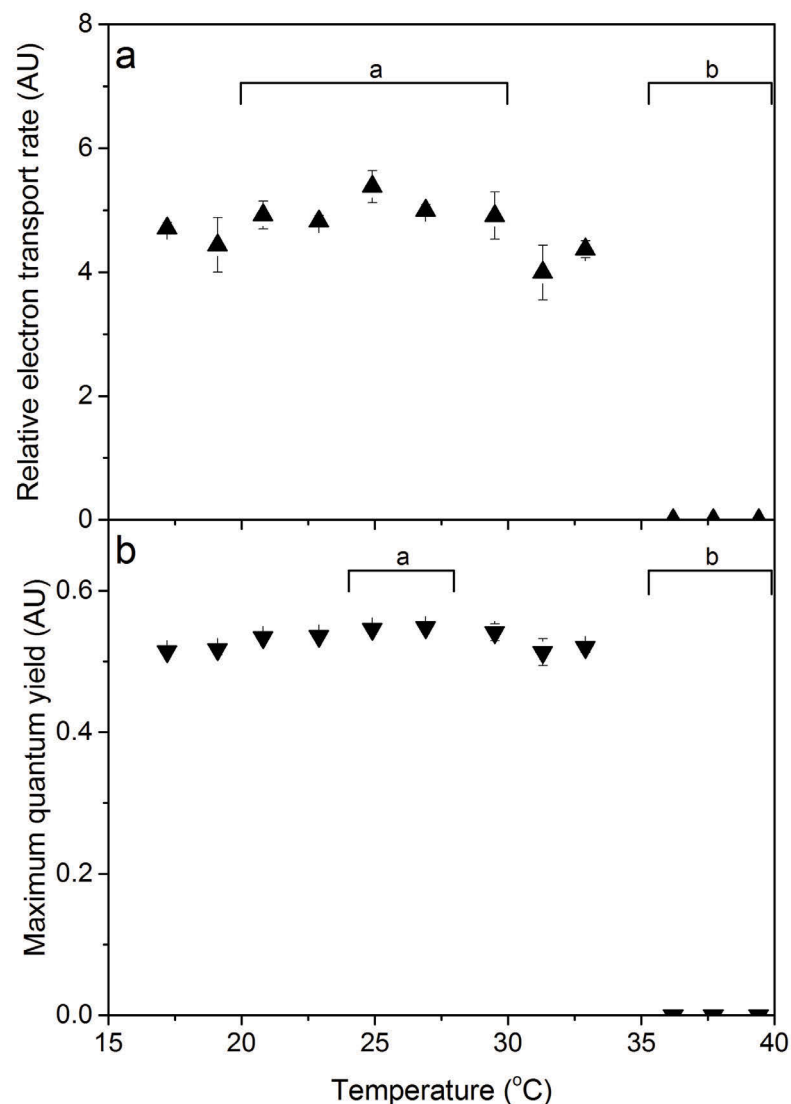


Figure 3.5 Relative electron transport rate (rETR) and maximum quantum yield of *N. oculata* after 96 hours at varying temperatures: (a) rETR corresponds to value at 2 seconds after induction of light performed on Imaging-PAM. (b) Maximum quantum yield was determined after dark adaption for 15 min. Symbols represent the average of triplicates ($n=3$) with errors corresponding to ± 1 standard deviation.

3.4 Discussion

In order to understand the direct implications of temperature (magnitude and duration) on large-scale microalgae cultures, we provided an in-depth characterisation of thermal responses in the biofuel candidate strain *N. oculata*, by obtaining time-resolved thermal performance curves for a number of algal traits. Furthermore, we demonstrated that the time scale of temperature exposure can shift thermal tolerance ranges and some algal traits, such as photophysiology responded more rapidly to changes in temperature, whereas other traits such as nutrient uptake and growth took longer to respond.

Early responses to temperature change in *N. oculata* were detected in subcellular responses such as photophysiological parameters, specifically rETR following thermal exposures as short as 5 min (**Figure 3.1**). Through deriving parameters from the RLC we were able to show that components of the photosynthetic process (rETR_{max} and I_K) reacted rapidly to changes in the surrounding environment such as light and temperature (Murchie et al. 1999; Hancke et al. 2008). Whilst studies have examined the rate of these thermal changes to the photosynthetic apparatus in *Nannochloropsis* (Figueroa et al. 1997), few studies measure photophysiological responses over a comprehensive range of temperatures (Salleh & McMinn 2011; Mackey et al. 2013) and until now was not available for *N. oculata*. This type of continuous data can be used to better inform models that predict growth of *N. oculata* in outdoor cultivation systems, particularly in response to temperature (Béchet et al. 2013).

The thermal responses of subcellular traits such as photosynthetic rate were dependent on the magnitude and duration of the temperature excursion and thermal acclimation of this trait was evidenced by acclimation of the TPC through time. Short-periods of exposure (5 min duration) of *N. oculata* to temperatures ± 15 °C from long-term culture conditions (25 °C) resulted in a 15% reduction in rETR in comparison to the thermal optima range between 25 – 40 °C (**Figure 3.2**). Following intermediate exposure times, this thermal optima range narrows, as the CT_{max} approaches 36 °C (24 h; **Figure 3.3a**) likely reflecting irreversible damage to PSII at these higher temperatures. Damage of this nature may occur due to the occurrence of Q_B non-reducing centres, the highly sensitive oxygen evolving complex (Suklenik et al. 2009), as well as, the impairment of repair to the reaction centre protein, D1. Previous observation in *Nannochloropsis* suggest that this repair is irreversible above 40 °C, (Figueroa et al. 1997). This thermal window of photosynthetic operation remains stable,

but acclimation to warmer temperatures becomes evident as rETR at temperatures greater than 27 °C is more similar to the thermal optima range producing a thermal performance curve that is less bell-shaped and more flat (**Figure 3.5**). These changes in photosynthesis through time may indicate the regulatory mechanisms that control thermal acclimation are triggered following exposure to either different magnitudes of temperature stress and/or duration of exposure.

Compared to sub-cellular traits, a definitive TPC of whole-organism traits (e.g. growth) manifested following much longer timeframes (days). Unlike rETR that exhibited clear differences following 24 h exposure (**Figure 3.2**, **Figure 3.3**), growth and nutrient uptake remained highly variable until 96 h of temperature exposure (**Supplementary Figure 3.1** and **Figure 3.4**, respectively). These differences in timeframes between whole-organism and sub-cellular response times are mostly likely due to differences in the underlying mechanisms that define the time limits of thermal exposure, whereby adaptive changes in population traits such as growth take longer to respond (Pörtner 2002). This is because growth is comprised of hundreds if not thousands of underlying sub-cellular traits, each with different tolerances, sensitivities and acclamatory capacity (Willmer et al. 2009). Trade-offs in these traits must first occur and reassemble if necessary, in order for the final thermal performance curve (growth) to take shape (Angilletta et al. 2003).

A rapid response in thermal acclimation was exhibited by *N. oculata*, as the thermal performance curve for growth appeared to stabilize following 96 h of exposure to new temperatures (**Figure 3.4**), reflecting thermal performance curves for this species following 10 days of exposure (Chen et al. 2012) and others of this genus (Sandnes et al. 2005). *N. oculata* showed similar productivity over a wide range of temperatures (continuous exposure between 15 and 30 °C) demonstrating a thermal ‘generalist’ response. These findings aid our understanding of why fluctuations in temperature (diel range of 10 °C; Tamburic et al. 2014 and **Chapter 2**) do not appear to affect productivity in this strain and furthers the potential of its use for large-scale cultivation (Shurin et al. 2013). This is because if large temperature excursions occur, it is less likely that the culture will ‘crash’ and production of reliable yields can be obtained over a large temperature range.

Temperature screening of *N. oculata* in this study has obtained empirical data in order to determine the appropriate conditions for growth and therefore suitable cultivation locations for this strain to be used as a biofuel stock. Firstly, our findings suggested

that monocultures of *N. oculata* would be ideal for cultivation locations where culture temperatures do not frequently exceed exposure to 30 °C for more than three consecutive days. Secondly, *N. oculata* could serve as a reliable generalist in polyculture biofuel feedstocks. At the cultivation locations deemed to be most suitable for biofuel microalgae production in Australia (north-west coast of Western Australia; Borowitzka et al. 2012), high temperature specialists are likely to be required because average daily air temperatures fluctuate around 30 °C or higher (BOM 2016) and may result in a high temperature culture environment. However, these high temperature specialist cultures are not very reliable because small swings in temperature can dramatically reduce productivity (Belay 1997). In order to ensure production at these cultivation systems is more predictable, the implementation of artificial algal assemblages could be highly effective, whereby *N. oculata* could serve as an ideal candidate to support high temperature specialist strains and ultimately yield a highly productive and consistent biofuel feedstock (Nalley et al. 2014).

The better understanding of thermal limits of *N. oculata* obtained in this study in conjunction with meteorological data (anticipated magnitude and duration of temperature conditions) can be used to monitor the productivity of the biofuel feedstock through time and better predict the production outputs. Non-invasive techniques such as fluorometry that can be used to probe sub-cellular processes that respond rapidly to changes in temperature such as photosynthesis, could serve as valuable tools in management strategies as early detectors of temperature stress. Especially, given that these non-invasive techniques couple well with other measures of productivity such as oxygen evolution and carbon fixation (Hancke et al. 2008; Sukenik et al. 2009). These findings are significant because the ability to detect significant reductions in photosynthetic capacity over 24 h timescales has important implications for large-scale cultivation of *N. oculata*. For example, the most suitable and highly productive locations for cultivation are found at coastal locations in tropical regions where temperatures are sustained close to those shown to disrupt photosynthetic mechanisms within *N. oculata* (Tredici 2010). In the present study, changes in photosynthesis, specifically rETR and F_v/F_m were detected within minutes after the onset of increased temperature and days before a change in cell yield could be detected. These findings provide further evidence of the capacity of fluorometry-derived photosynthetic parameters to be implemented as non-invasive tools in management strategies.

In this study, thermal screening of *N. oculata* has provided useful insights into potential cultivation locations for this strain as either monoculture or polyculture seeds for biofuel

feedstocks as its thermal 'generalist' nature provide thermally reliable cultivation seeds for algae farms where locations experience high variability in climate. It is likely that further screening of other biofuel candidate strains through bio-prospecting over multivariate conditions will shed light into other valuable strains that can be matched to specific locations. For example, cultures with high temperature and hypersaline tolerance would be ideal seed inoculums in regions that have sustained high temperatures, as these locations are also synonymous with high evaporative rates (Mata et al. 2010). The detailed active chlorophyll fluorometry characterisation of the thermal responses of *N. oculata* presented suggests that fluorometric-derived photosynthetic parameters provide useful measures of culture health as their short-term responses to changes in temperature enable rapid detection of thermal stress. Further understanding of how these indicators translate into longer term responses such as changes in final culture yields, will enable us to better predict when culture crashes are likely to occur by monitoring responses through time. Advancing our mechanistic understanding behind these responses over different timescales and how these changes translate into effects on biomass will better our management practices and improve productivity.

3.5 Acknowledgements

The authors would like to thank the Climate Cluster (C3), University of Technology Sydney for financial support and A/Prof. Martina Doblin and Prof. Maria Byrne for use of equipment.

The University of Dundee is a registered Scottish charity. No.SC015096.

3.6 References

- Angilletta, M.J., Wilson, R.S., Navas, C.A. & James, R.S. 2003, 'Tradeoffs and the evolution of thermal reaction norms', *Trends in Ecology & Evolution*, vol. 18, no. 5, article, pp. 234–40.
- Baker, K.G., Robinson, C.M., Radford, D.T., McInnes, A.S., Evenhuis, C. & Doblin, M.A. 2016, 'Thermal performance curves of functional traits aid understanding of thermally induced changes in diatom-mediated biogeochemical fluxes', *Frontiers in Marine Science*, vol. 3, e44.
- Béchet, Q., Shilton, A. & Guieysse, B. 2013, 'Modeling the effects of light and temperature on algae growth: state of the art and critical assessment for productivity prediction during outdoor cultivation.', *Biotechnology Advances*, vol. 31, no. 8, pp. 1648–63.
- Belay, A. 1997, 'Mass culture of *Spirulina* outdoors- The Earthrise Farms experience', in A. Vonshak (ed.), *Spirulina platensis (Arthrospira): Physiology, Cell-biology and Biotechnology*, Taylor & Francis Ltd, London, pp. 131–58.
- BOM 2016, 'Climate Data Online', *Bureau of Meteorology Climate Data online*, viewed 3 February 2016, <<http://www.bom.gov.au/climate/data/>>.
- Borowitzka, M.A. 1999, 'Commercial production of microalgae: ponds, tanks, tubes and fermenters', *Journal of Biotechnology*, vol. 70, no. 1, pp. 313–321.
- Borowitzka, M.A. 2013, 'High-value products from microalgae- their development and commercialisation', *Journal of Applied Phycology*, vol. 25, no. 3, pp. 743–56.
- Borowitzka, M.A., Boruff, B.J., Moheimani, N.R., Pauli, N., Cao, T., Smith, H., Michael A., B., Bryan J, B., Navid R., M., Natasha, P., Yinghui, C. & Helen, S. 2012, 'Identification of the optimum sites for industrial- scale microalgae biofuel production in WA using a GIS Model', *The Centre for Research into Energy for Sustainable Transport (CREST)*, pp. 1–35.
- Chen, S.Y., Pan, L.Y., Hong, M.J. & Lee, A.C. 2012, 'The effects of temperature on the growth of and ammonia uptake by marine microalgae', *Botanical Studies*, vol. 53, no. 1, pp. 125–33.
- Chisti, Y. 2007, 'Biodiesel from microalgae', *Biotechnology Advances*, vol. 25, no. 3, pp. 294–306.
- Falkowski, P.G. & La Roche, J. 1991, 'Acclimation to spectral irradiance in algae', *Journal of Phycology*, vol. 27, no. 1, pp. 8–14.
- Figuerola, F.L., Jiménez, C., Lubián, L.M., Montero, O., Lebert, M. & Häder, D.-P.P. 1997, 'Effects of high irradiance and temperature on photosynthesis and photoinhibition in *Nannochloropsis gaditana* Lubián (Eustigmatophyceae)', *Journal of Plant Physiology*, vol. 151, no. 1, pp. 6–15.
- Fisher, T., Minnaard, J. & Dubinsky, Z. 1996, 'Photoacclimation in the marine alga *Nannochloropsis* sp. (Eustigmatophyte): a kinetic study', *Journal of Plankton*

- Research*, vol. 18, no. 10, pp. 1797–818.
- Fon Sing, S., Isdepsky, A., Borowitzka, M.A. & Moheimani, N.R. 2013, 'Production of biofuels from microalgae', *Mitigation and Adaptation Strategies for Global Change*, vol. 18, no. 1, pp. 47–72.
- Genty, B., Briantais, J.-M. & Baker, N.R. 1989, 'The relationship between the quantum yield of photosynthetic electron transport and quenching of chlorophyll fluorescence', *Biochimica et Biophysica Acta (BBA)-General Subjects*, vol. 990, no. 1, pp. 87–92.
- Girden, E.R. 1992, *ANOVA: Repeated measures*, A. Virding (ed.), 1st edn., Sage, Newbury Park.
- Guillard, R. & Ryther, J. 1962, 'Studies of marine planktonic diatoms: I. *Cyclotella nana* Hustedt, and *Dentonula confervacea* (Cleve) Gran', *Canadian Journal of Microbiology*, vol. 8, pp. 229–39.
- Hancke, K., Hancke, T.B., Olsen, L.M., Johnsen, G. & Glud, R.N. 2008, 'Temperature effects on microalgal photosynthesis-light responses measured by O₂ production, pulse-amplitude-modulated fluorescence, and ¹⁴C assimilation', *Journal of Phycology*, vol. 44, no. 2, pp. 501–14.
- Hoening, M., Lee, R.J. & Ferguson, D.C. 1989, 'A microtiter plate assay for inorganic phosphate', *Journal of Biochemical and Biophysical Methods*, vol. 19, pp. 249–51.
- Huey, R.B., Kearney, M.R., Krockenberger, A., Holtum, J.A.M., Jess, M. & Williams, S.E. 2012, 'Predicting organismal vulnerability to climate warming: roles of behaviour, physiology and adaptation', *Philosophical Transactions of the Royal Society of London B: Biological Sciences*, vol. 367, no. 1596, pp. 1665–79.
- Huey, R.B. & Stevenson, R.D. 1979, 'Integrating thermal physiology and ecology of ectotherms: a discussion of approaches', *American Zoologist*, vol. 19, no. 1, pp. 357–66.
- Kroon, B.M.A., Latasa, M., Ibelings, B.W. & Mur, L.R. 1992, 'The effect of dynamic light regimes on *Chlorella*. Pigments and cross sections', *Hydrobiologia*, vol. 238, pp. 71–8.
- Lukeš, M., Procházková, L., Schmidt, V., Nedbalová, L. & Kaftan, D. 2014, 'Temperature dependence of photosynthesis and thylakoid lipid composition in the red snow alga *Chlamydomonas* cf. *nivalis* (Chlorophyceae)', *FEMS Microbiology Ecology*, vol. 89, no. 2, pp. 303–15.
- Lundquist, T.J., Woertz, I.C., Quinn, N.W.T. & Benemann, J.R. 2010, *A realistic technology and engineering assessment of algae biofuel production*, Energy Biosciences Institute- University of California, Berkeley, California.
- Mackey, K.R.M., Paytan, A., Caldeira, K., Grossman, A.R., Moran, D., McIlvin, M. & Saito, M.A. 2013, 'Effect of temperature on photosynthesis and growth in marine *Synechococcus* spp.', *Plant Physiology*, vol. 163, no. 2, article, pp. 815–29.
- Mallick, N. 2002, 'Biotechnological potential of immobilized algae for wastewater N, P and metal removal: A review', *BioMetals*, vol. 15, no. 4, pp. 377–90.
- Mata, T.M., Martins, A.A. & Caetano, N.S. 2010, 'Microalgae for biodiesel production and other applications: A review', *Renewable and Sustainable Energy Reviews*, vol. 14, no. 1, pp. 217–32.
- Moheimani, N.R. & Borowitzka, M.A. 2007, 'Limits to productivity of the alga *Pleurochrysis carterae* (Haptophyta) grown in outdoor raceway ponds', *Biotechnology and Bioengineering*, vol. 96, no. 1, pp. 27–36.
- Murchie, E.H., Chen, Y., Hubbart, S., Peng, S. & Horton, P. 1999, 'Interactions between senescence and leaf orientation determine in situ patterns of

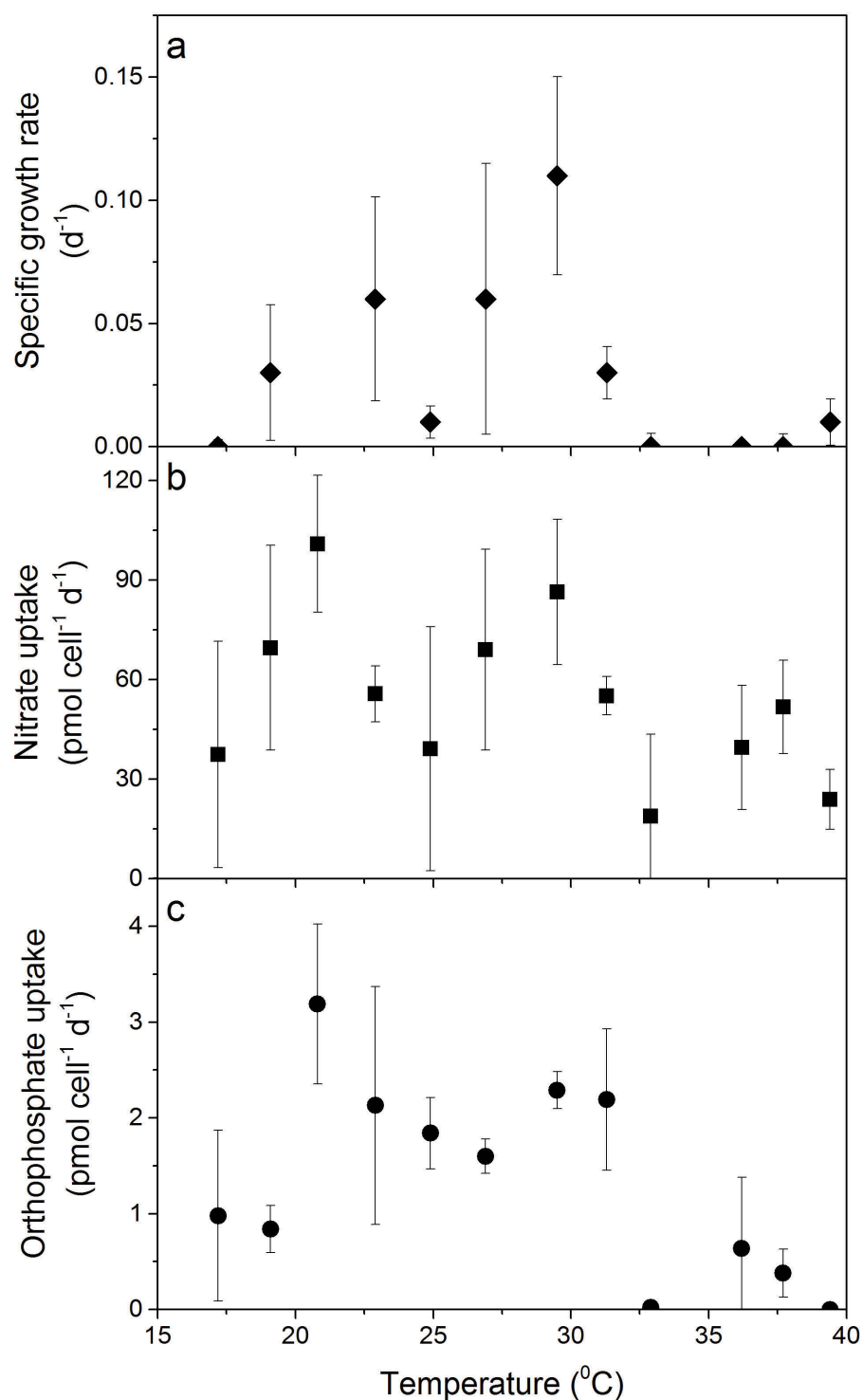
- photosynthesis and photoinhibition in field-grown rice', *Plant Physiology*, vol. 119, no. 2, pp. 553–64.
- Nalley, J.O., Stockenreiter, M. & Litchman, E. 2014, 'Community Ecology of Algal Biofuels: Complementarity and Trait-Based Approaches', *Industrial Biotechnology*, vol. 10, no. 3, pp. 191–201.
- Pörtner, H.-O. 2002, 'Climate variations and the physiological basis of temperature dependent biogeography: systemic to molecular hierarchy of thermal tolerance in animals', *Comparative Biochemistry and Physiology Part A: Molecular & Integrative Physiology*, vol. 132, no. 4, pp. 739–61.
- Ralph, P.J. & Gademann, R. 2005, 'Rapid light curves: A powerful tool to assess photosynthetic activity', *Aquatic Botany*, vol. 82, no. 3, pp. 222–37.
- Raven, J.A. & Geider, R.J. 2003, 'Adaptation, Acclimation and Regulation in Algal Photosynthesis', in A.W.D. Larkum, S.E. Douglas & J.A. Raven (eds), *Photosynthesis in Algae*, Springer Netherlands, pp. 385–412.
- Richmond, A., Vonshak, A. & Arad, S.M. 1980, *Environmental limitations in outdoor production of algal biomass, Algae biomass: production and use*, National Council for Research and Development, Israel and the Gesellschaft für Strahlen-und Umweltforschung (GSF), Munich, Germany.
- Salleh, S. & McMinn, A. 2011, 'Photosynthetic response and recovery of Antarctic marine benthic microalgae exposed to elevated irradiances and temperatures', *Polar Biology*, vol. 34, no. 6, pp. 855–69.
- Sandnes, J.M., Wenner, D., Källqvist, T., Wenner, D. & Gislerød, H.R. 2005, 'Combined influence of light and temperature on growth rates of *Nannochloropsis oceanica*: linking cellular responses to large-scale biomass production', *Journal of Applied Phycology*, vol. 17, no. 6, pp. 515–25.
- Schnetger, B. & Lehnert, C. 2014, 'Determination of nitrate plus nitrite in small volume marine water samples using vanadium(III)chloride as a reduction agent', *Marine Chemistry*, vol. 160, pp. 91–8.
- Schreiber, U. 2004, 'Pulse-Amplitude-Modulation (PAM) Fluorometry and Saturation Pulse Method: An Overview', in G.C. Papageorgiou (ed.), *Chlorophyll a fluorescence*, Springer Netherlands, pp. 279–319.
- Sforza, E., Simionato, D., Giacometti, G.M., Bertucco, A. & Morosinotto, T. 2012, 'Adjusted light and dark cycles can optimize photosynthetic efficiency in algae growing in photobioreactors.', *PloS One*, vol. 7, no. 6, e38975.
- Shurin, J.B., Abbott, R.L., Deal, M.S., Kwan, G.T., Litchman, E., McBride, R.C., Mandal, S. & Smith, V.H. 2013, 'Industrial-strength ecology: trade-offs and opportunities in algal biofuel production', *Ecology Letters*, vol. 16, no. 11, pp. 1393–404.
- Suggett, D.J., Goyen, S., Evenhuis, C., Szabó, M., Pettay, D.T., Warner, M.E. & Ralph, P.J. 2015, 'Functional diversity of photobiological traits within the genus *Symbiodinium* appears to be governed by the interaction of cell size with cladal designation.', *The New Phytologist*, vol. 208, no. 2, pp. 370–81.
- Sukenik, A., Beardall, J., Kromkamp, J.C., Kopecký, J., Masojídek, J., van Bergeijk, S., Gabai, S., Shaham, E. & Yamshon, A. 2009, 'Photosynthetic performance of outdoor *Nannochloropsis* mass cultures under a wide range of environmental conditions', *Aquatic Microbial Ecology*, vol. 56, no. 2–3, pp. 297–308.
- Tamburic, B., Guruprasad, S., Radford, D.T., Szabó, M., Lilley, R.M., Larkum, A.W.D., Franklin, J.B., Kramer, D.M., Blackburn, S.I., Raven, J.A., Schliep, M. & Ralph, P.J. 2014, 'The effect of diel temperature and light cycles on the growth of *Nannochloropsis oculata* in a photobioreactor matrix.', *PloS One*, vol. 9, no. 1,

e86047.

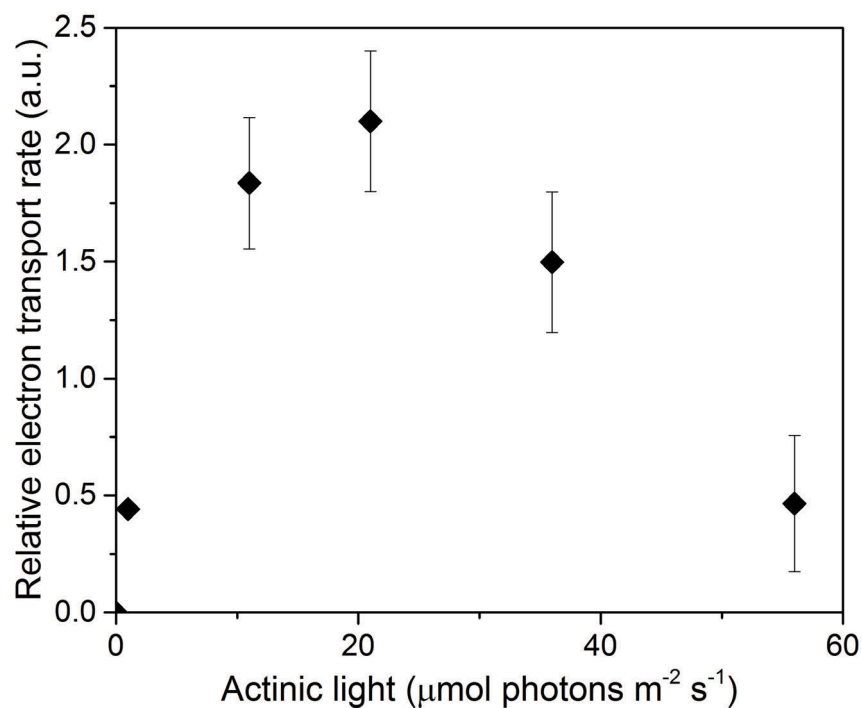
Tredici, M.R. 2010, 'Photobiology of microalgae mass cultures: understanding the tools for the next green revolution', *Biofuels*, vol. 1, no. 1, pp. 143–62.

Willmer, P., Stone, G. & Johnston, I. 2004, *Environmental physiology of animals*, P. Willmer, G. Stone & I. Johnston (eds), 2nd edn., Wiley-Blackwell, Oxford.

3.7 Supplementary figures



Supplementary Figure 3.1 Physiological responses of *N. oculata* after 24 hours at varying temperatures: (a) specific growth rate (diamonds), (b) nitrate uptake rate (squares) and (c) orthophosphate uptake rate (circles) where symbols represent the average of triplicates (n=3) with errors corresponding to ± 1 standard deviation.



Supplementary Figure 3.2 Steady state light curve of *N. oculata*: rETR was calculated using the Imaging-PAM (Walz, Germany), samples were exposed to 5 min actinic light prior determination of relative electron transport rate. Symbols represent the average of triplicates ($n=3$) with errors corresponding to ± 1 standard deviation. Data from this analysis was used to determine the actinic light required for the induction curves.

Chapter 4 Satisfying the nutrient tank of *Nannochloropsis oculata*

Dale T. Radford¹, Kirralee G. Baker¹, Unnikrishnan Kuzhiumparambil¹, John A. Raven^{1,2}, Milán Szabó^{1,3} and Peter J. Ralph¹.

Affiliations

¹ Climate Change Cluster (C3), University of Technology Sydney, Broadway, NSW 2007, Australia

² Division of Plant Sciences, University of Dundee at the James Hutton Institute, Invergowrie, Dundee DD2 5DA, UK

³ Division of Plant Sciences, Research School of Biology, The Australian National University, Sullivans Creek Road, Acton, ACT 2601, Australia

Keywords

sustainable microalgae cultivation, nutrient input, N:P, nitrogen, phosphorus

Abbreviations:

N: nitrogen

P: phosphorus

FAME: fatty acid methyl ester

EPA: eicosapentaenoic acid

NO₃⁻: nitrate

PO₄³⁻: orthophosphate

O.D.: optical density

The following chapter is formatted to be submitted to *Bioresource Technology* and is therefore structured according to its journal requirements in atypical outline to the other chapters.

4.1 Introduction

Microalgae have potential for many 'renewable' commercial applications such as bioremediation and the production of nutraceuticals and bioenergy (Mata et al. 2010). In order to ensure that these microalgal applications are commercially viable, maximum quantities of microalgae must be produced at minimal input costs. Life cycle analysis (LCA) of production at cultivation scale indicates the nutrient requirement of microalgae will ultimately determine whether these applications will be both economically and environmentally viable (Johnson et al. 2013; Markou et al. 2014).

In order to produce the algal biomass required for commercial scale production, large quantities of nitrogen (N) and phosphorus (P) are necessary to support growth, as these nutrients are essential elements for all organisms. The absolute nutrient requirements scale as a function of yield, for example, to produce 1000 kg of algal biomass, up to 50 - 80 kg of N and 5 kg of P are required (Borowitzka & Moheimani 2013c) and are delivered to these cultivation systems in the form of fertilisers. At present, these fertilisers are dispensed in an unsustainable and poorly controlled manner because their initial production from present sources uses fossil fuels and involve considerable greenhouse gas emissions (Wood & Cowie 2004; Johnson et al. 2013). Furthermore, the use of P-based fertilisers in competition with agriculture is not sustainable in the long-term since exploitable sources are finite, with estimates of exhaustion of P reserves on the order of a few centuries (Cordell et al. 2009; Fixen & Johnston 2012). To ensure these fertilisers are used effectively, the potential for reuse of N and P from microalgal biomass (post-harvest) and reuse in the spent culture medium must be explored, as well as the quantity of fertiliser added initially.

A major limitation in the mass-cultivation of microalgae for the bioenergy market is the price of fertilisers which contribute towards a significant portion of the overall energy and financial cost of production. The lower profit margins of the bioenergy industry based on calculations of Borowitzka (2013), dictate that a barrel of algae crude oil needs to be produced at an overall production cost of \$AU 59.73 per barrel in order to be equivalent to market price of crude oil. This algal derived product is more expensive to produce in comparison to high-lipid containing cells, as they require a greater amount of fertilisers to support production on a per cell basis (Borowitzka 2013). This is because microalgae acquire inorganic N and P from the surrounding environment via active transport (Hipkin et al. 1983; Gauthier & Turpin 1997) in order to synthesise key cellular components for growth and photosynthesis and ultimately generates a positive

feedback loop that regulates its own cellular synthesis (Ticconi & Abel 2004). This means that in order to generate biomass rapidly, the provision of optimal growth conditions is a necessity, meaning N and P macronutrients must be delivered in quantities equal to algae requirements. The delivery of a commercially viable alternative to fuel can be aided by cost-efficiency analysis and balancing nutrient inputs with algal requirements to ensure the product matches the quantity and quality of the market demand and to ensure that the usage of fertilisers is sustainable.

Whilst economics dictate nutrient inputs for the bioenergy industry, understanding algal metabolic pathways underpins the 'high-value product' market. Over the past decade, valuable algal metabolites (e.g. carotenoids, poly-unsaturated fatty acids and phycobilins) and their derived products have received significant interest by research and commercial communities (Maity et al. 2014). In particular, the decline of wild fish stocks have driven interest into alternative sources of the omega-3 fatty acids that these fish contain, for either direct extraction for use in nutraceuticals or as a supplement fish feed (including bivalves) for the aquaculture industry (Robert & Trintignac 1997; Li et al. 2009; Lim et al. 2012; Rasdi & Qin 2014). As a result, market interest has driven research to investigate specific metabolic pathways, such as eicosapentaenoic acid (EPA) production. It is known that unfavorable growth conditions such as nutrient stress result in the accumulation of lipid components including fatty acids such as EPA (Adarme-Vega et al. 2012) that ultimately yields a lower biomass, but with a greater lipid-content on a cellular basis. A greater understanding of how the quantity and quality (% of targeted fatty acid) of cellular lipid changes as a function of N and P concentration would better facilitate the production of these high-value metabolite algal products.

Much research has focused on limiting N inputs whereby an algae stress response increases cellular lipid content (Suen et al. 1987; Hu & Gao 2003; Converti et al. 2009). In contrast, using phosphate stress to increase lipid production has received a limited amount of attention with mixed conclusions as to the role in algal physiology (Liang et al. 2013; Roopnarain et al. 2014). Fewer studies have coupled N and P limitation to understand the complex relationship between the two nutrients and the influence this has upon the final product (Mayers et al. 2014; Rasdi & Qin 2015). In all of these cases, the final product has been found to be a function of physiological changes by the alga to different N:P supplies but the effect of varying starting concentrations of N and P (but with stable N:P ratios) remains relatively unexplored. This aspect is particularly important in the context of biomass production, as final productivity is directly

proportional to the initial nutrient supply (Liebig's limitation), but also in terms of cellular lipid accumulation for the "high-value product" industry (Borowitzka 2013). This is because the initial nutrient supply will determine the length of the exponential growth phase, where lower starting supplies result in earlier onset of the stationary phase and therefore higher lipid accumulation than conditions where higher starting supplies are given and growth continues for longer (Haney 1996). To advance our understanding of the minimum inputs of both N and P required for commercial cultivation (i.e. to achieve the maximum rate of biomass production with the greatest lipid content per unit biomass), we need to investigate a more comprehensive N:P matrix over varying N and P starting concentrations.

In this study, we examined the effect of different starting N to P concentrations (but keeping the N:P ratios fixed at 24:1) on algal productivity by measuring growth, nutrient uptake and photosynthetic performance in *N. oculata*. This will aid management practices with regards to the quantities of fertiliser for use in mass-cultivation. To further the potential of algae for metabolites as industrial products, we then compared the effects of optimal and non-optimal N:P on total lipid content and fatty acid methyl ester (FAME) composition over a comprehensive N:P matrix. This will determine whether all nutrient stress conditions increase lipid accumulation or if there is characteristic FAME profile that is specific to N:P ratios. In both cases, algal characteristics were analysed over timescales (e.g. growth) relevant to commercial applications in order to understand how initial starting concentrations affect the final microalgal product.

4.2 Materials and methods

4.2.1 Microalgal culture and medium

Nannochloropsis oculata (Droop) Green (CS-179) was obtained from the ANACC (Australian National Algae Culture Collection, CSIRO, Hobart, Australia) and grown in f/2 media (0.2 µm filtered artificial seawater enriched with; 8.82×10^{-4} M NaNO₃; 3.62×10^{-5} M, NaH₂PO₄·H₂O; trace metal solution and vitamin solution; Guillard & Ryther 1962). Stock cultures of *N. oculata* were maintained at 25 °C under cool-white fluorescent irradiance at 120 ± 10 µmol photons m⁻² s⁻¹ (12 h: 12 h light: dark cycle).

4.2.2 Experimental nutrient matrix

Prior to experimental growth, 40 mL cultures of *N. oculata* were pre-acclimated for 3-4 generations to different starting nutrient concentration, light and temperature conditions. All cultures had the following trace metals (1.17×10^{-5} M FeCl₃·6H₂O; 1.17×10^{-5} M Na₂EDTA·2H₂O; 9.10×10^{-7} M MnCl₂·4H₂O; 7.65×10^{-8} M ZnSO₄·7H₂O; 4.20×10^{-8} M CoCl₂·6H₂O; 3.93×10^{-8} M CuSO₄·5H₂O; 2.60×10^{-8} M Na₂MoO₄·2H₂O) and vitamin concentrations (2.96×10^{-7} M Thiamine HCl; 2.05×10^{-9} M Biotin; 3.69×10^{-10} M Cyanocobalamin). The concentrations of macronutrients nitrogen (NaNO₃) and phosphorus (NaH₂PO₄·H₂O) were manipulated (**Figure 4.1** and **Supplementary Table 4.1**). *N. oculata* was cultivated at 25 °C under cool-white fluorescent irradiance at 120 ± 10 µmol photons m⁻² s⁻¹ (12 h: 12 h light: dark cycle) on an orbital shaker table (Bioline, Australia) to provide gentle agitation. Carbon addition was provided daily through bubbling with 100% CO₂ to return the pH to 6.77 ± 0.29 , maintaining carbon-replete conditions. All treatments were grown under batch conditions.

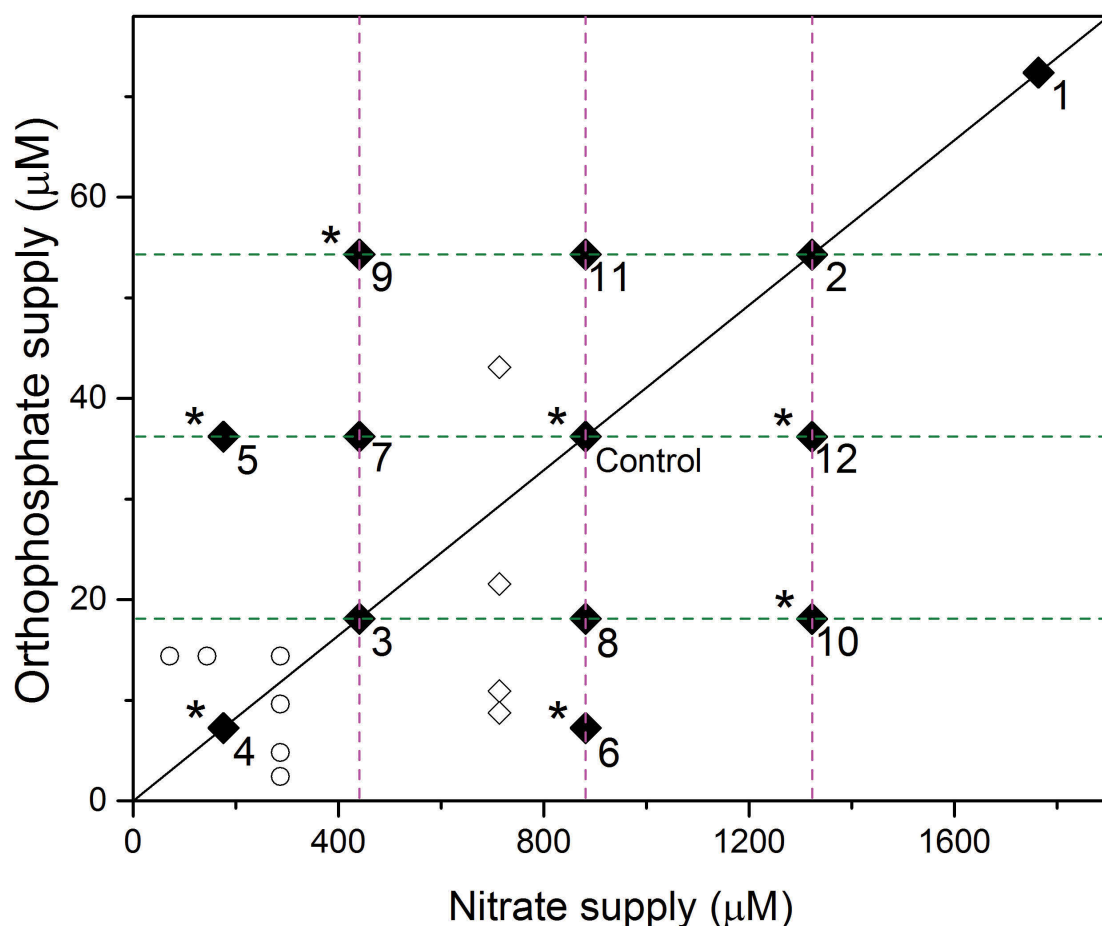


Figure 4.1 Schematic of nutrient supply experimental design. Solid diamonds represents treatments performed in this study with three replicates per treatment ($n=3$). Open diamonds represent treatments performed in Mayer et al. 2013 and open circles represent Rasdi and Qin 2015. Numbers represent treatment identification and asterisks indicate those samples chosen for total lipid quantification and fatty-acid methyl ester (FAME) analysis. Black diagonal line represents constant N:P ratios (24:1) with different magnitude of nutrient supply. Magenta and green broken lines represent samples cultivated under changing N:P, whilst maintaining consistent nitrogen and orthophosphate supply, respectively. The control treatment is traditional f/2 media (882 μM nitrate and 36.2 μM orthophosphate).

4.2.3 Growth analysis

Daily optical density (O.D.) was measured at 750 nm using a microplate spectrophotometer (Infinite 200 PRO series, TECAN). O.D. measurements were then correlated to cell density ($R^2=0.951$), using the image analysis method described in Suggett et al. (2015) and **Chapter 2.2.3**. Specific growth rate was calculated from changes in cell density (cells mL^{-1}) using the following equation:

$$\text{Specific growth rate } (\mu) = \frac{\ln N_1 - \ln N_0}{t_1 - t_0} \quad \text{(Equation 4.1)}$$

where, N_0 and N_1 are the cell densities at time t_0 and t_1 .

4.2.4 Nutrient analysis

Cell suspensions of *N. oculata* were centrifuged at 5000 g for 5 min (Eppendorf 5424R), and the supernatant removed and stored at -20 °C until analysis. Analysis of NO₃⁻ and PO₄³⁻ were performed according to the methods described in **Chapter 3.2.4.4**. Nutrient uptake rates were calculated as the amount of nutrient removal from the media as a function of time and standardised on a per cell basis.

4.2.5 Photophysiological analysis

Maximum quantum efficiency of PSII (F_V/F_M) in *N. oculata* was measured with an Imaging-PAM (Heinz Walz GmbH, Effeltrich, Germany). Samples were dark-adapted for 15 min, subjected to a saturation pulse ($> 3000 \mu\text{mol photons m}^{-2} \text{s}^{-1}$, 800 milliseconds), values were derived according to the following equation:

$$\text{Maximum quantum efficiency of PSII } (F_V/F_M) = \frac{F_M - F_O}{F_M} \quad (\text{Equation 4.2})$$

Where, F_O is the minimum fluorescence of dark-adapted samples and F_M the maximum PSII fluorescence in dark-adapted state.

4.2.6 Lipid content and fatty acid composition analysis

N. oculata biomass (10 mL) for lipid and FAME analysis were harvested in the early stationary phase (n=3) by centrifugation at 3600 g for 10 min. Cells were washed by three repeated cycles of centrifugation and re-suspension in 0.1 M phosphate buffer prior to freeze-drying. Extraction of total lipids from dry biomass was performed according to the Folch et al. (1957) method. Lyophilized samples were extracted with 3 mL of chloroform/methanol mixture (2/1, v/v) by vortexing (1 min) followed by centrifugation. Supernatants were collected and residues re-extracted twice with 2 mL of chloroform/methanol mixture as stated above. Pooled supernatants were dried under a stream of N and total lipid contents were determined gravimetrically. FAMES were prepared by transmethylation of lipid samples following the reactions given as below. One microlitre of 1% NaOH in MeOH was added, followed by heating for 15 min at 55 °C, adding 2 mL of 5% methanolic HCl and further heated for 15 min at 55 °C. Nonadecanoic acid (10 ppm) was used as the internal standard. FAMES were extracted by with hexane (3 x 1 mL) and evaporated to dryness under nitrogen, re-dissolved in 300 μL of hexane and analysed by GC-MS.

GC-MS analysis was performed on an Agilent 7890 series GC coupled to an Agilent quadrupole MS (5975N) using a HP-5MS fused capillary column (5%-phenyl-methylpolysiloxane, 30 m long, 0.25 mm i.d., film thickness 0.25 μm , Agilent

Technologies). The GC carrier gas was helium at a flow rate of 0.9 mL/min. The GC inlet temperature was 280 °C and a splitless mode of injection was used with a purge time of 1 min. Injection volume was 5 µL. The column temperature program was as follows: initial oven temperature 50 °C (held for 2 min), followed by a 4 °C/min ramp up to 220 °C, and then to 300 °C at 60 °C/min (held for 3 min). Peaks were identified by comparison of their retention times with authentic standards (Sigma Aldrich, NSW, Australia).

4.2.7 Statistical analysis

The different treatments were assessed by one-way analysis of variance (ANOVA). If the result was significant ($p < 0.05$), a Tukey's Post Hoc Analysis was performed on the comparisons between means. All statistical analyses were computed using OriginPRO 2015 software (version b9.2.272).

4.3 Results and discussion

In this study, we used different starting concentrations of N and P in order to determine the minimum inputs required to seed *N. oculata* cultures. The impact of various N:P ratios on the final product were examined by assessing growth and biochemical composition.

4.3.1 Growth and nutrient uptake dynamics

The highest specific growth rate ($0.49 \pm 0.07 \text{ d}^{-1}$) was obtained in the control treatment using traditional f/2 medium concentrations at optimal N:P. However, growth rate did not significantly deviate from this value in seven out of the twelve treatments tested (**Figure 4.2**; $p > 0.05$). When N:P were supplied in the optimal ratio of 24:1, growth was comparable for most N and P concentrations assessed, except when N and P concentrations were below $442 \mu\text{M}$ and $18.1 \mu\text{M}$, respectively. These results suggest that the growth rate rather than the final cell yield was restricted by these nutrient concentrations. These findings are unexpected as they are indicative of Blackman rather than Liebig limitation (Andersen 2005). Cellular acclimation to nutrient concentration is controlled by the density of uptake sites on the plasmalemma and in turn controls growth and nutrient uptake (Beardall et al. 2001). We see further evidence of this acclimation in *N. oculata* following the usual response where N and P uptake scale with growth (**Figure 4.3a**) and supply until maximum uptake capacity is reached (**Figure 4.3b**). The time scale of acclimation over which this occurs remains unclear (Smith et al. 2009). It is possible that acclimation period is a function of N and P concentration; thus acclimation may take longer when there is a greater differential in concentrations (i.e. between Control and Treatment 4). This may help to explain why the lowest concentrations of N and P showed signs of nutrient stress, as the cells had not had a chance to completely acclimate like the optimal N:P treatments.

Additionally, this study demonstrated that the N:P provided in f/2 (24:1) is close to the optimal ratio for *N. oculata*, as treatments which were supplied with higher P or N (Treatments 7 and 8, respectively) did not significantly enhance growth rates under the conditions tested (**Figure 4.2**). This is because the N:P uptake rate saturates around 20 moles of N to every mole of P (**Figure 4.3b**), which is similar to the Redfield ratio of 16:1 (Redfield 1958). Unexpectedly, when N was supplied at high N:P ratios (120:1; Treatment 10), uncharacteristically high values of N:P uptake were observed (**Figure 4.3b**). This may indicate non-saturable or biphasic N uptake kinetics, as has been observed for obligate requirements of silicate in diatoms (Collos et al. 1992). Under

these conditions, when nutrient concentrations are in excess of what is required for growth, diffusional uptake can occur and as a result the net flux of N is greatest, but does not necessarily enhance growth and N may get compartmentalised intracellularly (Figure 4.3b).

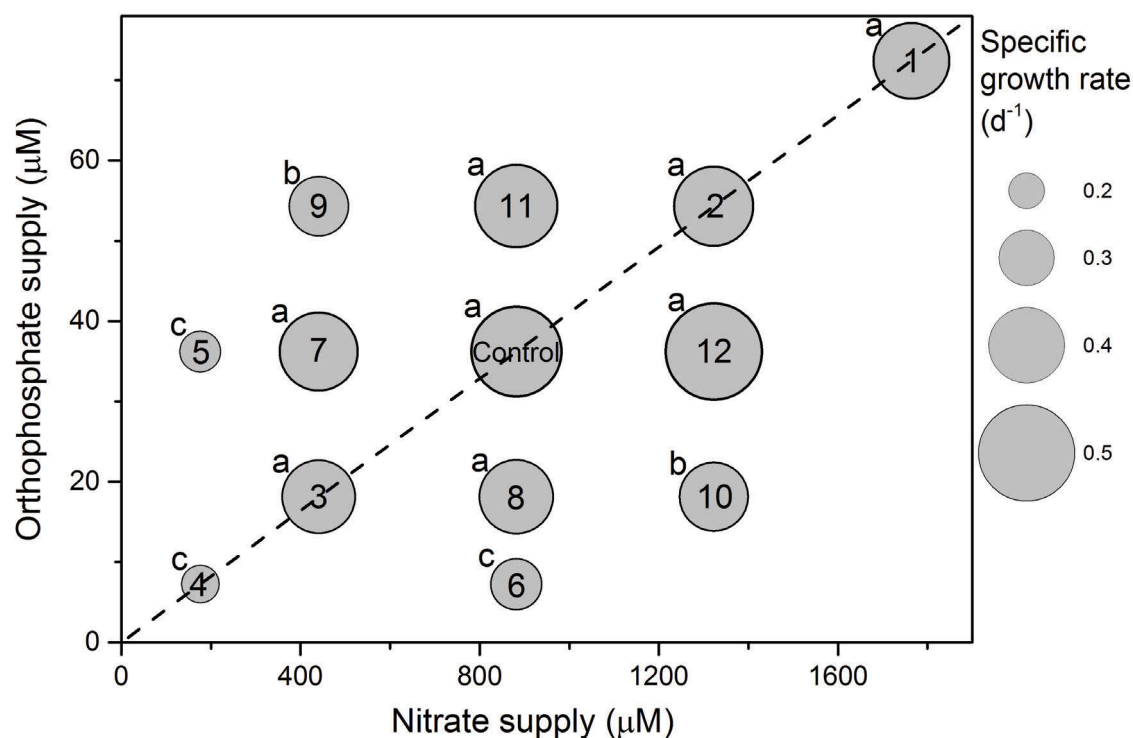


Figure 4.2: Specific growth rates of *N. oculata* cultivated under a matrix of varying nitrate and orthophosphate supply. Bubbles size corresponds to the magnitude of growth rate; bigger bubbles indicate higher growth rates. Each bubble represents the average of triplicate samples ($n=3$). Similarities between treatments are denoted by same letters (one way ANOVA with post hoc Tukeys $p > 0.05$), differences in treatments are denoted by different letters ($p < 0.05$).

Monitoring growth and uptake kinetics over the comprehensive matrix in this study has demonstrated that harnessing the physiological acclimation capacities in *N. oculata* can reduce the absolute N and P concentrations required. As a result, initial starting concentrations of these nutrients can be used in order to avoid excess nutrient usage that could support further batch cultures. Our findings show that under the light and temperature condition used in this experimental set up the initial starting concentrations of f/2 media are currently twofold greater than that required for growth and reducing this by 50% can support the same productivity. Secondly, the matrix experiment showed that it is possible that by providing a longer acclimation period, these nutrient concentrations could be reduced further. Finally, whilst under the conditions tested in this study the optimal ratio of N: P was consistent with f/2 media (24:1). For both optimal ratio and the potential reduction of initial concentrations, it remains unknown

how the response of the microalgae may differ under conditions likely to be experienced in large-scale cultivation systems (i.e. open pond or closed photobioreactor). In these commercial applications, nutrient requirements of either N and/or P may be greater (shift in N:P ratio) under increased mean incident irradiance, temperature or fluctuations of these abiotic parameters and should be investigated further, as the N:P ratio in the cells of a given alga is not constant but may be regulated by environmental conditions (Geider & La Roche 2002).

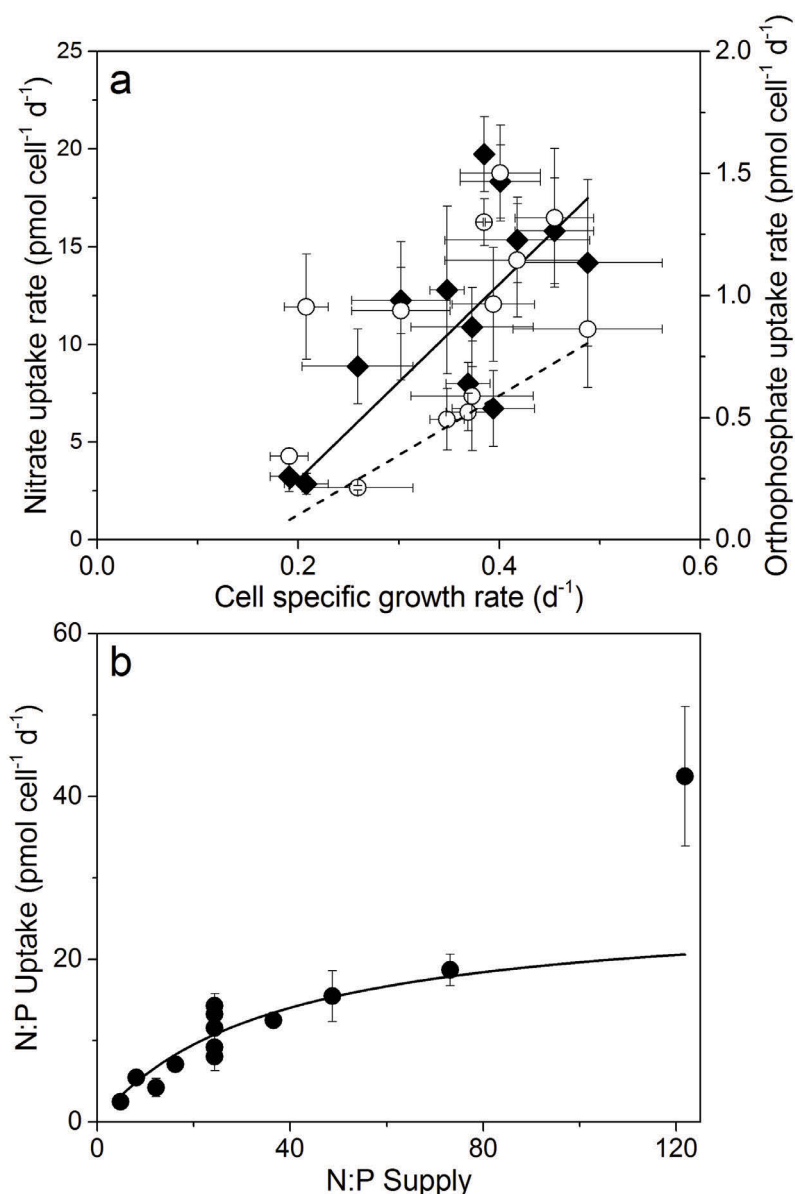


Figure 4.3: Nutrient uptake dynamics of *N. oculata*; (a) Nitrate uptake (solid diamonds) and orthophosphate uptake (open circles) compared to the resulting cell specific growth rate. Solid and broken lines represent the linear regressions ($y = mx + c$) for nitrate ($m = 50.1$; $R^2 = 0.71$) and orthophosphate uptake ($m = 2.44$; $R^2 = 0.20$) respectively. (b) Moles of N uptake per mole of P taken up in *N. oculata* cultivated under different N:P supply ratio. Closed circles represent the average of triplicate samples ($n=3$) with error bars corresponding to ± 1 standard deviation, a Michaelis-Menten model was fitted to the data (solid line; $R^2 = 0.80$).

4.3.2 Physiological dynamics:

Monitoring the maximum quantum efficiency of PSII (F_V/F_M) of *N. oculata* through time provided an indication of PSII operating efficiency under variable N and P concentrations. Specifically, we observed a relationship between F_V/F_M and N and P concentrations as a function of time, where during the period of nutrient uptake (decrease in residual N and P), F_V/F_M increased until nutrients became depleted (dotted line; **Figure 4.4a, b**). At the start of the experiment low F_V/F_M (~0.2 a.u.) values are observed, this may be due to the cultures being inoculated with cells from late exponential phase, where they would have been under a certain level of nutrient (N, P) and carbon stress. An additional decrease may have been the result of culture inoculation (culture transfer to new vessel); this has previously been seen in **Chapter 2** where upon inoculation low F_V/F_M were observed in all treatments. Despite the low initial F_V/F_M , all experimental cultures started to grow as a result of nutrient replenishment. Additionally, we showed that the absolute concentrations of initial N and P supply determine the time of depletion. For example, in the control treatment where N and P concentrations were five-fold greater than in Treatment 4, nutrient depletion occurred two days later (time differential indicated by arrow; **Figure 4.4b**). These F_V/F_M dynamics through time aid an explanation to the significant reduction in F_V/F_M observed in treatments where initial N concentrations were reduced (Treatments 4 and 5; **Figure 4.4c**) and therefore experience a longer period in N-depletion. Nitrogen is known to be a fundamental component of the synthesis of chlorophyll molecules and associated apoprotein involved in capturing light energy for photosynthesis is nitrogen intensive (Raven 1984). Severe nitrogen limitation will cause the reduction in the PSII reaction centres, as well as, the energetic uncoupling of light harvesting antenna from reaction centres (Simionato et al. 2013), strongly impacting the F_V/F_M . Comparatively, when initial P concentrations were reduced, no significant differences in F_V/F_M were observed (Treatments 6 and 10), suggesting that these specific concentrations of P limited growth (**Figure 4.2**) but not the light reactions of photosynthesis.

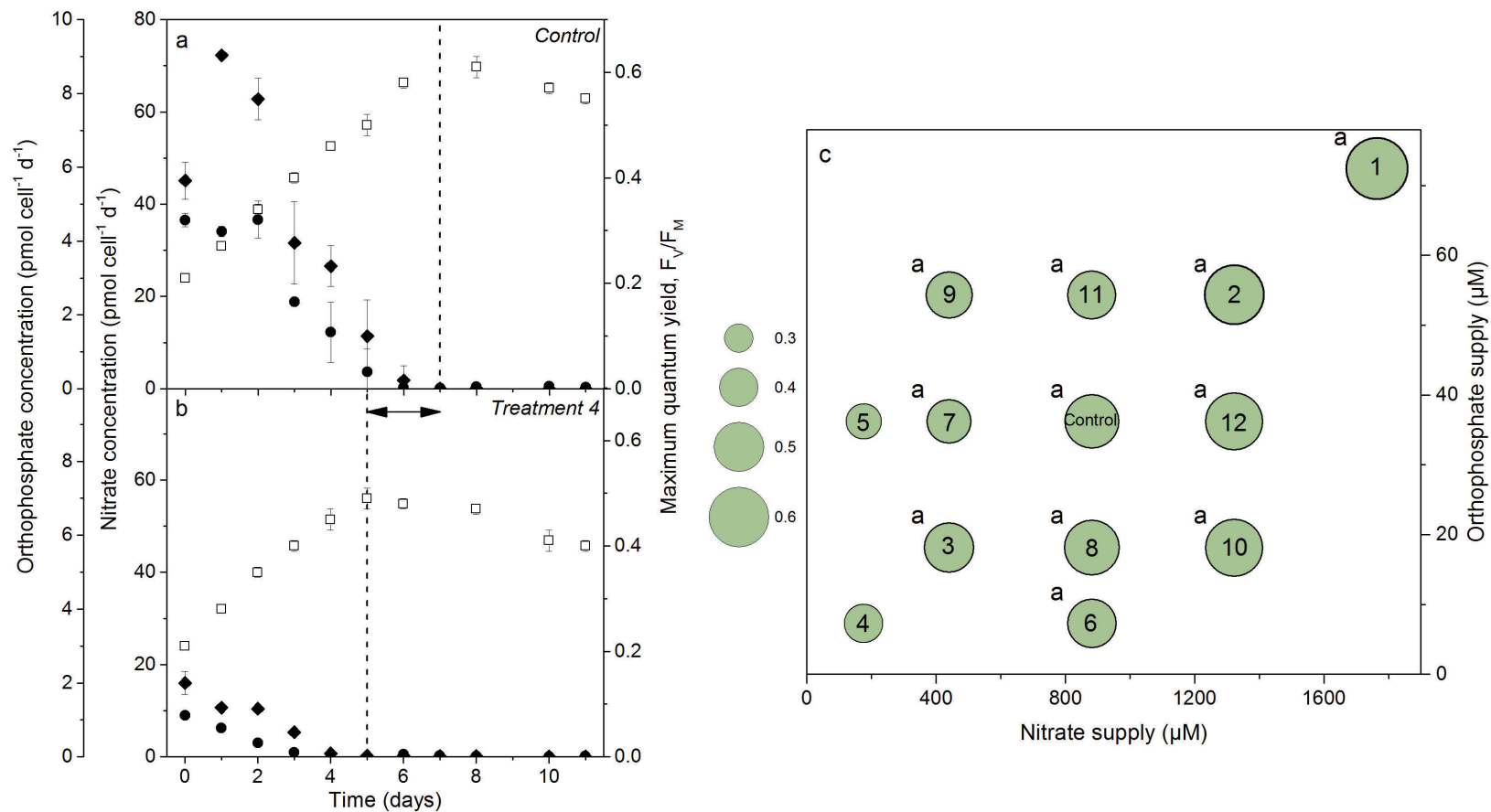


Figure 4.4 (a, b) Nutrient concentration of nitrate (solid diamonds), orthophosphate (solid circles) and maximum quantum yield, F_V/F_M (open squares) over a batch growth of *N. oculata* cultivated under (a) control (882 μM N and 36.2 μM P) and (b) treatment 4 (176 μM N and 7.24 μM P) starting nutrient conditions. Vertical broken line represents the day in which nutrient depletion occurred, double headed arrow indicates time differential of nutrient depletion between the control and treatments 4. (c) Maximum quantum yield (F_V/F_M) of *N. oculata* cultivated under a nutrient matrix measured on the day of harvest. Bubbles size corresponds to the magnitude F_V/F_M (n=3) values are represented by scale-bar adjacent. Letters denote similarity to control (882 μM N and 36.2 μM P; one way ANOVA with post hoc Tukeys $p > 0.05$), numbers represent the different treatment identification.

4.3.3 Biochemical response

Under optimal nutrient conditions for growth (N:P 24:1) total lipid content was $2.58 \pm 0.23 \text{ pg cell}^{-1}$. Deviations from this ratio produced different outcomes in terms of cellular lipid accumulation. Total lipid content increased when N:P was reduced below 24:1. When N supply was reduced by 80% and 50% in Treatments 5 and 9, respectively, a ~20% increase in total lipid content was observed compared to the Control ($p < 0.05$; **Figure 4.5a**), supporting findings that it is solely N-limitation that induces the production of cells with high cellular lipid content (Suen et al. 1987; Sukenik & Carmeli 1990; Gong et al. 2013). This is further supported by the total lipid contents of treatments with N:P ratios greater than 24:1 (Treatment 6; 120:1 and Treatment 10; 73:1) was found when P was limiting and higher N, showed no associated increase in lipid content despite reduced growth rates. These findings are contradictory to those of Rasdi & Qin (2015) who show greatest lipid production occurred at the highest N:P studied (120:1) and are likely due to differences in the way the N:P ratio was experimentally obtained. In the present study, the 120:1 was obtained at threefold higher concentrations of N and P in comparison to Rasdi & Qin (2015), demonstrating that it is not only the N:P, but the importance of specific concentrations of N and P in determining total cellular lipid accumulation.

It is not exclusively lipid content that is targeted for commercial applications but specific fatty acids are also high-value products. The major fatty acids found in all treatments were myristic acid (C14:0), palmitic acid (C16:0), palmitoleic acid (C16:1) and eicosapentaenoic acid (EPA; C20:5), the complete fatty acid composition of *N. oculata* are shown in **Table 4.1**. In this study, an inverse relationship between EPA% and the total cellular lipid was observed (**Figure 4.5**). For example, in Treatments 5 and 9 where cellular lipid content was highest, the EPA% was significantly reduced ($p < 0.05$; **Figure 4.5b**). The largest EPA% was found in Treatment 12 where a 30% increase in N (relative to the control) showed an EPA increase by 36%. Increasing N supply in this way has been found to increase the EPA content similarly within *Nannochloropsis* sp. (Sukenik 1991). Further to cellular nutrient requirements external conditions, i.e. light and temperature have been shown to impact EPA productivity. Chrismadha & Borowitzka (1994) observed increased EPA concentration in *Phaeodactylum tricornutum* with increased cell density and increased irradiance but observed a decreased in EPA content when cultures were supplemented with additional CO₂, suggesting a shift in storage of carbon from lipid to carbohydrate. Similarly, Zittelli et al. 1999, showed EPA productivity of *Nannochloropsis* sp. cultivated in outdoor

bioreactors mimicked biomass productivity which was shown to seasonal, where summer irradiances and temperatures had the best results. Inducing significant changes in EPA would be of particular interest for the aquaculture industry with microalgae such as *N. oculata* with greater EPA content providing high quality feedstocks for marine larvae (Adarme-Vega et al. 2012).

Table 4.1 Fatty acid composition of *N. oculata* cultivated under different nutrient concentrations: Fatty acids are expressed as a % of total fatty acid. Values are means of triplicate samples (n=3), ± 1 standard deviation.

Treatment ID	Control	4	6	12	5	10	9
Starting [NO ₃ ⁻] (μM)	882	176.4	882	1323	176.4	1323	441
Starting [PO ₄ ³⁻] (μM)	36.2	7.24	7.24	36.2	36.2	18.1	54.3
Percentage of FAME							
<i>Saturated fatty acids</i>							
C14:0	5.37±0.24	5.07±0.02	4.02±0.07	5.29±0.21	4.85±0.20	4.51±0.22	5.18±0.25
C15:0	0.44±0.02	0.30±0.02	0.33±0.03	0.55±0.04	0.29±0.01	0.46±0.02	0.32±0.01
C16:0	43.55±1.31	43.93±0.55	40.37±1.08	39.54±0.22	45.72±0.48	39.67±0.42	46.27±0.43
C17:0	0.23±0.03	0.17±0.01	0.17±0.01	0.29±0.02	0.16±0.01	0.26±0.02	0.13±0.01
C18:0	2.37±0.06	2.99±0.16	4.05±0.06	2.91±0.54	2.41±0.17	4.12±0.23	2.44±0.01
<i>Unsaturated fatty acids</i>							
C16:1 n-7	24.61±0.68	27.84±0.33	28.92±0.69	28.34±0.37	27.07±0.50	29.84±0.28	27.89±0.14
C18:1 n-9	8.47±0.31	11.71±0.63	15.56±1.75	7.79±0.74	10.59±0.09	9.98±0.66	10.69±0.35
C18:2 n-6	1.07±0.05	0.85±0.04	0.41±0.06	1.16±0.06	1.07±0.12	0.81±0.07	0.41±0.18
C18:3 n-6	0.24±0.01	0.27±0.01	0.25±0.02	0.27±0.00	0.34±0.02	0.17±0.01	0.36±0.02
C20:3 n-6	0.19±0.07	0.78±0.15	0.95±0.11	0.21±0.03	0.28±0.02	0.5±0.02	0.27±0.02
C20:4 n-6	2.12±0.81	2.07±0.08	1.54±0.10	2.43±0.3	2.58±0.04	1.72±0.22	1.81±0.10
C20:5 n-3	8.35±1.37	4.02±0.04	3.24±0.23	11.21±0.95	4.64±0.31	7.69±0.76	4.22±0.36
Sum SFA ^a	51.95	52.46	48.94	48.59	53.43	49.02	54.35
Sum MUFA ^b	36.08	39.55	44.48	36.13	37.66	39.82	38.58
Sum PUFA ^c	11.97	7.99	6.58	15.28	8.91	11.16	7.07

^a SFA- saturated fatty acids, ^b MUFA- monounsaturated fatty acids, ^c PUFA- polyunsaturated fatty acids.

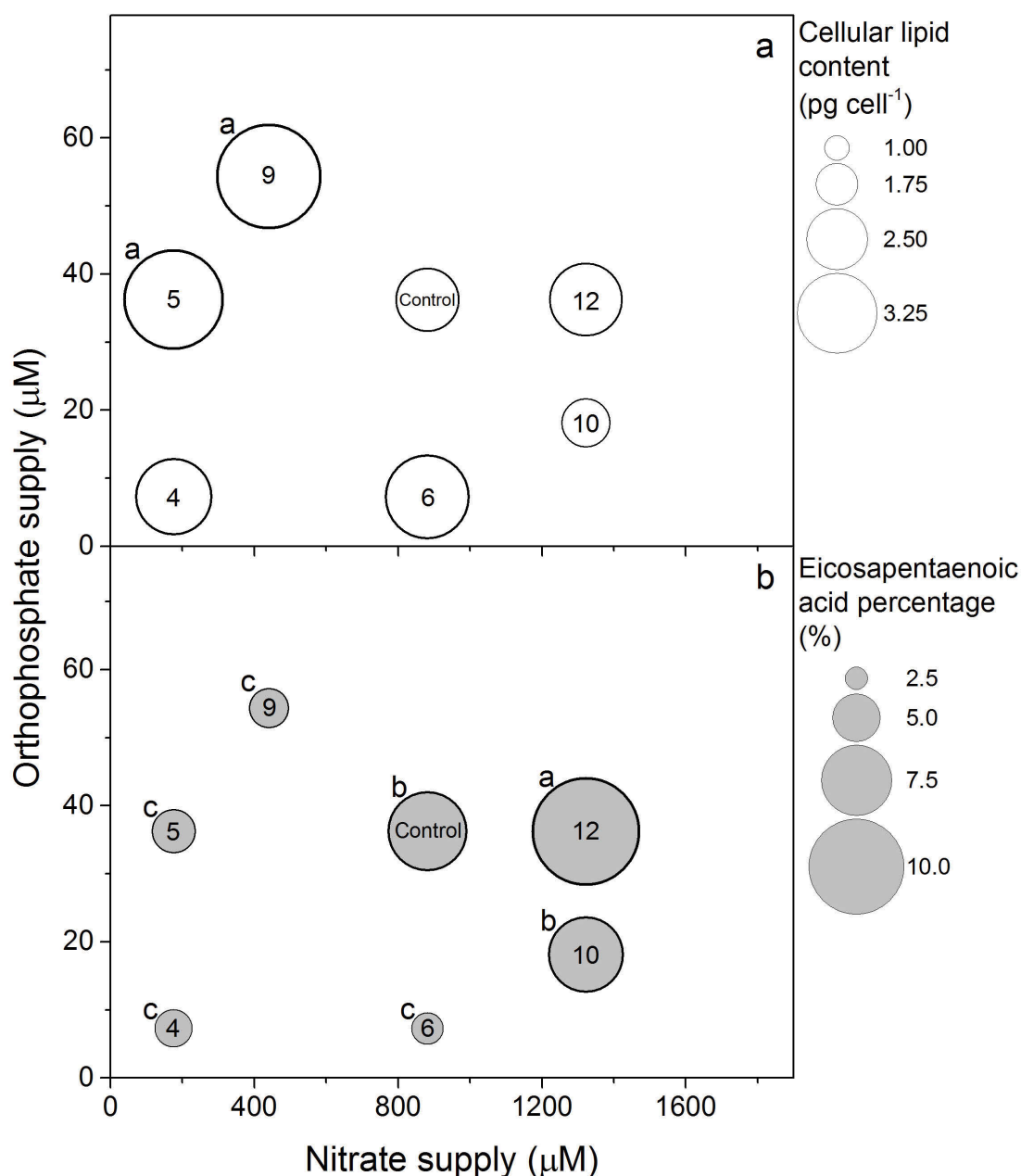


Figure 4.5 Biochemical analysis of *N. oculata* cultivated under a matrix of varying nitrate and orthophosphate supply. (a) Cellular lipid content (pg cell⁻¹), bubble size corresponds to the cellular lipid content according to scale adjacent, where values represents the average of duplicate samples. Letters denoted significant difference in lipid content when compared with control (one way ANOVA with post hoc Tukeys $p < 0.05$). (b) Eicosapentaenoic acid (EPA) percentage, bubble size corresponds to the magnitude of EPA % in scale adjacent. Each bubble represents the average of triplicate samples ($n=3$). Similarity in treatments are denoted by same letters (one way ANOVA with post hoc Tukeys $p > 0.05$), whilst different between treatments are denoted by different letters ($p < 0.05$).

4.3.4 Implications to large-scale

From a bioenergy perspective (i.e. bulk biomass or lipid-derived biofuel) the N:P ratio in the traditionally used f/2 media, provides the optimal ratio of N:P, however the concentrations supplied are twice that required to saturate growth. Scaling back the N and P concentration in equal proportions to 442 μM N and 18.1 μM P showed no reduction of growth rates. Therefore, the nutrient supply cost can be reduced by 50% for production of bulk biomass for conversion into 'green' crude. Alternatively, if the final product is to be used in lipid-derived biofuels, the starting N:P ratio needs to be decreased below 24:1 providing a surplus of P, producing cells with higher cellular lipid content (Treatment 5). Whilst producing greater lipid yield may be of economic benefit, the additional P requirement is not sustainable given the finite availability of usable rock P (Fixen & Johnston 2012). In terms of higher value products such as secondary metabolites (e.g. EPA-rich cells), we found that EPA increases proportionally to the amount of excess N supplied (i.e. 30% increase in EPA when N supplied in 30% excess; Treatment 12). Whilst the increased initial supply is economically more costly, the final product attracts a higher market value due to the 'superior' quality.

4.3.5 Future directions

Whilst this study has provided quantitative information regarding nutrient supply inputs and final product outputs, data were obtained under controlled laboratory environments of constant light and temperature. It is known that these environmental conditions alters the optimal N:P ratio of microalgae and in turn is likely to have implications on growth, lipid content and fatty acid composition (Sukenik 1991; Converti et al. 2009). Previous studies have shown irradiance to effect fatty acid composition, for example, Fábregas et al. (2004) observed in *Nannochloropsis* sp. that as the irradiance increased from 40 to 480 $\mu\text{mol photons m}^{-2} \text{s}^{-1}$ the degree of unsaturation of fatty acids decreased. It is unknown whether these changes in nutrient supply along with the environmental changes experienced at a commercial scale (i.e. varying irradiances) will result in similar final products.

Evidence for the commercial sustainability of industries involving microalgae-derived products remains inconclusive. In this study, we showed the final product varies as a response to starting N and P supply and/or N:P ratio. Bulk production of biomass can be achieved with a N and P supply of 442 μM and 18.1 μM (i.e. at a optimal ratio of 24:1), whereas a lipid derived biofuel will need a surplus of P. By altering the N:P ratio through increasing N supply it would be possible for the aquaculture industry to yield cells with higher EPA content improving the quality of feedstocks.

4.4 Acknowledgments

The authors would like to thank the Climate Change Cluster (C3), University of Technology Sydney for financial support.

The University of Dundee is a register Scottish charity, no. SC 015096.

4.5 References

- Adarme-Vega, T.C., Lim, D.K.Y., Timmins, M., Vernen, F., Li, Y. & Schenk, P.M., 2012. Microalgal biofactories: a promising approach towards sustainable omega-3 fatty acid production. *Microbial Cell Factories*, 11(1), p.96.
- Andersen, R.A., 2005. *Algal Culturing Techniques* 1st edn. R. A. Andersen, ed., Cambridge, MA: Elsevier Academic Press.
- Baker, K.G., Robinson, C.M., Radford, D.T., McInnes, A.S., Evenhuis, C. & Doblin, M.A., 2016. Thermal performance curves of functional traits aid understanding of thermally induced changes in diatom-mediated biogeochemical fluxes. *Frontiers in Marine Science*, 3, p.e44.
- Beardall, J., Young, E. & Roberts, S., 2001. Approaches for determining phytoplankton nutrient limitation. *Aquatic Sciences*, 63(1), pp.44–69.
- Borowitzka, M.A., 2013. High-value products from microalgae- their development and commercialisation. *Journal of Applied Phycology*, 25(3), pp.743–756.
- Borowitzka, M.A. & Moheimani, N.R., 2013. Sustainable biofuels from algae. *Mitigation and Adaptation Strategies for Global Change*, 18(1), pp.13–25.
- Chrimadha, T. & Borowitzka, M.A., 1994. Effect of cell density and irradiance on growth, proximate composition and eicosapentaenoic acid production of *Phaeodactylum tricornutum* grown in a tubular photobioreactor. *Journal of Applied Phycology*, 6(1), pp.67–74.
- Collos, Y., Siddiqi, M.Y., Wang, M.Y., Glass, A.D.M. & Harrison, P.J., 1992. Nitrate uptake kinetics by two marine diatoms using the radioactive tracer ¹³N. *Journal of Experimental Marine Biology and Ecology*, 163(2), pp.251–260.
- Converti, A., Casazza, A.A., Ortiz, E.Y., Perego, P. & Del Borghi, M., 2009. Effect of temperature and nitrogen concentration on the growth and lipid content of *Nannochloropsis oculata* and *Chlorella vulgaris* for biodiesel production. *Chemical Engineering and Processing: Process Intensification*, 48(6), pp.1146–1151.
- Cordell, D., Drangert, J.-O. & White, S., 2009. The story of phosphorus: Global food security and food for thought. *Global Environmental Change*, 19(2), pp.292–305.
- Fábregas, J., Maseda, A., Domínguez, A., Otero, A., Domí, A. & Otero, A., 2004. The cell composition of *Nannochloropsis* sp. changes under different irradiances in semicontinuous culture. *World Journal of Microbiology and Biotechnology*, 20(1), pp.31–35.
- Fixen, P.E. & Johnston, A.M., 2012. World fertilizer nutrient reserves: a view to the future. *Journal of the Science of Food and Agriculture*, 92(5), pp.1001–1005.

- Folch, J., Lees, M. & Stanley, S.G.H., 1957. A simple method for the isolation and purification of total lipids from animal tissues. *Journal of Biological Chemistry*, 226(1), pp.497–509.
- Gauthier, D.A. & Turpin, D.H., 1997. Interactions between inorganic phosphate (P_i) assimilation, photosynthesis and respiration in the P_i -limited green alga *Selenastrum minutum*. *Plant, Cell & Environment*, 20(1), pp.12–24.
- Geider, R. & La Roche, J., 2002. Redfield revisited : variability of C : N : P in marine microalgae and its biochemical basis. *European Journal of Phycology*, 37(1), pp.1–17.
- Gong, Y., Guo, X., Wan, X., Liang, Z. & Jiang, M., 2013. Triacylglycerol accumulation and change in fatty acid content of four marine oleaginous microalgae under nutrient limitation and at different culture ages. *Journal of Basic Microbiology*, 53(1), pp.29–36.
- Guillard, R. & Ryther, J., 1962. Studies of marine planktonic diatoms: I. *Cyclotella nana* Hustedt, and *Dentonula confervacea* (Cleve) Gran. *Canadian Journal of Microbiology*, 8, pp.229–39.
- Haney, J.D., 1996. Modeling phytoplankton growth rates. *Journal of Plankton Research*, 18(1), pp.63–85.
- Hipkin, C.R., Thomas, R.J. & Syrett, P.J., 1983. Effects of nitrogen deficiency on nitrate reductase, nitrate assimilation and photosynthesis in unicellular marine algae. *Marine Biology*, 77(2), pp.101–105.
- Hoening, M., Lee, R.J. & Ferguson, D.C., 1989. A microtiter plate assay for inorganic phosphate. *Journal of Biochemical and Biophysical Methods*, 19, pp.249–251.
- Hu, H. & Gao, K., 2003. Optimization of growth and fatty acid composition of a unicellular marine picoplankton, *Nannochloropsis* sp., with enriched carbon sources. *Biotechnology Letters*, 25(5), pp.421–425.
- Johnson, M.C., Palou-Rivera, I. & Frank, E.D., 2013. Energy consumption during the manufacture of nutrients for algae cultivation. *Algal Research*, 2(4), pp.426–436.
- Li, Y., Qin, J., Ball, A. & Moore, R., 2009. Perspectives of marine phytoplankton as a source of nutrition and bioenergy. In W. T. Kersey & S. P. Munger, eds. *Marine Phytoplankton*. New York: Nova Science, pp. 187–202.
- Liang, K., Zhang, Q., Gu, M. & Cong, W., 2013. Effect of phosphorus on lipid accumulation in freshwater microalga *Chlorella* sp. *Journal of Applied Phycology*, 25(1), pp.311–318.
- Lim, D.K.Y., Garg, S., Timmins, M., Zhang, E.S.B., Thomas-Hall, S.R., Schuhmann, H., Li, Y. & Schenk, P.M., 2012. Isolation and evaluation of oil-producing microalgae from subtropical coastal and brackish waters. *PLoS One*, 7(7), p.e40751.
- Maity, J.P., Bundschuh, J., Chen, C.-Y. & Bhattacharya, P., 2014. Microalgae for third generation biofuel production, mitigation of greenhouse gas emissions and wastewater treatment: Present and future perspectives--A mini review. *Energy*, 78, pp.104–113.
- Markou, G., Vandamme, D. & Muylaert, K., 2014. Microalgal and cyanobacterial cultivation : The supply of nutrients. *Water Research*, 65, pp.186–202.

- Mata, T.M., Martins, A.A. & Caetano, N.S., 2010. Microalgae for biodiesel production and other applications: A review. *Renewable and Sustainable Energy Reviews*, 14(1), pp.217–232.
- Mayers, J.J., Flynn, K.J. & Shields, R.J., 2014. Influence of the N:P supply ratio on biomass productivity and time-resolved changes in elemental and bulk biochemical composition of *Nannochloropsis* sp. *Bioresource Technology*, 169, pp.588–95.
- Rasdi, N.W. & Qin, J.G., 2015. Effect of N: P ratio on growth and chemical composition of *Nannochloropsis oculata* and *Tisochrysis lutea*. *Journal of Applied Phycology*, 27(6), pp.1–10.
- Rasdi, N.W. & Qin, J.G., 2014. Improvement of copepod nutritional quality as live food for aquaculture: a review. *Aquaculture Research*, 47(1), pp.1–20.
- Raven, J.A., 1984. A cost-benefit analysis of photon absorption by photosynthetic unicells. *New Phytologist*, 98(4), pp.593–625.
- Redfield, A.C., 1958. The biological control of chemical factors in the environment. *American Scientist*, 46(3), pp.205–221.
- Robert, R. & Trintignac, P., 1997. Substitutes for live microalgae in mariculture: a review. *Aquatic Living Resources*, 10(5), pp.315–327.
- Roopnarain, A., Gray, V.M. & Sym, S.D., 2014. Phosphorus limitation and starvation effects on cell growth and lipid accumulation in *Isochrysis galbana* U4 for biodiesel production. *Bioresource Technology*, 156, pp.408–11.
- Schnetger, B. & Lehnert, C., 2014. Determination of nitrate plus nitrite in small volume marine water samples using vanadium(III)chloride as a reduction agent. *Marine Chemistry*, 160, pp.91–98.
- Smith, S.L., Yamanaka, Y., Pahlow, M. & Oschlies, A., 2009. Optimal uptake kinetics: physiological acclimation explains the pattern of nitrate uptake by phytoplankton in the ocean. *Marine Ecology Progress Series*, 384, pp.1–12.
- Suen, Y., Hubbard, J.S., Holzer, G. & Tornabene, T.G., 1987. Total lipid production of the green alga *Nannochloropsis* sp. QII under different nitrogen regimes. *Journal of Phycology*, 296(s2), pp.289–296.
- Suggett, D.J., Goyen, S., Evenhuis, C., Szabó, M., Pettay, D.T., Warner, M.E. & Ralph, P.J., 2015. Functional diversity of photobiological traits within the genus *Symbiodinium* appears to be governed by the interaction of cell size with cladal designation. *The New Phytologist*, 208(2), pp.370–81.
- Sukenik, A., 1991. Ecophysiological considerations in the optimization of eicosapentaenoic acid production by *Nannochloropsis* sp. (Eustigmatophyceae). *Bioresource Technology*, 35(3), pp.263–269.
- Sukenik, A. & Carmeli, Y., 1990. Lipid synthesis and fatty acid composition in *Nannochloropsis* sp. (Eustigmatophyceae) grown in a light-dark cycle. *Journal of Phycology*, 26, pp.463–469.
- Tamburic, B., Guruprasad, S., Radford, D.T., Szabó, M., Lilley, R.M., Larkum, A.W.D., Franklin, J.B., Kramer, D.M., Blackburn, S.I., Raven, J.A., Schliep, M. & Ralph, P.J., 2014. The effect of diel temperature and light cycles on the growth of

- Nannochloropsis oculata* in a photobioreactor matrix. *PloS One*, 9(1), p.e86047.
- Ticconi, C.A. & Abel, S., 2004. Short on phosphate: plant surveillance and countermeasures. *Trends in Plant Science*, 9(11), pp.548–55.
- Wood, S. & Cowie, A., 2004. A review of greenhouse gas emission factors for fertiliser production. *IEA Bioenergy Task*, 38(1), pp.1–20.
- Zittelli, G.C., Lavista, F., Bastianini, A., Rodolfi, L., Vincenzini, M. & Tredici, M.R., 1999. Production of eicosapentaenoic acid by *Nannochloropsis* sp. cultures in outdoor tubular photobioreactors. *Journal of Biotechnology*, 70(1), pp.299–312.

4.6 Supplementary Figures

Supplementary Table 4.1 Starting macronutrient concentrations (NO_3^- and PO_4^{3-}): Asterisk (*) represent samples chosen for lipid/ fatty acid methyl ester (FAME) analysis.

Treatment ID	NO_3^- μM	PO_4^{3-} μM	N:P
Control*	882	36.2	24.36
1	1764	72.4	24.36
2	1323	54.3	24.36
3	441	18.1	24.36
4*	176.4	7.24	24.36
5*	176.4	36.2	4.87
6*	882	7.24	121.82
7	441	36.2	12.18
8	882	18.1	48.72
9*	441	54.3	8.12
10*	1323	36.2	73.09
11	882	54.3	16.24
12*	1323	36.2	36.55

Chapter 5 Assessing gas transfer rates as an essential link in scale-up studies for mass microalgal cultivation

Authors:

Dale T. Radford¹, Christian Evenhuis¹, Joseph R. Crosswell¹, Milán Szabó^{1,2}, John A. Raven^{1,3} and Peter J. Ralph¹

Affiliations

¹ Climate Change Cluster (C3), University of Technology Sydney, NSW 2007, Australia

² Division of Plant Sciences, Research School of Biology, The Australian National University, Sullivans Creek Road, Acton, ACT 2601, Australia

³ Division of Plant Sciences, University of Dundee at the James Hutton Institute, Invergowrie, Dundee DD2 5DA, UK

Keywords

Nannochloropsis oculata, oxygen transfer coefficient, environmental PBR platform.

Abbreviations

CO₂: carbon dioxide

k_La: gas transfer coefficient

CCM: carbon concentrating mechanism

ePBR: environmental photobioreactor

O₂: oxygen

P: photosynthesis rate

R: respiration rate

5.1 Introduction

Microalgae have an important role for the future fuel security of the planet. They offer the potential to sequester anthropogenic carbon dioxide (Wang et al. 2008; Ho et al. 2011), treatment of wastewater (Mallick 2002), and produce high-value compounds and bioenergy products (Borowitzka 1999; Borowitzka & Moheimani 2013a). However, to effectively replace existing raw material for these applications, mass outdoor cultivation is required. To obtain commercial quantities of algae, optimal growth conditions are required for example, ideal light and temperature conditions, as well as sufficient macronutrients; nitrogen, phosphorus and carbon (Geider & La Roche 2002). Manual control over light and temperature conditions is difficult, as these factors will ultimately be governed by the location of the cultivation facility; however, control over the addition of macronutrient is possible, as the operator ultimately dictates quantities added. However, unlike nitrogen and phosphorus that are delivered in salt form, the precise control of gas exchange (e.g. CO₂) in large-scale cultivations is more challenging, and must be optimised for maximal productivity.

The rate at which any gas (e.g. O₂, CO₂) can be dissolved into a liquid is defined by the mass (gas) transfer rate (k_La ; h⁻¹), for example, the addition of CO₂ into culture medium. Conceptually, the k_La value consists of two terms, (i) k_L and (ii) a . In the case of the former, k_L is a function of the gas and the physicochemical properties of the liquid phase, whereas, a is dependent upon the hydrodynamic conditions, which in turn, are inherent properties of the reactor and the gas production rate (Lee & Pirt 1984). As a result, k_La values will vary depending on the geometry of the operational gas input and reactor design (i.e., factors that control a), type of gas and physicochemical characteristics of the solution/ growth media (i.e., factors that control k_L).

The understanding of k_La in biological processes was initially focused upon oxygen (O₂) transfer in aerobic processes (Paus et al. 1990). It was then recognised the importance of mass transfer in microalgae reactor design (Märkl 1977; Grima et al. 1993). For microalgae cultivation, the addition of carbon is essential for enhanced production rates and is achieved by bubbling cultures with carbon dioxide (CO₂). In large-scale applications, such as closed tubular or flat panel photobioreactors (PBRs), and open raceway ponds, observed values of k_La are low (Richmond 2004). Subsequently, low values of k_La often result in inefficient, and therefore expensive supply of CO₂ because most of this gas is lost to the atmosphere via outgassing (Fon Sing et al. 2013; Asadollahzadeh et

al. 2014).

At the biological level, the availability of gases especially CO₂ ultimately governs growth and because poor gas to liquid transfer rates are usually observed in natural conditions, microalgae have developed biological mechanisms to cope with low gas availabilities. For example, the process of CO₂ diffusion into the cell is slow, often causing carbon to be limiting at the cellular level. As a result, microalgae have evolved carbon concentrating mechanisms (CCMs) that mediate the acquisition of inorganic carbon via; active, direct uptake of HCO₃⁻, a CO₃²⁻ active transport mechanism, and external carbonic anhydrase (CA) (Colman et al. 2002). At the cellular level, the operation of CCMs are energy consuming processes (Giordano, Beardall & Raven 2005) and can use a significant proportion of the cells total energy budget (Raven, Beardall & Giordano 2014). Therefore, from the cellular perspective, any means by which a system (e.g. reactor) set-up can be used to improve the bioavailability of inorganic carbon this may reduce the cells reliance on CCMs for carbon uptake. Subsequently, cellular energy that would otherwise be used to operate CCMs could be used for growth (Raven, Beardall & Giordano 2014) and therefore facilitate a more productive cultivation system.

Additionally, poor gas transfer rates of oxygen can also be problematic in some cultivation systems. This is because inefficient removal of oxygen from the cultivation system can result in O₂ super-saturation within the culture, which subsequently reduces biomass production (Moheimani & Borowitzka 2007; Peng, Lan & Zhang 2013). Attempts to alleviate this issue have been made through improved reactor design and additional devices such as; sumps, baffles/ static mixers (Ugwu et al. 2002; de Godos et al. 2014). Furthermore, the implementation of strategies such as counter-current injection of gas (Weissman, Goebel & Benemann 1988), hollow fiber modules (Carvalho & Malcata 2001), and carbonation columns (Putt et al. 2011) have also been used. Despite all of these techniques, O₂ super saturation remains a problem in all large-scale reactor designs. At the decision-making level, this results in a trade-off between energy required (Grima et al. 1993) to remove inhibitory levels of O₂ (i.e., through bubbling) and the benefit of increased in culture productivity through the addition of CO₂ (Mendoza et al. 2013).

The use of flue-gas as the sole carbon source in cultivation is seen as a favorable option for the overall success of a microalgal cultivation facilities because carbon addition is estimated to be relatively costly, equating to 8 – 27% of the overall production cost (Ho et al. 2011; de Godos et al. 2014). As a result, many manipulative

laboratory experiments have measured utilisation of carbon by microalgae to optimise the concentration of CO₂ input. These studies have shown the concentrated CO₂ delivered to the system enhances the overall productivity of the culture (Chiu et al. 2009; Ho et al. 2012). However, these experiments often use a wide variety of experimental aeration (i.e., gas input) techniques making it difficult to distinguish genuine biological responses from what may be operational differences (i.e., inappropriate data collection, poor consistency between experimental designs; Riebesell et al. 2010). For example, providing high concentrations of CO₂ using less efficient set-up may be equivalent to delivering low concentrations of CO₂ in a more efficient manner. As a result, our current level of understanding of microalgal performance under different CO₂ input conditions remains ambiguous (Kumar et al. 2010).

Furthermore, it is likely that other inconsistencies between CO₂ enrichment studies (Chiu et al. 2009; Ho et al. 2012; Sforza et al. 2012; Kao et al. 2014) in terms of the physical variables applied (i.e., temperature and light) are not only likely to affect microalgal growth rates (**Figure 1.5 and 1.6**) but also change the physicochemical properties of the culture medium and therefore the exchange of CO₂ from gas to liquid phase. These differences can affect gas transfer rates and ultimately dictate gas bioavailability for the microalgae (Shene et al. 2016). For example, temperature can change the solubility of gas in liquids, whereby higher temperatures decrease solubility (Henry's Law, Talbot et al. 1991). As a result, we hypothesise gas transfer rates should increase with increasing temperature. Other physical variables such as light may indirectly influence gas transfer rates through their effect on biological processes such as photosynthesis and respiration (Geider 1987). For example, photosynthesis (i.e., the production of oxygen) increases with increasing light until a saturation point (Falkowski & Raven 2007; **Figure 1.5**). In this case, we hypothesise that gas transfer rates should decrease with increasing light levels because of changes in the oxygen concentration gradient due to photosynthesis. It is therefore apparent, that physical variables such as temperature and light are likely to affect the efficiency of gas transfer within the culture medium, however our understanding of these dynamics remains unknown. Further to this the ratio of the different carbon species (CO₂(l): HCO₃⁻: CO₃⁻) in the culture medium must be considered as these have been shown to be a function of temperature, salinity and alkalinity, as microalgae are only capable of utilising CO₂(l) and HCO₃⁻. CO₂ addition experiments are often conducted using unrealistic environmental conditions, for example constant light (Chiu et al. 2009; Ho et al. 2012) and/or constant temperature (Sforza, Cipriani, et al. 2012). The simplistic nature of these experiments

makes it difficult to relate that data to large-scale outdoor systems (Kumar et al. 2010) in which these environmental conditions are continuously changing. Whilst CO₂ addition experiments have been conducted outdoors (Kao et al. 2014), the effects of environmental conditions on gas transfer rates has not yet been explicitly tested. For example, it is likely that both temperature and light have direct and indirect effects respectively on gas transfer rates by changing gas solubility (as described above). Yet, how changes in the frequency and amplitude of changes in temperature and light affect gas transfer rates remains unknown. Understanding these dynamics will allow us to predict how gas transfer efficiencies may change temporally and are essential for providing data for dynamic predictive models that are used to determine the feasibility of large-scale cultivation systems (Bernard 2011).

Finally, whilst previous works on gas transfer (of both O₂ and CO₂) has been carried out in the context of photobioreactors, both in closed tubular (Talbot et al. 1991; Grima et al. 1993; Grima, Ación Fernández & Chisti 1999; Babcock, Malda & Radway 2002) and open pond systems (Weissman, Goebel & Benemann 1988; Lívansky 1990; Lívansky & Doucha 1996), these studies have only described the mass transfer characteristics in order to understand the spatial variability of dissolved gases (dissolved O₂ and CO₂) within the cultivation medium. Despite this data being fundamental to the development of earlier predictive models to facilitate reactor design (Rubio et al. 1999), it remains unknown how the dynamics of gas transfer will change under highly variable conditions (e.g. light and temperature) like those found outdoors. Fortunately, since these past experiments the development of new sensor technology has allowed for the high-resolution detection of small changes in concentrations of dissolved gases, in particular, oxygen (Suresh, Srivastava & Mishra 2009; Zhao et al. 2015). This high-resolution capacity of the technology is important as microalgae are known to respond to their external environment on timescales as short as seconds to minutes (Geider et al. 1993). Therefore, the application of such *in-situ* gas monitoring technology can provide a comprehensive understanding of the influence of variable light and temperature on temporal gas transfer rates.

This study assessed the gas transfer of oxygen, k_La (O₂), which has been shown to relate to k_La (CO₂) by a correction factor involving the diffusivity of the two gases (Talbot et al. 1991; Grima et al. 1993). Using the ePBR platform, we first characterised k_La (O₂) coefficients under environmentally relevant abiotic conditions in the absence of biological material. Next, in order to determine whether the presence of microalgae influences gas transfer rates, the k_La (O₂), photosynthesis and respiration rates of

biofuel candidate microalgae, *Nannochloropsis oculata* were analysed under: (i) laboratory controlled conditions using (square-wave diel light and constant temperature), and (ii) simulated outdoor conditions using *in situ* light and temperature data.

5.2 Materials and methods

5.2.1 ePBR gas transfer characterisation set-up

For gas transfer characterisation, vessels used in environmental photobioreactors (ePBR, Phenometrics Inc.) were filled with 500 mL of solutions of desired physicochemical characteristics. Dissolved oxygen was measured with oxygen probes (OXROB3; oxygen probe, Firesting O₂, Pyroscience). Nitrogen or ambient air was supplied via a hypodermic needle (0.34 mm, NN-2338R, Terumo) positioned 2 cm from the base of the vessel and additional agitation was provided by a magnetic stirrer set at 200 rpm. Gas flow rates were controlled using programmable mass flow controller (FMA5400/5500, Omega Engineering), whilst two solenoid valves (SS0905, Jaycar Electronics) allowed for the delivery of either nitrogen or ambient air according to the set-up shown in **Supplementary Figure 5.1**. Gas transfer rates in the ePBR were determined using a method similar to that described in Mendoza et al. (2013). Briefly, the ePBR was filled with 500 mL of sample solution; nitrogen gas was bubbled to reduce the oxygen concentration in the solution. Once the oxygen concentrations were reduced, the gas flow was switched to ambient air using the solenoid switch. The solution was then bubbled until the oxygen concentration returned to equilibrium, denoted by horizontal broken line (**Figure 5.1**). Through this method the gas transfer coefficient of oxygen (k_La) was calculated using the following equation derived from the exponential curve fit (OriginPRO 2015; version b9.2.272):

$$d[O_2](t) = [O_2]_0 + \Delta[O_2]e^{-k_Lat} \quad \text{(Equation 5.1)}$$

Where, $[O_2]$ is the dissolved oxygen concentrations at time points t_0 and t_1 , $\Delta[O_2]$ is the change in oxygen concentration and k_La is the gas transfer coefficient of oxygen. To determine the changes in gas transfer rate as a function of (1) different experimental set-ups and, (2) physiochemical characteristics of solutions, samples were bubbled with different gas inputs devices (i.e., varied needle aperture; 0.21 mm, 0.34 mm, NN-2613R, NN-2328R, Terumo), different gas flow rates (0 – 500 mL min⁻¹) and solutions with different physiochemical characteristics (temperature, pH and salinity). For physiochemical gas transfer characterisation, a 0.34 mm needle (NN-2328R, Terumo) at a flow rate of 450 mL min⁻¹ was used as it was shown to provide the most reproducible gas transfer data (data not shown).

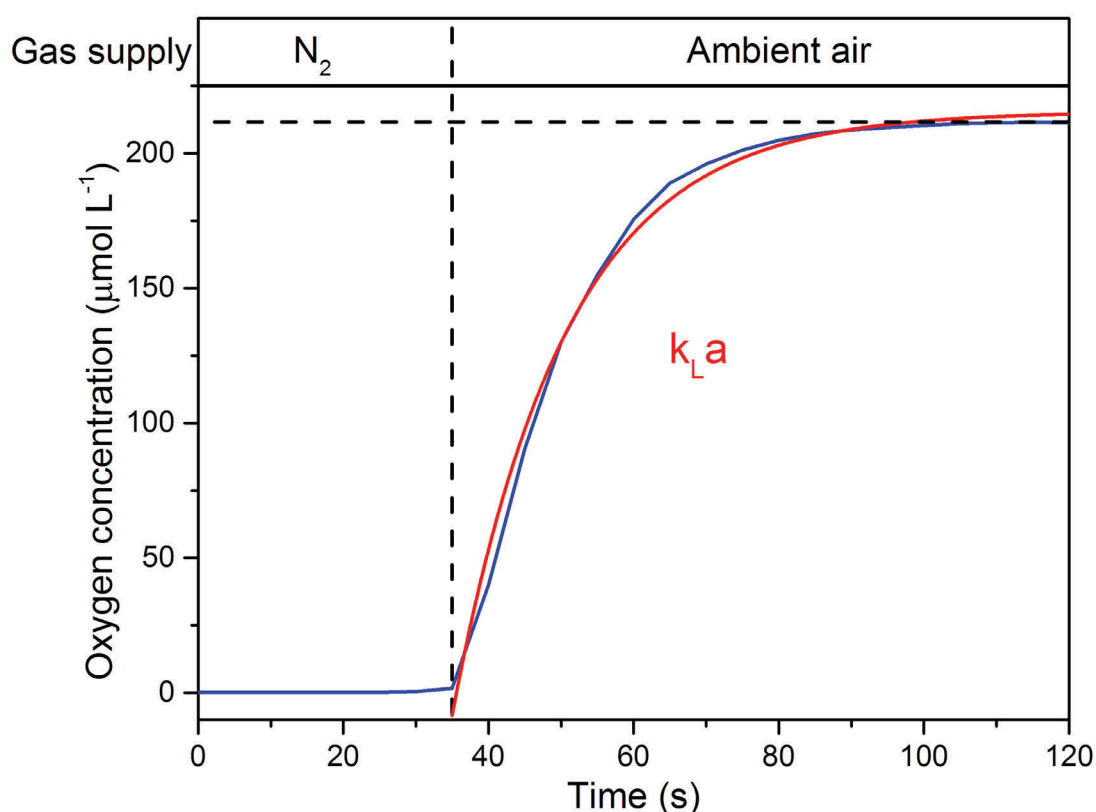


Figure 5.1 Schematic of oxygen concentration trace (blue line) used to calculate the gas transfer coefficient. Gas transfer rates were derived from equation 5.1 where the red solid line represents a typical fit, $R^2 > 0.98$. The vertical broken line represents the switching of gas types from N_2 to ambient air and the horizontal broken line represents oxygen saturation.

5.2.2 Microalgal culture and medium

Nannochloropsis oculata (Droop) Green (CS-179) was obtained from the ANACC (Australian National Algae Culture Collection, CSIRO, Hobart, Australia). For all biological experiments performed, *N. oculata* was grown in f/2 medium lacking silicate (0.2 μm filtered artificial seawater enriched with; 8.82×10^{-4} M NaNO_3 ; 3.62×10^{-5} M, $\text{NaH}_2\text{PO}_4 \cdot \text{H}_2\text{O}$; trace metal solution and vitamin solution; Guillard & Ryther 1962).

5.2.3 Static cultivation (tank reactor) setup

N. oculata was cultivated in a clear plastic tank (14 L) to ensure a culture depth of 21 cm (equivalent to the depth of 500 mL in the ePBR vessel). The culture was illuminated from above using white light emitting diodes (LEDs; WLED50, IronHorse) providing 300 $\mu\text{mol photons m}^{-2} \text{s}^{-1}$ irradiance at the surface of the culture under a 12 h: 12 h light: dark cycle. Temperature and dissolved oxygen ($p\text{O}_2$) were continuously recorded (OXROB3; oxygen probe, Firesting O_2 , Pyroscience) and constant pressurised gas (ambient air) was provided through custom-made gas input systems.

5.2.4 Simulated outdoor condition (ePBR) setup

Environmental PBRs (ePBRs) with a working volume of 500 mL were programmed with light and temperature data from the UTS rooftop facility, Sydney, Australia (33.88 °S, 151.20 °E), collected between 1st and 12th August 2015. Here, environmental light and temperature values were obtained using HOBO temperature/ light logger (UA-002-64, Onset) placed at the surface of a 435 L raceway pond agitated using a paddlewheel. In the ePBR, the culture was illuminated from above using a solar LED (Phenometrics Inc.) calibrated to provide programmed irradiance level at the surface of the 500 mL culture. Gas (ambient air under constant pressure) was supplied through 0.34 mm needles. Temperature, dissolved oxygen and pH were measured continuously, whereby in-built sensors were used to measure temperature and pH (Phenometrics Inc.) and optode sensors (OXROB3; oxygen probe, Firesting O₂, Pyroscience) were used to measure dissolved oxygen.

5.2.5 Growth measurements

Growth rate measurements were calculated from optical density and cell count basis. For these measurements, 1 mL sub-samples were harvested for optical density measurements (at 750 nm) using a spectrometer (Varian Cary 50 Bio, Agilent). For cell counting, the same samples were stored in glutaraldehyde solution (1% (v/v) final concentration). Stored samples were then used to correlate optical density measurements with cell counts. Cells were enumerated using an automated microscopy method complemented with image analysis software as previously described in **Section 2.2.3**.

5.2.6 In situ photosynthesis, respiration rate and gas transfer calculations

The concentration of oxygen in an algal culture is determined by three processes: equilibrium with atmosphere and is determined by the gas transfer rate, photosynthesis which contributes oxygen, and respiration which consumes oxygen. Mathematically these fluxes of oxygen are described by the following differential equation:

$$\frac{d[O_2]}{dt} = k_L a ([O_2]_{eq} - [O_2]) + P - R \quad (\text{Equation 5.2})$$

The equilibrium concentration of oxygen in solution depends on the concentration of oxygen in the atmosphere, the salinity and the temperature and has been extensively parameterised (Garcia & Gordon 1992).

It is possible to analytically solve the above equation if the mass transfer coefficient, the equilibrium oxygen concentration and rates of photosynthesis and respiration can be assumed to be constant over time. This approach was employed in Tamburic et al.

(2015) (**Figure 5.2**). Two cases are presented: (i) when the gas flow is stopped (**Figure 5.2b**) and (ii) when the gas flow is switched back on (**Figure 5.2c**):

(i) Gas flow stopped:

When the gas flow is stopped the gas transfer term is removed and the oxygen deviates from equilibrium. The rate the oxygen accumulates is the net photosynthesis (P) -respiration (R) rate:

$$[O_2](t) = [O_2]_0 + (P - R)t \quad (\text{Equation 5.3})$$

where t is time since the gas flow was stopped and $[O_2]_0$ is concentration of oxygen was the gas flow was stopped. These are the spikes shown in (**Figure 5.2 and Supplementary Figure 5.2**), as a result, net photosynthesis (**Figure 5.2b**) or dark respiration (**Figure 5.2c**) was calculated as a linear function during this period.

(ii) Gas switched back on:

When the gas flow is resupplied, the oxygen concentration returns to steady state equilibrium. Solving **Equation 5.1** gives

$$d[O_2](t) = [O_2]_0 + \Delta[O_2] e^{-k_L a(t-t_1)} \quad (\text{Equation 5.4})$$

Where, $[O_2]$ dissolved oxygen concentration at time points t_0 and t_1 , $\Delta[O_2]$ is the change in oxygen concentration and $k_L a$ is gas-transfer coefficient of oxygen. The gas transfer rate can be determined by fitting this data to an exponential decay function.

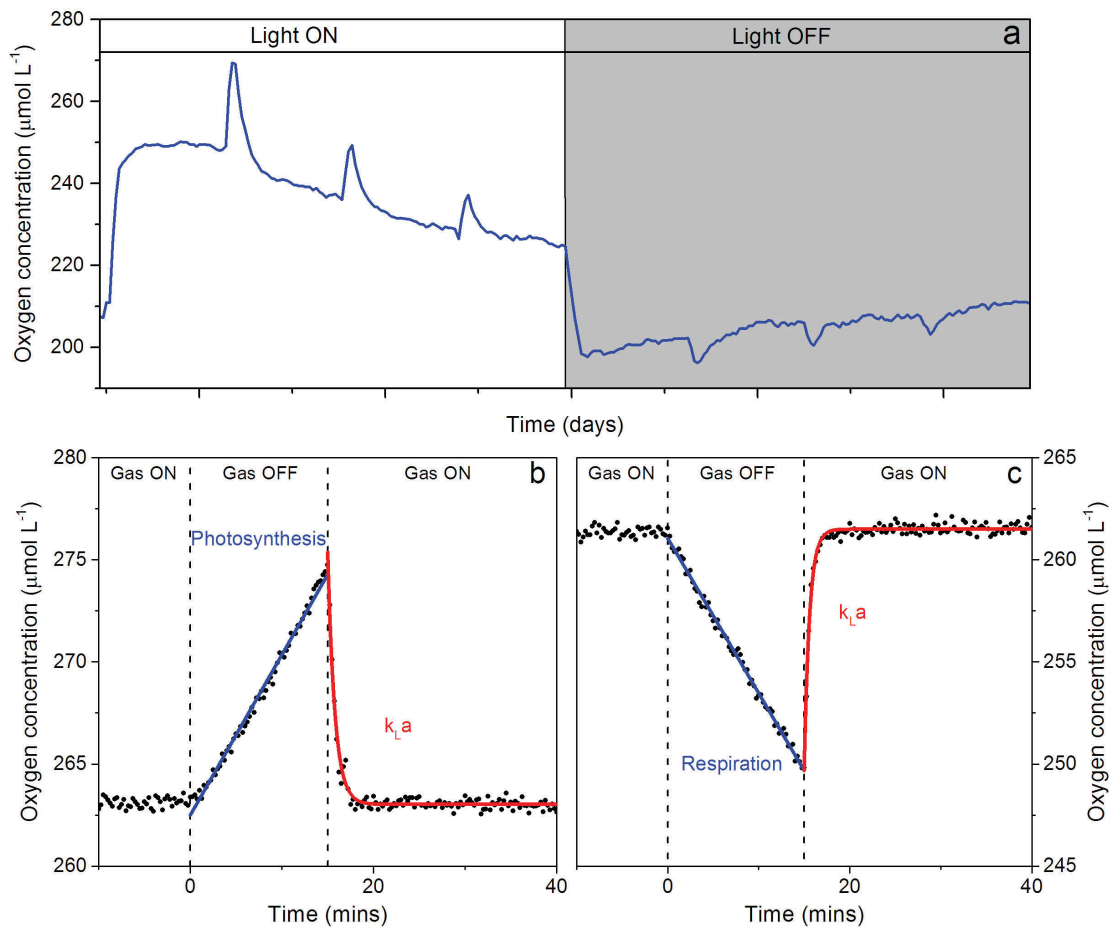


Figure 5.2 (a) A typical dissolved oxygen trace of microalgae (solid blue line) cultivated under square wave light, white and gray background represents light on and light off respectively. Where the spike in the dissolved oxygen trace (a) were used to calculate (b) net photosynthesis and (c) respiration rates, both indicated by blue lines and gas transfer coefficient ($k_L a$; b, c) indicated by red line.

5.2.7 Modeling gas-transfer rates, photosynthesis and respiration

The above analysis only holds if photosynthesis and respiration and temperature are constant. In a fluctuating environment all of these terms are changing so it is necessary to solve **Equation 5.4** numerically. **Equation 5.4** was solved using the Runge Kutta 4th-order method. Here, it is necessary to allow the terms to be dependent on temperature and light. The equilibrium solubility of oxygen is particularly sensitive to temperature (e.g. as temperature decreases, more O_2 is dissolved in solution). As the fluctuations in temperature are relatively small and have low frequency, these changes are comparatively minor, but must be accounted for across the day.

The most important terms but hardest to characterise are ones associated with biological processes. Photosynthesis (P) is the most rapidly changing term, as it directly proportional to light intensity (I) and responds very rapidly to changes (<1 sec).

These fast changes are described with a PI-curve (**Figure 1.5**). The maximum photosynthesis (P_{max}) term can vary diurnally due to increased biomass. Additionally P_{max} can decrease due to limitations such as nutrients or dissolved carbon. Respiration (R) also depends on the light, but to a lesser extent. Respiration is low at night-time and increases during the day, due to the up regulation of metabolic processes associated with photosynthesis (light-enhanced respiration). It is assumed that light-enhanced respiration reflects the average photosynthesis that can take place in preceding 15 min or so. In addition to this, photosynthesis and respiration depend on temperature (T). The changes in photosynthesis and respiration rates through the day were represented using Hermite spline functions (h). This function allows complex changes to be easily captured by adding more spline points. In addition, constraints were placed on the behavior of respiration and photosynthesis. Respiration was constrained to increase monotonically in the light and the decrease monotonically in the dark, consistent with light enhanced respiration. Photosynthesis was allowed to either increase during the light due to cell division or to decrease due to limitation (such as carbon or light).

$$\frac{dO_2}{dt} = k_L a(1 + dKT)[O_{2equ}(T) - O_2] + P_{max}(3pts)(1 - \exp\left(-\frac{I}{Ih}\right)) - R(10pts) \quad (\text{Equation 5.5})$$

For a given set of parameters, the above equation was integrated across the day and the squared difference between model and observations calculated. By minimising the least squares error, the unknown photosynthesis and the unknown parameters could be estimated.

5.3 Results

5.3.1 Gas transfer characterisation

Gas input techniques were found to have a significant effect on gas transfer coefficients, with needle diameter and flow rates significantly altering gas transfer of oxygen (**Figure 5.3**). Gas transfer rate was observed to increase with increasing flow rate. Maximum flow rate did not result in maximum gas transfer rate once a threshold flow rate was reached, 450 mL min⁻¹ and 350 mL min⁻¹ for 0.34 mm and 0.21 mm needle gauge respectively. In these cases, additional flow rates did not increase the gas transfer rate. Irrespective of flow rate, larger needle gauges resulted in greater oxygen gas transfer.

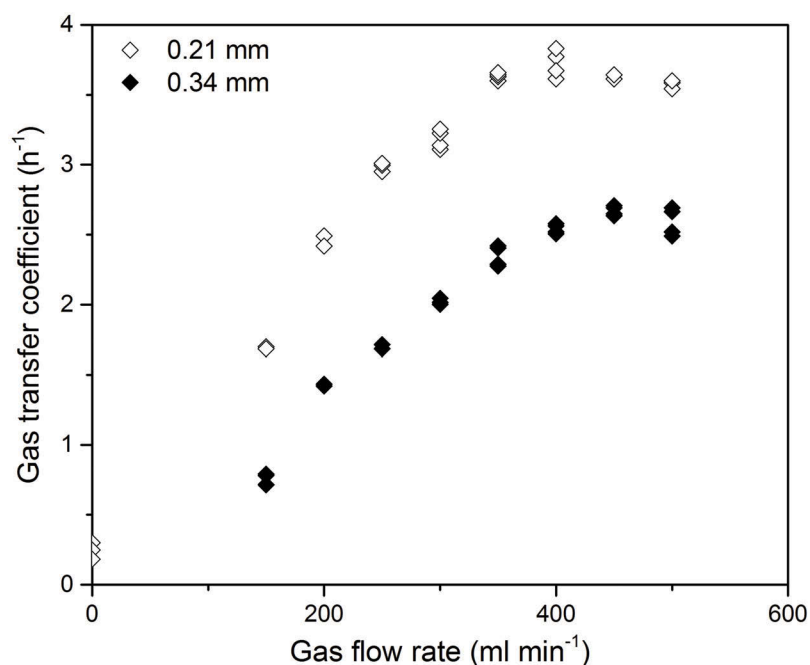


Figure 5.3 Characterisation of gas transfer coefficient at different gas flow rates provided through different needle diameters of 0.21 mm (open diamond) and 0.34 mm (solid diamond).

Gas transfer coefficients were affected by some, but not all physicochemical characteristics. Temperature appeared to have the most significant effect, whereby the gas transfer coefficient increased with temperature from 1.5 h⁻¹ at 11 °C in comparison to 3.5 h⁻¹ at 40 °C (**Figure 5.4a**). In contrast, when all other variables remained equal (i.e. needle aperture, temperature, flow rate), a gas transfer of 2.6 h⁻¹ was maintained over a pH range between 2 and 12 (**Figure 5.4b**). Similarly, a gas transfer of 2.6 h⁻¹ remained consistent over a salinity range from 0 to 40 gL⁻¹ (**Figure 5.4c**). Together these results indicate that it is more difficult to transfer oxygen at colder temperatures but other media characteristics such as dissolved salts and pH have negligible effects.

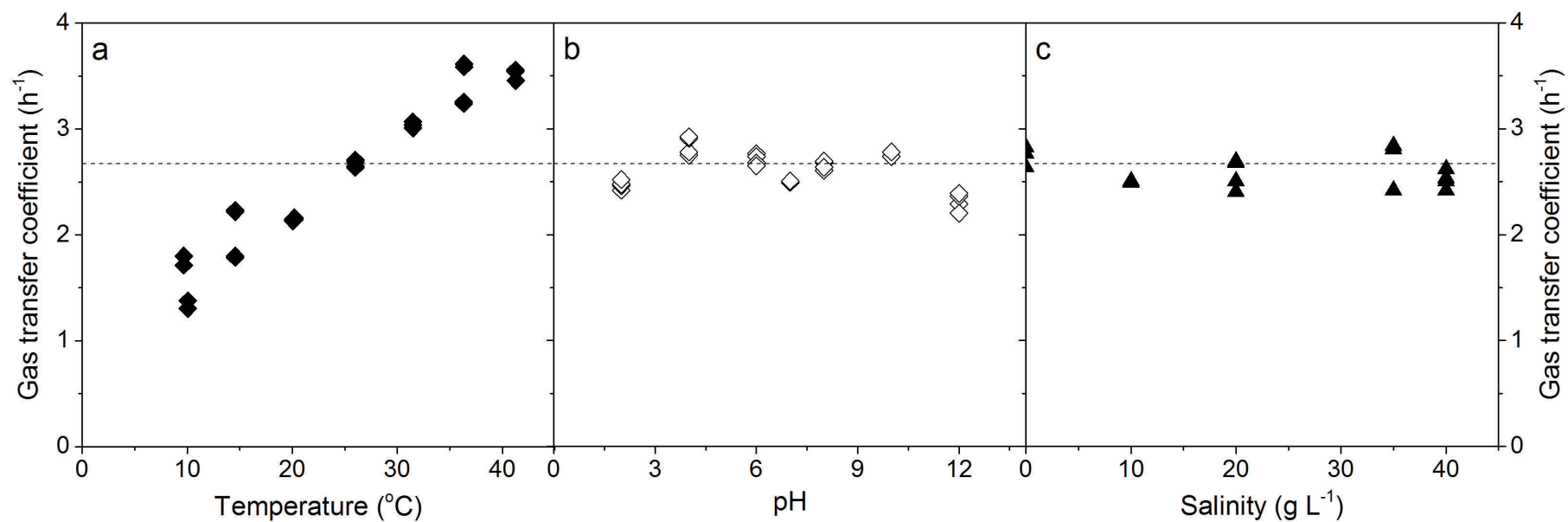


Figure 5.4 Characterisation of gas transfer coefficients at different (a) temperature, (b) pH and (c) salinity using the ePBR set-up, each symbol represents the individual replicates. Broken line represents the gas transfer coefficient at 450 mL min⁻¹ at 26 °C, 0 g L⁻¹ and pH 5.93.

5.3.2 Response to static growth conditions

Under static growth conditions of constant light ($300 \mu\text{mol photons m}^{-2} \text{ s}^{-1}$) and temperature ($28 \pm 2 \text{ }^{\circ}\text{C}$), *N. oculata* remained in lag phase between day 0 and day 5 as cell numbers remained relatively stable until day 6 (**Figure 5.5a**). Cell numbers began to double from day 6, corresponding to exponential growth phase until day 12, with an overall growth rate of 0.083 d^{-1} ($R^2=0.87$) (**Figure 5.5a**). Diel changes in temperature, oxygen gas transfer and rates of photosynthesis and respiration were observed throughout the growth cycle and appeared consistent between days (data not shown); day 4 (lag phase) and day 9 (exponential phase) shown in (**Figure 5.5b - e**) are representative of these diel trends.

Our model revealed changes in gas transfer coefficients over a diel cycle, increasing from a rate of 0.9 h^{-1} at the onset of the light period to a rate of 1.1 h^{-1} at the end of the light period (**Figure 5.5b**). These results indicate that the gas to liquid transfer of oxygen becomes more efficient over the course of the day. These changes were concomitant with a gradual change in temperature over the light period, increasing in the morning from $25 \text{ }^{\circ}\text{C}$ to $28 \text{ }^{\circ}\text{C}$. A decrease in temperature was observed at the onset of the dark period. These trends were consistent between lag phase (**Figure 5.5b**) and exponential growth phase (**Figure 5.5c**). Photosynthetic rate was maximal at the onset of light and then decreased over the light period. In lag phase (**Figure 5.5d**) this decrease is linear, whereas, later in growth the photosynthetic decline follows a more exponential decline over the light period (**Figure 5.5e**). Modeled response of respiration showed a similar trend between the days observed (day 4 and day 9; **Figure 5.5d, e**).

5.3.3 Response to simulated outdoor growth conditions

Under winter simulated outdoor conditions in Sydney, Australia, no growth in *N. oculata* was observed between day 0 and day 7 as cell numbers remained relatively stable until day 8 (**Figure 5.6a**), indicating a longer lag period than that observed under static laboratory conditions. Significant differences in cell number were observed after day 7, corresponding to exponential growth phase until day 12, with an overall growth rate of 0.048 d^{-1} ($R^2=0.78$) (**Figure 5.6a**). Diel changes in temperature and light varied significantly between days over this growth cycle (**Figure 5.6a**).

Day 4 (lag phase) and day 9 (exponential phase, **Figure 5.6b - e**) revealed diel patterns in light, temperature, as well as in the rate of oxygen transfer, photosynthesis

and respiration. Consistent with results obtained under static laboratory conditions, gas transfer appeared to follow changes in temperature. For example, during lag phase (day 4 to 5), gas transfer increased with increasing temperature to approximately midday and then decreased with decreasing temperature until nightfall (**Figure 5.6b**). This pattern was similar during exponential growth phase between day 9 and 10 (**Figure 5.6c**). However, in contrast to static conditions where oxygen gas transfer varied consistently over a diel cycle (between 0.9 to 1.1 h⁻¹; **Figure 5.5b - e**), the rates were greater and more variable under simulated outdoor conditions. For example, during lag phase (day 4 to 5) transfer rates varied between 2.0 and 5.0 h⁻¹ (**Figure 5.5b**) and between 1.5 and 4.0 h⁻¹ during exponential phase (**Figure 5.6c**).

Unlike static laboratory conditions, where maximal photosynthetic rates coincided with the onset of light period (**Figure 5.5d, e**), photosynthetic and respiration rates trailed light onset in both lag and exponential growth (**Figure 5.6d, e**). Furthermore, these rates were far more variable in comparison to controlled laboratory conditions. In contrast to a maximal photosynthetic rate in the morning followed by a smooth decline towards the afternoon, photosynthetic rates of *N. oculata* grown in simulated outdoor conditions were far more difficult to predict (**Figure 5.6d, e**).

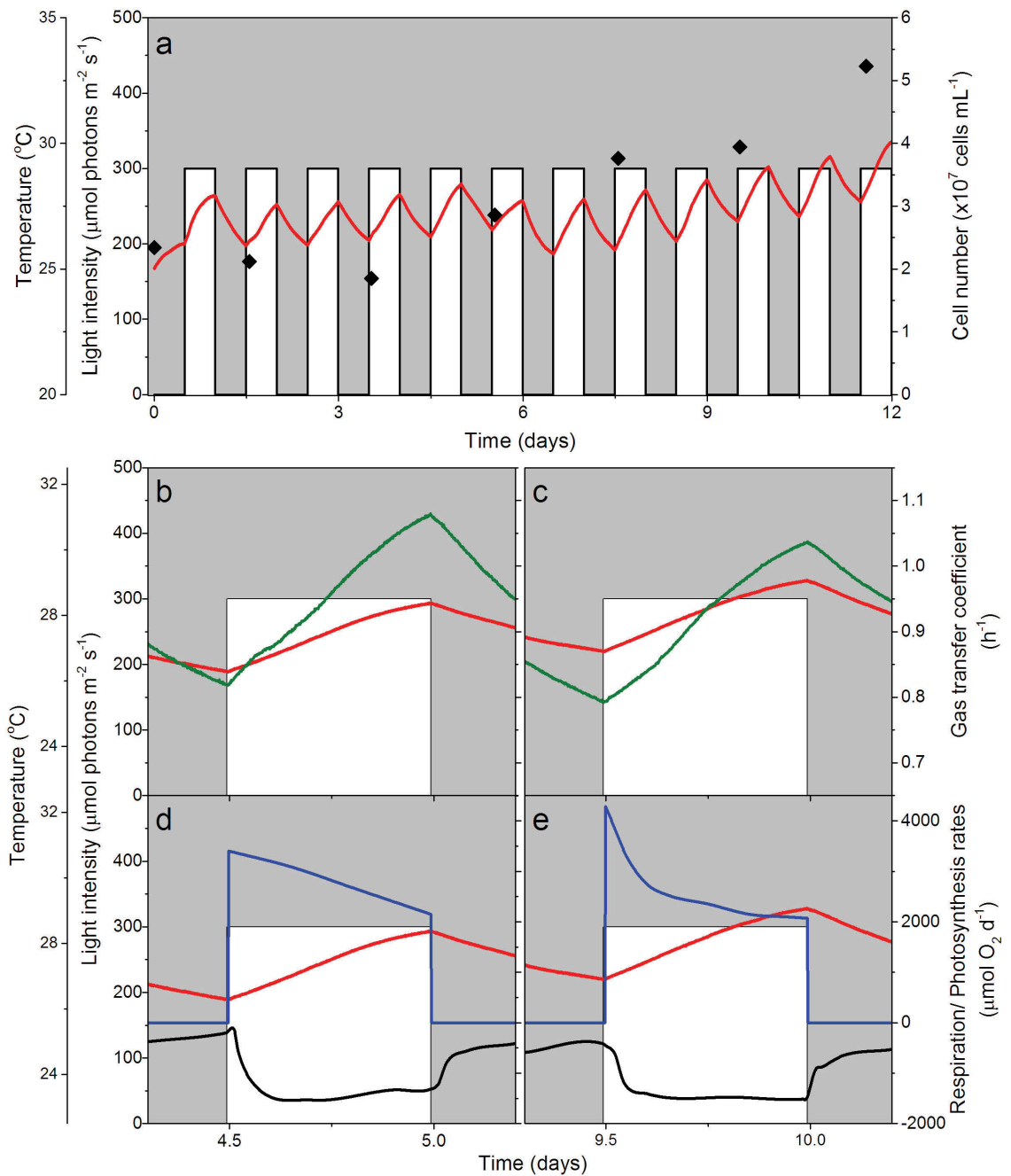


Figure 5.5 (a) Growth of *N. oculata* under laboratory conditions (light intensity, white blocks), where temperature (red line), cell number (closed diamonds) were monitored over the growth cycle. Modelled rates of gas transfer (green line), photosynthesis (blue line), and respiration (black line) are shown during lag (a, d) and exponential (b,c) growth phases.

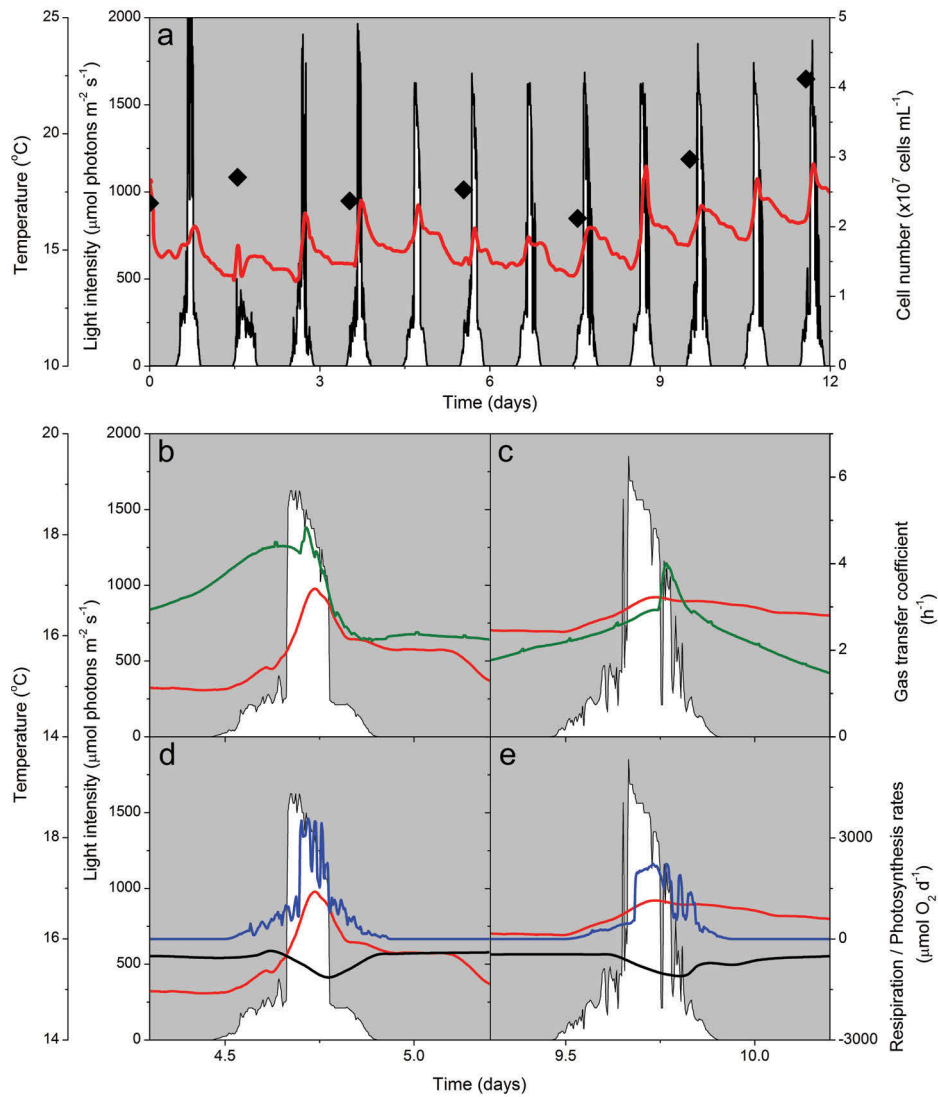


Figure 5.6 (a) Growth of *N. oculata* under simulated outdoor conditions obtained from raceway pond at UTS rooftop facility, where light intensity (white blocks), temperature (red line) and cell number (closed diamonds) were monitored over the growth cycle. Modelled rates of gas transfer (green line), photosynthesis (blue line), and respiration (black line) are shown during lag (a, d) and exponential (b,c) growth phases.

5.4 Discussion

This study demonstrates the importance of thorough analysis of the gas to liquid mass transfer coefficient when conducting gas addition experiments. Whilst previous studies have reported gas flow rates in order to create reproducibility between experimental set-ups (Hu & Gao 2003; Sforza et al. 2012), we have shown that flow rates alone are not indicative of the efficiency of the gas to liquid mass transfer (k_La) (Carvalho, Meireles & Malcata 2006). This is because the geometry of the operational set-up can significantly affect bioreactor hydrodynamics and gas production rates, as these factors influence the 'a' component of the k_La term (Pauss et al. 1990). For example, a 75% increase in k_La (from 1.70 to 2.98 h⁻¹) could be achieved by decreasing the aperture of the gas input device (from 0.34 mm to 0.21 mm at the same flow rate of 250 mL min⁻¹; **Figure 5.3**). Changes in the needle aperture altered characteristics of the gaseous stream, such as bubble size and velocity, as well as the distribution of bubbles throughout the culture medium (Shah et al. 1982; Ugwu et al. 2008), which in turn altered hydrodynamics within the culture medium. Needle aperture followed theoretical predictions, where smaller apertures resulted in higher gas transfer rates as a result of smaller bubbles being produced (Miller 1974). It is evident that geometry of the operational set-up has a significant impact upon the k_La (Carvalho & Malcata 2001). Likewise, we were also able to manipulate k_La by changing gas production/flow rates (**Figure 5.3**). Together, these findings demonstrate that operational differences can have profound effects on the rate of gas transfer. Therefore, reporting k_La values as part of experimental documentation can help to alleviate these experimental obstacles and allow consistencies between experimental designs.

Unlike the operational set-up, which influences the 'a' component of the k_La term, physicochemical properties of the liquid determines the ' k_L ' (Pauss et al. 1990). In this study, no relationship was observed between k_La (O₂), and the pH and salinity of the solution (**Figure 5.4b, c**). Whilst this may not affect the k_La of O₂, changes in pH and salinity are likely to be significant for CO₂ addition studies. For example, pH changes have been shown to alter k_La (CO₂) coefficients due to changes in diffusivity, the gas bubble size, and reaction kinetics at the gas/liquid boundary (Lee & Pirt 1984). In contrast, liquid temperature significantly changed k_La (O₂) coefficients, whereby warmer temperatures facilitated more efficient oxygen transfer (**Figure 5.4a**). These results are consistent with our hypothesis based on Henry's Law, whereby, the gas to liquid solubility decreases with increasing temperature, and hence the rate of transfer occurs more rapidly. However, because the k_La coefficient describes the rate of

transfer in either direction (gas to liquid or liquid to gas), the rate of oxygen being lost from the liquid to gaseous phase also increases (Talbot et al. 1991). These findings are significant in the context of the culturing of microalgae, especially in outdoor bioreactors/ ponds that are exposed to temperature fluctuations over relatively short timescales e.g. diurnal (Tamburic et al. 2014). This is because gas transfer efficiencies may vary over a temporal timescales and may need to be corrected for over the course of the day in order to ensure stable gas to liquid transfer rates.

To further understand how temporal variation in temperature influences the efficiency of gas to liquid transfer, we obtained k_La coefficients at high resolution over several diel cycles. Under more static laboratory-like conditions, gas transfer efficiencies were more predictable compared to simulated environmental conditions. This was evidenced by differing degrees of variation in k_La coefficients between laboratory and environmental conditions, despite consistent operational set-ups. For example, we controlled for variation in component 'a' of the k_La term; under laboratory-like settings, gas transfer rates varied by approximately 10% over a diurnal cycle in comparison to 50% when exposed to simulated 'natural' environments. These findings indicate that simulated 'natural' environments create more fluctuation in the ' k_L ' (physicochemical properties of the liquid; Pauss et al. 1990; Talbot et al. 1991). These findings are significant in the context of CO₂ addition experiments, as the temperature of the culture medium will influence CO₂ transfer efficiencies. For example, in bioreactors which are exposed to large daily deviations in temperature e.g. greater than 20 °C, (Belay 1997), operators may need to consider alterations to the system set-up (i.e. increased gas flow) that help to increase the 'a' in order to compensate for the loss in k_L component of the k_La term (Grima et al. 1993).

To implement these operational strategies effectively, model-based predictive controls (MPC) could be used (Camacho & Bordons 1995). By incorporating meteorological data into the models, we can use forecasted future conditions to predict their influence on gas to liquid mass transfer coefficient. For example, as demonstrated in this study, high temperatures increase the k_La for oxygen. By tailoring the gaseous stream characteristics e.g. flow rate, we can manipulate the k_La to suit forecasted *in situ* conditions. In this way, productivity can be maximised without oversaturating gas requirements. For example, García Sánchez et al. (2003) implemented MPC controllers in outdoor closed tubular photobioreactors to increase profits margins, whereby productivity was increased by 15.6% and biomass production costs were reduced by 6%. This was achieved by reducing the mean daily CO₂ flow rate as a well

as an on-off CO₂ value to balance culture requirements. Similarly, MPCs could be used to predict conditions where O₂ concentrations could become inhibiting for growth e.g. over 100% air saturation (Raso et al. 2012; Peng, Lan & Zhang 2013; Shene et al. 2016). In comparison to the continuous oxygen concentrations provided in Raso et al. (2012), the oxygen concentrations observed in this study (**Supplementary Figure 5.2**) do not appear to inhibit growth. As a result, we suggest that k_La values between 0.8 and 5.0 h⁻¹ are sufficient to prevent the accumulation of inhibitory O₂ concentrations for *N. oculata* under the temperature and light conditions examined in this study (**Figure 5.5 and 5.6**).

To advance our understanding of the importance of k_La on large-scale cultivation the use of a 'standard platform' is essential (Lucker et al. 2014). This is because, as shown in the current study, the geometric operational set-up (e.g. gas input) as well as physicochemical characteristics of the solution (e.g. temperature) influences the magnitude of k_La (**Figure 5.5b**). For example, developing existing infrastructure, such as ePBRs, would allow for the collection of robust, reproducible data. Firstly, the fabrication of a platform with capacities to measure and analyse CO₂ concentrations would improve the relevance of the data for commercial scale production. It would also provide the capability to carry out studies that accurately resolve the complex nature of the biological CO₂ absorption story (i.e., CO₂ influencing the carbonate chemistry). Furthermore, the development of more sophisticated gas input and control systems that are capable of programming a specific gas transfer coefficients would enable multiple avenues of exploration. For example the accurate gas transfer simulation of reactor design (e.g. raceway pond or closed PBR) would allow studies to test the effect of different reactor designs, i.e. additional sumps, mixers, dimensions etc. on the productivity of the culture. At the same time, the microalgal culture would receive light and temperature conditions that are representative of field scenarios. All of these future studies could be completed cost-efficiently in the laboratory prior to more costly large-scale field trials.

In conclusion, this study highlights the necessity for gas transfer coefficients to be correctly described in the literature to facilitate accurate interpretation and prevent conflicting conclusions due to operational differences. These operational differences are often overlooked and warrant more thorough consideration. The methods presented here contribute to producing a standard protocol of gas exchange rates and aim to harmonise data analysis among different research groups (Riebesell et al. 2010). Further growth experiments should attempt to separate biological and physical

Chapter 5: A practical approach to optimise gas exchange

controls on gas exchange using empirical data under laboratory and simulated natural conditions. The methods used in this manuscript represent a practical approach to optimise gas exchange, as opposed to complex modeling of bubble dynamics. In order to directly scale these results to commercial facilities, further studies should implement these methods on a case-by-case scenario.

5.5 Acknowledgements

The authors would like to thank the Climate Change Cluster (C3), University of Technology Sydney for financial support. A Taninec and Dr. B Tamburic for the collection of light and temperature data from the UTS Algal Biosystems rooftop facility, J Hanna for use of pressure regulators used in the growth experiment and K. Baker for assistance in the collection and analysis of data, and preparation of final manuscript.

The University of Dundee is a registered Scottish charity. No.SC015096.

5.6 References

- Asadollahzadeh, M.J., Ardjmand, M., Seafkordi, A.A. & Heydarian, S.M. 2014, 'Efficient storage and utilization of CO₂ in open raceway ponds for cultivation of microalgae', *Korean Journal of Chemical Engineering*, vol. 31, no. 8, pp. 1425–32.
- Babcock, R.W., Malda, J. & Radway, J.C. 2002, 'Hydrodynamics and mass transfer in a tubular airlift photobioreactor', *Journal of Applied Phycology*, vol. 14, no. 3, pp. 169–84.
- Belay, A. 1997, 'Mass culture of *Spirulina* outdoors- The Earthrise Farms experience', in A. Vonshak (ed.), *Spirulina platensis (Arthrospira): Physiology, Cell-biology and Biotechnology*, Taylor & Francis Ltd, London, pp. 131–58.
- Bernard, O. 2011, 'Hurdles and challenges for modelling and control of microalgae for CO₂ mitigation and biofuel production', *Journal of Process Control*, vol. 21, no. 10, pp. 1378–89.
- Borowitzka, M.A. 1999, 'Commercial production of microalgae: ponds, tanks, tubes and fermenters', *Journal of Biotechnology*, vol. 70, no. 1, pp. 313–321.
- Borowitzka, M.A. & Moheimani, N.R. 2013, *Algae for Biofuels and Energy*, M.A. Borowitzka & N.R. Moheimani (eds), *Algae for Biofuels and Energy*, 1st edn., Springer Netherlands, Dordrecht, New York.
- Camacho, E.F. & Bordons, C. 1995, *Model Predictive Control in the Process Industry*, M.J. Grimble & M.A. Johnson (eds), *Model Predictive Control in the Process Industry*, 1st edn., Springer, London.
- Carvalho, A.P. & Malcata, F.X. 2001, 'Transfer of carbon dioxide within cultures of microalgae: plain bubbling versus hollow-fiber modules', *Biotechnology Progress*, vol. 17, no. 2, pp. 265–72.
- Carvalho, A.P., Meireles, L.A. & Malcata, F.X. 2006, 'Microalgal reactors: a review of enclosed system designs and performances', *Biotechnology Progress*, vol. 22, no. 6, pp. 1490–506.
- Chiu, S., Kao, C., Tsai, M., Ong, S., Chen, C. & Lin, C. 2009, 'Lipid accumulation and CO₂ utilization of *Nannochloropsis oculata* in response to CO₂ aeration', *Bioresource Technology*, vol. 100, no. 2, pp. 833–8.
- Colman, B., Huertas, I.E., Bhatti, S. & Dason, J.S. 2002, 'The diversity of inorganic carbon acquisition mechanisms in eukaryotic microalgae', *Functional Plant Biology*, vol. 29, no. 3, article, pp. 261–70.

- Costache, T.A., Acién Fernández, F.G., Morales, M.M., Fernández-Sevilla, J.M., Stamatini, I., Molina, E. & Fernández, F.G.A. 2013, 'Comprehensive model of microalgae photosynthesis rate as a function of culture conditions in photobioreactors.', *Applied Microbiology and Biotechnology*, vol. 97, no. 17, pp. 7627–37.
- Falkowski, P.G. & Raven, J.A. 2007, *Aquatic Photosynthesis*, 2nd edn., Princeton University Press, Princeton, NJ.
- Fon Sing, S., Isdepsky, A., Borowitzka, M.A. & Moheimani, N.R. 2013, 'Production of biofuels from microalgae', *Mitigation and Adaptation Strategies for Global Change*, vol. 18, no. 1, pp. 47–72.
- Garcia, H.E. & Gordon, L.I. 1992, 'Oxygen solubility in seawater: Better fitting equations', *Limnology and Oceanography*, vol. 37, no. 6, pp. 1307–12.
- García Sánchez, J.L., Berenguel, M., Rodríguez, F., Fernández Sevilla, J.M., Brindley Alias, C. & Acién Fernández, F.G. 2003, 'Minimization of carbon losses in pilot-scale outdoor photobioreactors by model-based predictive control', *Biotechnology and Bioengineering*, vol. 84, no. 5, pp. 533–43.
- Geider, R. & La Roche, J. 2002, 'Redfield revisited: variability of C : N : P in marine microalgae and its biochemical basis', *European Journal of Phycology*, vol. 37, no. 1, pp. 1–17.
- Geider, R.J. 1987, 'Light and temperature dependence of the carbon to chlorophyll a ratio in microalgae and cyanobacteria: implications for physiology and growth of phytoplankton', *New Phytologist*, vol. 106, no. 1, pp. 1–34.
- Geider, R.J., Roche, J., Greene, R.M. & Olaizola, M. 1993, 'Response of the photosynthetic apparatus of *Phaeodactylum tricornutum* (Bacillariophyceae) to nitrate, phosphate, or iron starvation', *Journal of Phycology*, vol. 29, no. 6, pp. 755–66.
- Giordano, M., Beardall, J. & Raven, J.A. 2005, 'CO₂ concentrating mechanisms in algae: Mechanisms, environmental modulation, and evolution', *Annual Review of Plant Biology*, vol. 56, Annual Reviews, Palo Alto, pp. 99–131.
- de Godos, I., Mendoza, J.L., Acién, F.G., Molina, E., Banks, C.J., Heaven, S., Rogalla, F., Godos, I. De, Mendoza, J.L., Acién, F.G., Molina, E., Banks, C.J., Heaven, S. & Rogalla, F. 2014, 'Evaluation of carbon dioxide mass transfer in raceway reactors for microalgae culture using flue gases', *Bioresource Technology*, vol. 153, pp. 307–14.
- Grima, E.M., Acién Fernández, F.G. & Chisti, Y. 1999, 'Photobioreactors: light regime, mass transfer and scaleup', *Journal of Biotechnology*, vol. 70, pp. 231–47.
- Grima, E.M., Pérez, J.A., Camacho, G., Ía, F. & Medina, A.R. 1993, 'Gas-liquid transfer of atmospheric CO₂ in microalgal cultures', *Journal of Chemical Technology and Biotechnology*, vol. 56, no. 4, pp. 329–37.
- Guillard, R. & Ryther, J. 1962, 'Studies of marine planktonic diatoms: I. *Cyclotella nana* Hustedt, and *Dentonula confervacea* (Cleve) Gran', *Canadian Journal of Microbiology*, vol. 8, pp. 229–39.
- Ho, S.-H., Chen, C., Lee, D. & Chang, J. 2011, 'Perspectives on microalgal CO₂ - emission mitigation systems — A review', *Biotechnology Advances*, vol. 29, no. 2, pp. 189–98.
- Ho, S.-H., Chen, C.-Y. & Chang, J.-S. 2012a, 'Effect of light intensity and nitrogen starvation on CO₂ fixation and lipid/carbohydrate production of an indigenous

- microalga *Scenedesmus obliquus* CNW-N.', *Bioresource technology*, vol. 113, pp. 244–52.
- Ho, S.-H., Lu, W.-B. & Chang, J.-S. 2012b, 'Photobioreactor strategies for improving the CO₂ fixation efficiency of indigenous *Scenedesmus obliquus* CNW-N: Statistical optimization of CO₂ feeding, illumination, and operation mode', *Bioresource Technology*, vol. 105, pp. 106–13.
- Hu, H. & Gao, K. 2003, 'Optimization of growth and fatty acid composition of a unicellular marine picoplankton, *Nannochloropsis* sp., with enriched carbon sources', *Biotechnology Letters*, vol. 25, no. 5, pp. 421–5.
- Kao, C.-Y., Chen, T.-Y., Chang, Y.-B., Chiu, T.-W., Lin, H.-Y., Chen, C.-D., Chang, J.-S. & Lin, C.-S. 2014, 'Utilization of carbon dioxide in industrial flue gases for the cultivation of microalga *Chlorella* sp.', *Bioresource Technology*, vol. 166, pp. 485–93.
- Kumar, A., Ergas, S., Yuan, X., Sahu, A., Zhang, Q., Dewulf, J., Malcata, F.X. & van Langenhove, H. 2010, 'Enhanced CO₂ fixation and biofuel production via microalgae: recent developments and future directions', *Trends in Biotechnology*, vol. 28, no. 7, pp. 371–80.
- Lee, Y.-K. & Pirt, S.J. 1984, 'CO₂ absorption rate in an algal culture: effect of pH', *Journal of Chemical Technology and Biotechnology. Biotechnology*, vol. 34, no. 1, pp. 28–32.
- Lívansky, K. 1990, 'Losses of CO₂ in outdoor mass algal cultures: determination of the mass transfer coefficient K_L by means of measured pH course in NaHCO₃ solution', *Archiv für Hydrobiologie.*, vol. 85, pp. 87–97.
- Lívansky, K. & Doucha, J. 1996, 'CO₂ and O₂ gas exchange in outdoor thin-layer high density microalgal cultures', *Journal of Applied Phycology*, vol. 8, no. 4–5, pp. 353–8.
- Lucker, B.F., Hall, C.C., Zegarac, R. & Kramer, D.M. 2014, 'The environmental photobioreactor (ePBR): An algal culturing platform for simulating dynamic natural environments', *Algal Research*, vol. 6 Part B, pp. 242–9.
- Mallick, N. 2002, 'Biotechnological potential of immobilized algae for wastewater N, P and metal removal: A review', *BioMetals*, vol. 15, no. 4, pp. 377–90.
- Märkl, H. 1977, 'CO₂ transport and photosynthetic productivity of a continuous culture of algae', *Biotechnology and Bioengineering*, vol. 19, no. 12, pp. 1851–62.
- Mendoza, J.L., Granados, M.R., Godos, I. De, Acien, F.G., Molina, E., Heaven, S., Banks, C.J., de Godos, I., Acien, F.G., Molina, E., Heaven, S. & Banks, C.J. 2013, 'Oxygen transfer and evolution in microalgal culture in open raceways', *Bioresource Technology*, vol. 137, pp. 188–95.
- Miller, D.N. 1974, 'Scale-up of agitated vessels gas-liquid mass transfer', *AIChE Journal*, vol. 20, no. 3, pp. 445–53.
- Moheimani, N.R. & Borowitzka, M.A. 2007, 'Limits to productivity of the alga *Pleurochrysis carterae* (Haptophyta) grown in outdoor raceway ponds', *Biotechnology and Bioengineering*, vol. 96, no. 1, pp. 27–36.
- Pauss, A., Andre, G., Perrier, M. & Guiot, S.R. 1990, 'Liquid-to-gas mass transfer in anaerobic processes: inevitable transfer limitations of methane and hydrogen in the biomethanation process', *Applied and Environmental Microbiology*, vol. 56, no. 6, pp. 1636–44.
- Peng, L., Lan, C.Q. & Zhang, Z. 2013, 'Evolution, detrimental effects, and removal of

- oxygen in microalga cultures: A review', *Environmental Progress & Sustainable Energy*, vol. 32, no. 4, pp. 982–8.
- Putt, R., Singh, M., Chinnasamy, S. & Das, K.C. 2011, 'An efficient system for carbonation of high-rate algae pond water to enhance CO₂ mass transfer', *Bioresource Technology*, vol. 102, no. 3, pp. 3240–5.
- Raso, S., Van Genugten, B., Vermuë, M. & Wijffels, R.H. 2012, 'Effect of oxygen concentration on the growth of *Nannochloropsis* sp. at low light intensity', *Journal of Applied Phycology*, vol. 24, no. 4, pp. 863–71.
- Raven, J.A., Beardall, J. & Giordano, M. 2014, 'Energy costs of carbon dioxide concentrating mechanisms in aquatic organisms', *Photosynthesis Research*, vol. 121, no. 2–3, pp. 111–24.
- Richmond, A. 2004, 'Principles for attaining maximal microalgal productivity in photobioreactors: An overview', *Hydrobiologia*, vol. 512, pp. 33–7.
- Riebesell, U., Fabry, V.J., Hansson, L. & Gattuso, J.-P. 2010, *Guide to best practices for ocean acidification research and data reporting*, U. Riebesell, V.J. Fabry, L. Hansson & J.-P. Gattuso (eds), 1st edn., vol. 260, Publications Office of the European Union Luxembourg, Luxembourg.
- Rubio, F.C., Fernandez, F.G., Perez, J.A., Camacho, F.G. & Grima, E.M. 1999, 'Prediction of dissolved oxygen and carbon dioxide concentration profiles in tubular photobioreactors for microalgal culture', *Biotechnology and Bioengineering*, vol. 62, no. 1, pp. 71–86.
- Sforza, E., Cipriani, R., Morosinotto, T., Bertucco, A. & Giacometti, G.M. 2012, 'Excess CO₂ supply inhibits mixotrophic growth of *Chlorella protothecoides* and *Nannochloropsis salina*', *Bioresource Technology*, vol. 104, pp. 523–9.
- Shah, Y.T., Kelkar, B.G., Godbole, S.P. & Deckwer, W.-D. 1982, 'Design parameters estimations for bubble column reactors', *AIChE Journal*, vol. 28, no. 3, pp. 353–79.
- Shene, C., Chisti, Y., Bustamante, M. & Rubilar, M. 2016, 'Effect of CO₂ in the aeration gas on cultivation of the microalga *Nannochloropsis oculata*: Experimental study and mathematical modeling of CO₂ assimilation', *Algal Research*, vol. 13, pp. 16–29.
- Suresh, S., Srivastava, V.C. & Mishra, I.M. 2009, 'Techniques for oxygen transfer measurement in bioreactors: a review', *Journal of Chemical Technology and Biotechnology*, vol. 84, no. 8, pp. 1091–103.
- Talbot, P., Gortares, M.P., Lencki, R.W. & la Noüe, J. 1991, 'Absorption of CO₂ in algal mass culture systems: A different characterization approach', *Biotechnology and Bioengineering*, vol. 37, no. 9, pp. 834–42.
- Tamburic, B., Evenhuis, C.R., Suggett, D.J., Larkum, A.W.D., Raven, J.A. & Ralph, P.J. 2015, 'Gas transfer controls carbon limitation during biomass production by marine microalgae', *ChemSusChem*, vol. 8, no. 16, pp. 2727–36.
- Tamburic, B., Guruprasad, S., Radford, D.T., Szabó, M., Lilley, R.M., Larkum, A.W.D., Franklin, J.B., Kramer, D.M., Blackburn, S.I., Raven, J.A., Schliep, M. & Ralph, P.J. 2014, 'The effect of diel temperature and light cycles on the growth of *Nannochloropsis oculata* in a photobioreactor matrix.', *PloS One*, vol. 9, no. 1, e86047.
- Ugwu, C.U., Aoyagi, H. & Uchiyama, H. 2008, 'Photobioreactors for mass cultivation of algae', *Bioresource Technology*, vol. 99, no. 10, pp. 4021–8.
- Ugwu, C.U., Ogonna, J.C., Tanaka, H. & Tanaka, C.U.U.J.C.O.H. 2002, 'Improvement

Chapter 5: A practical approach to optimise gas exchange

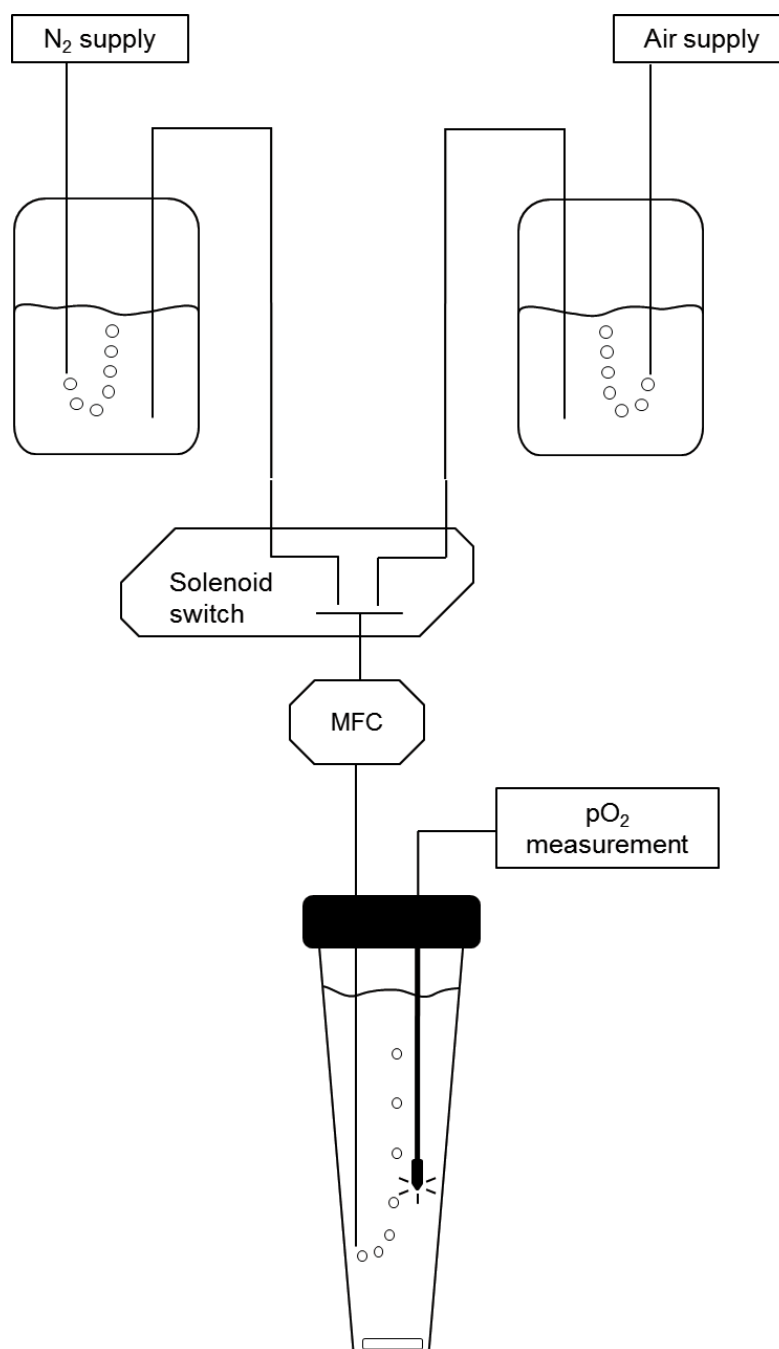
of mass transfer characteristics and productivities of inclined tubular photobioreactors by installation of internal static mixers.', *Applied Microbiology and Biotechnology*, vol. 58, no. 5, pp. 600–7.

Wang, B., Li, Y., Wu, N. & Lan, C.Q. 2008, 'CO₂ bio-mitigation using microalgae', *Applied Microbiology and Biotechnology*, vol. 79, no. 5, pp. 707–18.

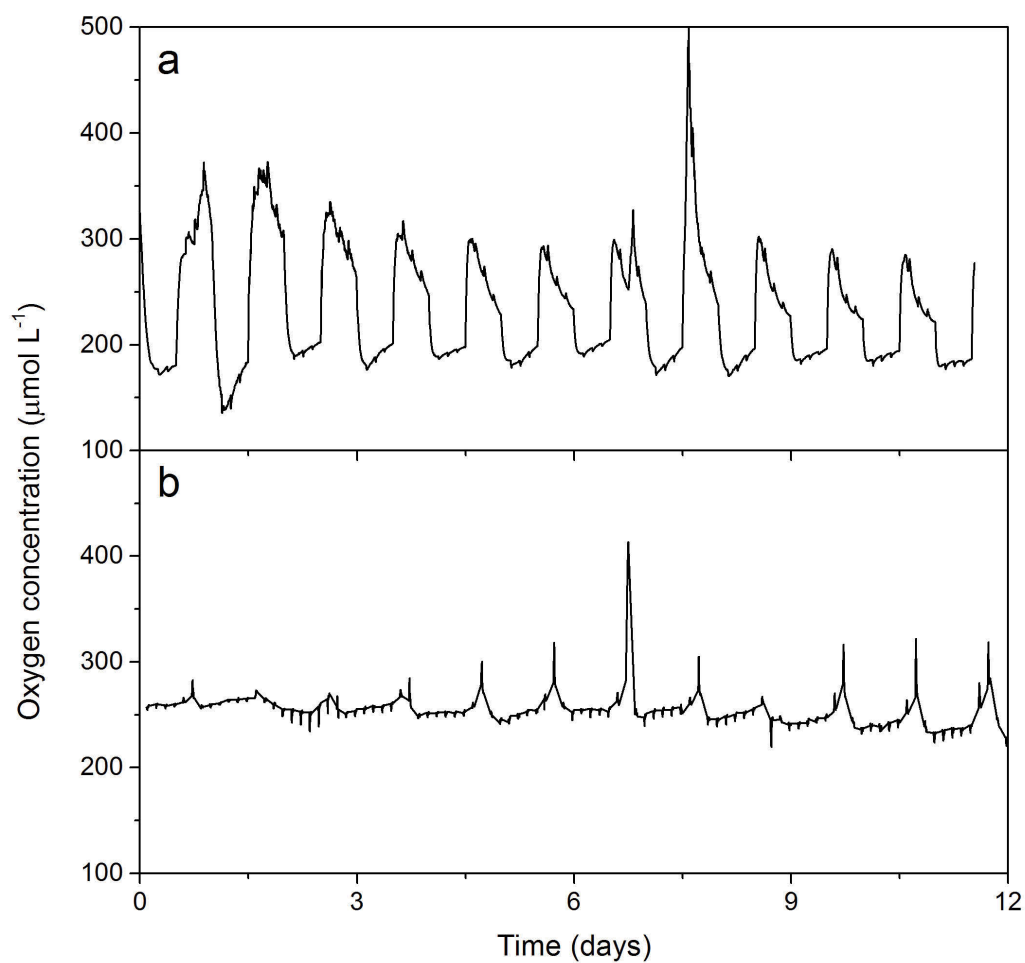
Weissman, J.C., Goebel, R.P. & Benemann, J.R. 1988, 'Photobioreactor design: Mixing, carbon utilization and oxygen accumulation', *Biotechnology and Bioengineering*, vol. 31, no. 4, pp. 336–44.

Zhao, L., Fu, H.-Y., Zhou, W. & Hu, W.-S. 2015, 'Advances in process monitoring tools for cell culture bioprocesses', *Engineering in Life Sciences*, vol. 15, no. 5, pp. 459–68.

5.7 Supplementary Figures



Supplementary Figure 5.1 The environmental PBR set up used to determine gas transfer within the solution, the top two reservoirs allow for the water to be humidified, MFC are gas flow controllers and the solenoid switch allowed for the switching between nitrogen and air.



Supplementary Figure 5.2 Dissolved oxygen trace ($p\text{O}_2$) of *N. oculata* cultivated under (a) laboratory conditions (square- wave light) and (b) under simulated outdoor conditions. Spikes correspond to time points in which gas supply was switched off in order to calculate net photosynthesis/ dark respiration and gas transfer coefficients.

Chapter 6 General Discussion

The work presented in my thesis investigates some of the key process constraints in the scale-up of the marine microalgae *Nannochloropsis oculata* (CS-179) for biofuel production. The application of quantitative physiological techniques has provided new insights into the microalgae response when cultivated under a range of different experimental and environmental conditions. Furthermore, the manipulative experiments and use of the ePBR platform expand the capacity to answer biological and economically relevant questions. For example assessing the response of *N. oculata* under environmental relevant conditions (**Chapters 2** and **5**) or minimising the nutrient inputs for growth (**Chapter 4**). The key outcomes and implications from these new insights are discussed in the subsequent sections. As a result of these new understandings, proposed and future research directions of the physiological/biological responses that constrain the scale-up of large-scale microalgae cultivation are examined in light of the of the insights gained through this research.

6.1 The ePBR platform - a suitable technique for improving large-scale biofuel production

Improving the production of biofuel from microalgae is a multifactorial problem, where many factors (e.g. light, temperature and nutrient availability) influence the overall systems productivity (Chisti 2007). This research has shown that these environmental factors interact with each other and becomes more complicated when cultures are exposed to dynamic environmental conditions. In order to understand these complex biological responses within a culture, high-throughput, non-invasive measurements of multiple traits are required (Lucker et al. 2014). Furthermore, to facilitate accurate comparison between data sets in order to provide robust empirical data for the biofuel industry, the use of a standard platform is necessary.

The ePBR has been used as an example of a standard platform. Data from **Chapters 2, 5** (and Tamburic et al. 2014) as well as studies by Lucker et al. (2014) have provided further evidence of the suitability for such technology to answer critical questions about the feasibility and scalability of microalgae for biofuel production. For example the capacity to fully program ecologically relevant temperature regimes (diel fluctuations) is something that previous photobioreactor technologies have lacked. Data presented in Tamburic et al. 2014 and **Chapter 2** highlight that when the daily temperatures fluctuation are between 15 – 25 °C and 20 – 30 °C, compared to constant temperatures

of 20 °C and 25 °C, no difference in growth rate is observed. On reflection of these results, the data presented in **Chapter 3** provides evidence to show that temperatures between 15 – 30 °C are not 'stressful' for *N. oculata*. Based on these findings of the research, it is proposed that future work upon determining the thermal fluctuation capacity (e.g. variation with higher amplitudes) of biofuel microalgae candidate strains is essential.

For advancements and discoveries to be made the cultivation of microalgae under ecologically relevant field conditions along with invasive and non-invasive analytical methods to monitor the condition of the microalgae is paramount. Whilst continual non-invasive techniques such as optical density, oxygen concentrations and chlorophyll fluorescence are informative, other more destructive but high-throughput analytical methods (e.g. lipid and FAME analyses, metabolic profiling) are required to provide absolute values of products (e.g. areal/ volumetric productivity) for biofuel industry (policies makers need predictions of production). One drawback of the ePBR systems is the small culture volume (500 mL). This limits the amount of culture able to be harvested for the collection of 'invasive' measurements at time points during the culture growth cycle. To overcome these challenges further developments of existing methodologies are required, for example one outcome of this thesis was a miniaturised nutrient analysis technique that allowed for the collection of daily nutrient samples and facilitated the calculation of nutrient uptake rates (see **Chapter 3.2.4.4** for more details). Further technical developments such as this will strengthen the reliability of the data collected with such an ePBR system.

The next step in the development of the ePBR system would be to determine how realistic and comparable the data is to an outdoor culture (Huesemann et al. 2016). Mixing in outdoor large scale cultures is a major factor that directly impacts the in-culture light dynamics and subsequently the culture productivity (Bernard & Rémond 2012). Whereby changes in light environment need to be considered on a daily time scale, incident irradiance on the culture (clear sky versus cloudy day) as well as over a time scale of seconds as cell are vertically mixed in the cultivation system (Hartmann, Béchet & Bernard 2013). Along with the affect upon in-culture light the uptake of nutrient and release of metabolites (e.g. O₂) as a result of must be considered.

Another, less discussed consideration is the availability of carbon (in the form of CO₂ (aq)). Many studies, both laboratory-based and outdoor, have performed experiments using poor mass transfer conditions which limits cultivation productivity (Grima et al. 1993; Moheimani & Borowitzka 2007; Peng, Lan & Zhang 2013). Evidence in **Chapter 5** highlights the suitability of the ePBRs platform to provide specific gas transfer rates, whilst demonstrating the complexities involved. The development of a programmable aeration system that facilitates gas transfer at specific time intervals would allow the simulation of paddle wheel (or sump, etc.) aerating a body of water. This would allow for the simulation of any reactor design (open or closed) to facilitate the improvement of reactor design without associated construction costs, whilst allowing the experiment to assess microalga responses under ecologically relevant conditions.

Taken together, once validation of both the light and gas availability has been achieved between laboratory and outdoor cultivation systems the ePBR robustness of the system will be known. Nevertheless, the future use of the ePBR platform will allow for accelerated microalgae biofuel research to help us overcome the challenges posed for the scale-up of microalgae cultivation.

6.2 New insights gained from an in-depth physiological characterisation of a biofuel candidate microalga. I. Understanding constraints on large-scale production.

New insights into the biological response of a biofuel-candidate microalga to dynamic outdoor conditions (**Chapter 2**) were gained by applying traditional physiology to characterise the biological constraints of temperature and irradiance (**Chapter 3**). The multivariate platform and development of analytical techniques described above facilitated the simulation of relevant outdoor conditions to assess these responses through time.

The biofuel candidate species used in this thesis, *N. oculata*, demonstrated high capacity to cope with large diel (sinusoidal) fluctuations in light intensity (0 - 2000 $\mu\text{mol photons m}^{-2} \text{s}^{-1}$), comparable to traditional laboratory conditions (square wave light) of equal daily quanta (**Chapter 2**) and temperatures between 15 – 25 °C (Tamburic et al. 2014) and 20 – 30 °C (**Chapter 2**). These findings were demonstrated by high resolution monitoring of photosynthetic responses to light of light harvesting and photochemistry processes of PSII (rETR; **Chapter 2**) and overall biological response (photosynthetic oxygen production; Tamburic et al. 2014) providing evidence of high

photosynthetic plasticity. Untangling these multivariate effects highlighted the importance identifying of thermal windows for optimal algal productivity and the response of the microalgae in periods of exposure outside the thermal window. Short periods (24 h) of lethal temperatures ($> 32\text{ }^{\circ}\text{C}$) are initially detected by declines in photosynthetic parameters (declined electron transport rates), followed shortly by declines in biomass, whereas longer exposures (96 h) to sub-lethal temperatures ($32\text{ }^{\circ}\text{C}$) affects other cellular mechanisms such as nutrient uptake leading to reductions in overall growth.

Further understanding of the ability of *N. oculata* to recover from different magnitudes of temperature excursions remains relatively unknown. Understanding different microalgae responses is essential for the optimisation of management practices in cultivation systems. For example, whether it would be more cost-effective to harvest the culture prior to a forecasted large temperature excursion would the culture acclimate or how long would it take to recover from that damage. The main non-invasive technique used throughout this thesis was *in vivo* chlorophyll fluorometry, as this measures a trait (photosynthetic electron transport rate) that rapidly responds to stress conditions (**Chapters 2 and 3**; Eberhard et al. 2008). Use of this technique allows for high-resolution sampling on scales that correspond to the timeframe over which detrimental damage occurs (0 - 24 h; **Chapter 3**). Furthermore, chlorophyll fluorometry has been shown to couple with other photosynthetic measurements (e.g. oxygen accumulation; Hancke et al. 2008; Kromkamp et al. 2009). Similarly designed experiments have been conducted in the context of terrestrial plants and temperature stress (Haldimann & Feller 2004), coral bleaching (Warner et al. 1999) and *Nannochloropsis* sp. (Figueroa et al. 1997; Sukenik et al. 2009). Advances could be facilitated through the ePBR platform by programming meteorological data into the instruments software and measuring rates of recovery after exposure to sub-optimal conditions e.g. high temperature. Specifically with regards to biofuel-related research, the collection of ancillary data such as cell composition through time of appropriate responses would be essential. Moreover, evidence provided in **Chapters 2 and 4** demonstrates how the culture's nutrient status determines capacity of the culture to recover from stressful conditions (**Figure 4.4**). For example, under nutrient depletion conditions cells have a decreased capacity to harvest light (Suggett et al. 2009; White et al. 2011). As a result, the timing of temperature excursions may also dictate how well the culture is able to recover from photoinhibition, ultimately responding to the dual

stress of high temperature and nutrient limitation. Despite the complexity, it is possible to untangle these effects by carefully designing experiments using standard platforms such as the ePBR.

The incorporation of complex thermal and light responses (magnitude and duration of exposure) in predictive models is limited and data of this nature are essential to increase efficiencies in large-scale cultivation. This thesis has demonstrated the significance of integrating the field of applied physiology within biofuels research towards understanding both the identity of environmental factor(s) and associated mechanisms that control large-scale outdoor microalgal cultivation to better inform dynamic predictive growth models.

6.3 New insights gained from an in-depth physiological characterisation of a biofuel candidate microalga. II. Harnessing the natural capacity of microalgae.

Harnessing the physiological capacity of microalga to acclimate to their surrounding nutrient environments (**Chapter 4**) whilst delivering the nutrients more efficiently specifically those in gaseous form (**Chapter 5**) has shed new light on how inputs can be minimised without affecting output and progressed our understanding on how to sustainably yield microalgal products.

In the past half-century, physiologists have regularly observed the capacity of microalgae to acclimate to their nutrient surroundings (Geider et al. 1997, 1998, MacIntyre and Cullen 2005). The traditional method of laboratory batch culturing of microalgae provides nutrients in excess of that required to support growth (Harrison, Thompson & Calderwood 1990). At the scale of cultivation required for biofuel production this nutrient requirement questions the sustainability of the production system (Mata et al. 2010; Borowitzka & Moheimani 2013). The most commonly used medium in laboratory experiments (e.g. f/2) may not necessarily be the most suitable for large-scale cultivation, any reductions in initial nutrient input without lower biomass would make the production process more cost-efficient. **Chapter 4** shows that by acclimating *N. oculata* to its nutrient surroundings a 50% reduction in supply of N and P supply can be made whilst maintaining the same productivity (growth rate) compared to cultures grown under traditional nutrient concentrations (f/2). Exploiting natural beneficial mechanisms such as nutrient acclimation will be a key to further improving the sustainability of the overall biofuel cultivation process. One possible approach to

harness this trait is through ‘contemporary evolution experiments’ and where it is possible to breed strains with beneficial characteristics (Reboud et al. 2007). These concepts of selective breeding have previously been applied in crops and cattle and more recently in phytoplankton, in the context of heavy metals (Huertas et al. 2010) and climate change (Jin et al. 2013; Hutchins et al. 2015; Schaum et al. 2015) and could be extended in the context of biofuels. A study completed by Huertas et al. (2011) provides evidence of these ‘evolution’ methodologies on the biofuel candidate strains, *Tetraselmis suecica* and *Isochrysis galbana* specifically selected for high-temperature adaptation. The method involves gradually exposing the microalgae to a specific selection pressure (i.e. increased temperature) whilst ensure the culture maintains the same levels in the trait of interest (e.g. growth). This gradual increase in selection intensity will facilitate random beneficial mutation in response to the selection pressure whilst not impacting the trait of interest (Huertas et al. 2010). For example, this method may increase the critical maximum temperature of *N. oculata* above 32 °C as described in **Chapter 3**. Further work in biofuel research could focus upon selectively evolving strains with low nutrient requirements. Whereby over long periods (months – years) the nutrient dose provided to the culture is gradual diminished, eliminating any ‘luxury uptake’ of nutrients, whilst ensuring that the culture maintains the capacity to produce the same level of a selected trait (e.g. growth rate). For example, it may be possible to generate a strain that requires 75% less nutrients to grow at the same rate as the original strain thereby producing four-times as much microalga product per unit of nutrient input. Other avenues of research could combine dual selection variables (e.g. high light and high temperature), or harness the capacity of the ePBRs to select for strains with the ability to grow rapidly under large diel fluctuations (> 30 °C; **Chapter 2**). For all the suggested avenues of research, in-culture evolution must also be considered as many cultures used in literature have been maintained in culture collections for decades, under square wave and static temperature conditions. Over this time scale strain selection will have occurred both physiological acclimation and genetic changes. As a result it is suggested that future experiments should use strains freshly isolated from the environment to prevent incorrect observations resulting from any potential in-culture evolution. Using this method of ‘evolution’ would also overcome the current governmental regulations preventing the cultivation of genetically modified microalgae strains in large open systems (Henley et al. 2013).

A greater understanding of how these physiological acclimation strategies in algae could reduce nutrient inputs further demonstrating the importance of incorporating applied physiology into biofuels in order to develop a sustainable industry into the future.

6.4 Perspectives for future research

My thesis has provided new insights into how incorporating the physiological response of microalga can enhance our understanding for large-scale cultivation conditions. The work provides evidence that the ePBR platform is a suitable, cost-effective and scalable platform to accelerate research into large-scale biofuel production. However, it is important to emphasise that the findings presented in this thesis raise further questions that should be addressed in future research, as discussed in the points below.

- In this thesis physiological response analysed under fluctuating conditions (**Chapter 2**) or through time with differing magnitudes of thermal conditions (**Chapter 3**), highlight the dynamic nature of physiological responses. Further research should focus upon the importance of both light and temperature history, in terms of magnitude and duration of exposure on growth and suitable biofuel product. Initially, this would be performed under static conditions and further expanded to examine diel fluctuating conditions. The results would determine whether environmentally resilient algae are ideal candidates for biofuel production especially when cultured under controlled conditions. Or whether it would be more suitable to use optimised algae to efficiently produce specified biofuel products.
- In conjunction with the findings from **Chapter 5**, it is apparent that a greater understanding of catabolic physiological responses during the night is required. Estimates suggest that the loss of daily biomass production through dark respiratory processes is greater than 30% of the total daily biomass gained during sunlight (Torzillo et al. 1991). Future research should aim to implement cost-effective management practices to alleviate, or at least minimise these potential losses (Raven & Ralph 2015). For example, a cost-benefit analysis of artificial culture illumination during the night; an experiment that could be completed within the ePBR system.
- This thesis used *Nannochloropsis oculata* as a model biofuel candidate strain due to its natural high lipid content; however, the cellular physical attributes

(small size and thick cell wall) are proven to be problematic for downstream processing techniques and the commercial potential for biofuel production of the strain remains unknown. Nevertheless, the findings of the thesis on *N. oculata* could be a prime example for further bio-prospecting and isolation of other strains to expand culture collections of potential candidates. In addition, the presented experimental procedures and outcomes may allow for the characterisation of strains with beneficial physiological traits suitable for all aspects of biofuel production. It is suggested that the ePBR matrix provides a reliable platform for these experiments. A suggested method to achieve this bio-prospecting using the ePBR is outlined in **Figure 6.1**.

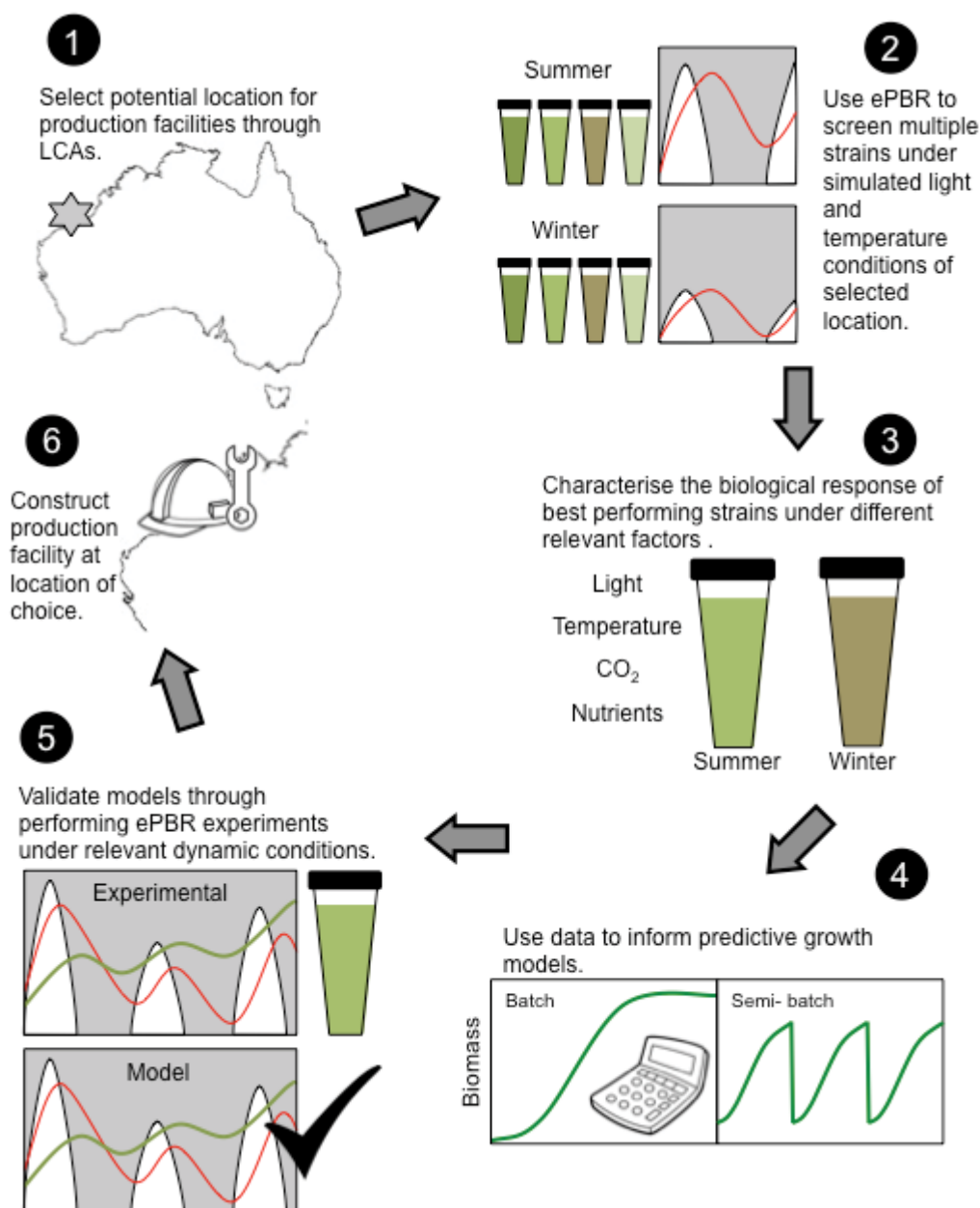


Figure 6.1: Proposed method of bio-prospecting potential site for microalgae cultivation for biofuel production using the ePBR platform.

6.5 The future of microalgae biofuel production- concluding remarks

The results presented in this thesis use newly developed tools and platforms (i.e. ePBR matrix) in combination with physiological techniques to provide new insights into the constraints associated with large-scale microalgae cultivation for biofuel production. The further development of these physiological insights, through harnessing natural cellular mechanisms will enhance our knowledge to improve the prospects for biofuel production. Moreover, it is imperative to integrate the expansive knowledge of agriculture practices that spans thousands of years with existing technology to ensure

that the biofuels industry does not 'reinvent the wheel'. Examples of these include the production of seasonal crops (product), the use of selective breeding techniques (to further improve algae strains).

Despite this, the goal posts for the biofuels industry are constantly changing. At the start of this thesis (February 2013), a barrel of crude oil (West Texas Intermediate) was on average US\$95.32 compared to the prices on near submission of US\$43.65 (US Office of Natural Resources and Revenue 2016; NASDAQ 2016). The only way to strive towards a stable biofuels industry is to supplement this with a secondary industry (non-commodity market), such as, high-value products (i.e. nutraceuticals) or waste utilisation (i.e. bioremediation) producing biomass for use as a biofuel feedstock. The signing of the recent Paris Agreement (United Nations 2015) has renewed interest in industry partnerships with research providers and has expressed the urgency to provide appropriate solutions.

6.6 General References

- Bernard, O. & Rémond, B. 2012, 'Validation of a simple model accounting for light and temperature effect on microalgal growth', *Bioresource Technology*, vol. 123, pp. 520–7.
- Borowitzka, M.A. & Moheimani, N.R. 2013, 'Sustainable biofuels from algae', *Mitigation and Adaptation Strategies for Global Change*, vol. 18, no. 1, pp. 13–25.
- Chisti, Y. 2007, 'Biodiesel from microalgae', *Biotechnology Advances*, vol. 25, no. 3, pp. 294–306.
- Eberhard, S., Finazzi, G. & Wollman, F.-A. 2008, 'The dynamics of photosynthesis', *Annual Review of Genetics*, vol. 42, pp. 463–515.
- Figuerola, F.L., Jiménez, C., Lubián, L.M., Montero, O., Lebert, M. & Häder, D.-P.P. 1997, 'Effects of high irradiance and temperature on photosynthesis and photoinhibition in *Nannochloropsis gaditana* Lubián (Eustigmatophyceae)', *Journal of Plant Physiology*, vol. 151, no. 1, pp. 6–15.
- Geider, R.J., MacIntyre, H.L. & Kana, T.M. 1998, 'A dynamic regulatory model of phytoplanktonic acclimation to light, nutrients, and temperature', *Limnology and Oceanography*, vol. 43, no. 4, pp. 679–94.
- Grima, E.M., Pérez, J.A., Camacho, G., Ía, F. & Medina, A.R. 1993, 'Gas-liquid transfer of atmospheric CO₂ in microalgal cultures', *Journal of Chemical Technology and Biotechnology*, vol. 56, no. 4, pp. 329–37.
- Haldimann, P. & Feller, U. 2004, 'Inhibition of photosynthesis by high temperature in oak (*Quercus pubescens* L.) leaves grown under natural conditions closely correlates with a reversible heat-dependent reduction of the activation state of ribulose-1, 5-bisphosphate carboxylase/oxy', *Plant, Cell & Environment*, vol. 27, no. 9, pp. 1169–83.
- Hancke, K., Hancke, T.B., Olsen, L.M., Johnsen, G. & Glud, R.N. 2008, 'Temperature effects on microalgal photosynthesis-light responses measured by O₂ production, pulse-amplitude-modulated fluorescence, and ¹⁴C assimilation', *Journal of Phycology*, vol. 44, no. 2, pp. 501–14.
- Harrison, P.J., Thompson, P.A. & Calderwood, G.S. 1990, 'Effects of nutrient and light limitation on the biochemical composition of phytoplankton', *Journal of Applied Phycology*, vol. 2, no. 1, pp. 45–56.
- Hartmann, P., Béchet, Q. & Bernard, O. 2013, 'The effect of time scales in photosynthesis on microalgae productivity', *Bioprocess and Biosystems Engineering*, vol. 37, no. 1, pp. 17–25.
- Henley, W.J., Litaker, R.W., Novoveská, L., Duke, C.S., Quemada, H.D. & Sayre, R.T. 2013, 'Initial risk assessment of genetically modified (GM) microalgae for commodity-scale biofuel cultivation', *Algal Research*, vol. 2, no. 1, pp. 66–77.
- Huertas, I.E., Rouco, M., López-Rodas, V. & Costas, E. 2011, 'Warming will affect phytoplankton differently: evidence through a mechanistic approach', *Proceedings of the Royal Society of London B: Biological Sciences*, vol. 278, no. 1724, pp. 3534–43.
- Huertas, I.E., Rouco, M., López-Rodas, V. & Costas, E. 2010, 'Estimating the capability of different phytoplankton groups to adapt to contamination: herbicides will affect phytoplankton species differently', *New Phytologist*, vol. 188, no. 2, pp.

478–87.

- Huesemann, M., Crowe, B., Waller, P., Chavis, A., Hobbs, S., Edmundson, S. & Wigmosta, M. 2016, 'A validated model to predict microalgae growth in outdoor pond cultures subjected to fluctuating light intensities and water temperatures', *Algal Research*, vol. 13, pp. 195–206.
- Hutchins, D.A., Walworth, N.G., Webb, E.A., Saito, M.A., Moran, D., McIlvin, M.R., Gale, J. & Fu, F.-X. 2015, 'Irreversibly increased nitrogen fixation in *Trichodesmium* experimentally adapted to elevated carbon dioxide', *Nature communications*, vol. 6, p. 8155.
- Jin, P., Gao, K. & Beardall, J. 2013, 'Evolutionary responses of a coccolithophorid *Gephyrocapsa oceanica* to ocean acidification.', *Evolution*, vol. 67, no. 7, pp. 1869–78.
- Kromkamp, J.C., Beardall, J., Sukenik, A., Kopecky, J., Masojidek, J., Bergeijk, van S., Gabai, S., Shaham, E. & Yamson, A. 2009, 'Short-term variations in photosynthetic parameters of *Nannochloropsis* cultures grown in two types of outdoor mass cultivation systems', *Aquatic Microbial Ecology*, vol. 56, no. 2–3, pp. 309–22.
- Lucker, B.F., Hall, C.C., Zegarac, R. & Kramer, D.M. 2014, 'The environmental photobioreactor (ePBR): An algal culturing platform for simulating dynamic natural environments', *Algal Research*, vol. 6 Part B, pp. 242–9.
- MacIntyre, H.L., Sharkey, T.D. & Geider, R.J. 1997, 'Activation and deactivation of ribulose-1,5-bisphosphate carboxylase/oxygenase (Rubisco) in three marine microalgae', *Photosynth Res*, vol. 51, no. 2, Journal Article, pp. 93–106.
- Moheimani, N.R. & Borowitzka, M.A. 2007, 'Limits to productivity of the alga *Pleurochrysis carterae* (Haptophyta) grown in outdoor raceway ponds', *Biotechnology and Bioengineering*, vol. 96, no. 1, pp. 27–36.
- NASDAQ 2016, *Crude Oil- WTI (NYMEX) Price*, viewed 8 January 2016, <<http://www.nasdaq.com/markets/crude-oil.aspx>>.
- Peng, L., Lan, C.Q. & Zhang, Z. 2013, 'Evolution, detrimental effects, and removal of oxygen in microalga cultures: A review', *Environmental Progress & Sustainable Energy*, vol. 32, no. 4, pp. 982–8.
- Raven, J.A. & Ralph, P.J. 2015, 'Enhanced biofuel production using optimality, pathway modification and waste minimization', *Journal of Applied Phycology*, vol. 27, no. 1, pp. 1–31.
- Reboud, X., Majerus, N., Gasquez, J. & Powles, S. 2007, '*Chlamydomonas reinhardtii* as a model system for pro-active herbicide resistance evolution research', *Biological Journal of the Linnean Society*, vol. 91, no. 2, pp. 257–66.
- Schaum, C.-E., Rost, B. & Collins, S. 2015, 'Environmental stability affects phenotypic evolution in a globally distributed marine picoplankton', *The ISME journal*, vol. 10, pp. 75–84.
- Suggett, D.J., Moore, C.M., Hickman, A.E. & Geider, R.J. 2009, 'Interpretation of fast repetition rate (FRR) fluorescence: signatures of phytoplankton community structure versus physiological state', *Marine Ecology Progress Series*, vol. 376, no. 1, pp. 1–19.
- Sukenik, A., Beardall, J., Kromkamp, J.C., Kopecký, J., Masojídek, J., van Bergeijk, S., Gabai, S., Shaham, E. & Yamshon, A. 2009, 'Photosynthetic performance of outdoor *Nannochloropsis* mass cultures under a wide range of environmental

- conditions', *Aquatic Microbial Ecology*, vol. 56, no. 2–3, pp. 297–308.
- Tamburic, B., Guruprasad, S., Radford, D.T., Szabó, M., Lilley, R.M., Larkum, A.W.D., Franklin, J.B., Kramer, D.M., Blackburn, S.I., Raven, J.A., Schliep, M. & Ralph, P.J. 2014, 'The effect of diel temperature and light cycles on the growth of *Nannochloropsis oculata* in a photobioreactor matrix.', *PloS One*, vol. 9, no. 1, e86047.
- Torzillo, G., Sacchi, A., Materassi, R. & Richmond, A. 1991, 'Effect of temperature on yield and night biomass loss in *Spirulina platensis* grown outdoors in tubular photobioreactors', *Journal of Applied Phycology*, vol. 3, no. 2, pp. 103–9.
- United Nations 2015, 'Adoption of the Paris Agreement', *Framework Convention on Climate Change*, Paris, pp. 1–32.
- US Office of Natural Resources and Revenue 2016, *NYMEX Oil Prices*, viewed 6 January 2016, <<http://onrr.gov/Valuation/NYMEX.htm>>.
- Warner, M.E., Fitt, W.K. & Schmidt, G.W. 1999, 'Damage to photosystem II in symbiotic dinoflagellates: a determinant of coral bleaching', *Proceedings of the National Academy of Sciences*, vol. 96, no. 14, pp. 8007–12.
- White, S., Anandraj, A. & Bux, F. 2011, 'PAM fluorometry as a tool to assess microalgal nutrient stress and monitor cellular neutral lipids.', *Bioresource Technology*, vol. 102, no. 2, pp. 1675–82.